FACILITATED TRANSPORT OF GROUNDWATER CONTAMINANTS IN THE VADOSE ZONE: COLLOIDS AND PREFERENTIAL FLOW PATHS

A Dissertation

Presented to the Faculty of the Graduate School

of Cornell University

In Partial Fulfillment of the Requirements for the Degree of

Doctorate in Philosophy

by

Verónica Lorena Morales

January 2011

FACILITATED TRANSPORT OF GROUNDWATER CONTAMINANTS IN THE VADOSE ZONE: COLLOIDS AND PREFERENTIAL FLOW PATHS

Verónica L. Morales, Ph.D.

Cornell University, 2011

Although a wide variety of studies have been conducted to understand the numerous processes responsible for the transport of solutes and particulates through soils in order to prevent groundwater contamination, many gaps remain. This thesis presents the findings of two mechanisms (colloid facilitated transport and development of preferential flow infiltration) by which contaminants are able to expedite their transport through unsaturated soils (i.e., the vadose zone), easily reach deeper groundwater, and lower the filtering capacity of soils.

The first study of this thesis bridges the gap between changes in polymeric characteristics of dissolved organic matter-colloid complexes induced by solution composition, and the effect these have on colloid transport through unsaturated soils. The second study presents a semi-empirical approach to improve existing models that predict attachment efficiency (α) of electrosterically stabilized suspensions moving through a porous medium using direct measurements of polymeric characteristics. The fourth study elucidates the capillary forces responsible for the transition between pinning or allowing particles to slip when they approach an air-water-solid interface. Lastly, bioclogging and soil-water repellency from dehydrated microbial exudates are studied in terms of biotic changes in structure and surface properties that generate points of wetting instability that can result in the formation of persistent preferential flow paths.

BIOGRAPHICAL SKETCH

From the first ten years of her life, Veronica grew up listening to constant warnings from the Mexican government about preventative measures that should be taken with tap water to protect Mexico City's residents from water born diseases; particularly from cholera. The next two years of life, her family moved to the northernmost desert of the country, the state of Chihuahua. In this region, Veronica had to quickly adapt to a different water consumption routine, as this public utility service to date is only supplied during a restricted number of hours each day. In 1994, Veronica's family immigrated to Southern California where they enjoyed a carefree and water-plentiful life. During her college years at the University of California at Santa Barbara, Veronica was educated on water politics and became painfully aware that the lifestyle of residents along in the lower Colorado River basin is artificially maintained by excessive allocation of water flow from the Colorado River. It was clear that the unrestricted urban growth of and clashing consumption of water in this desert region of the country were allowed at the expense of the river basin's ecosystems and the Mexican communities on the Sea of Cortez where the river water no longer flows. For these reasons Veronica decided to continue her higher education in the field of hydrology in hopes to contribute professionally to protect and restore natural water systems so that clean water may be naturally available to ecosystems and people that need it in a sustainable and just manner.

I dedicate this thesis to my family, but especially to mom, dad, and Lili; to my best friends Nate and Amy; the amazing people I've met at the hippy commune called Stewart Little Coop, a truly great place to live; the mud buddies; the steadfast Lane 5 swim team; the Chappy; all the planti friends I've made over the years; to my first (and probably best) set of college students at CPEP for being an amazing inspiration to strive to be a great educator; and to Maria Harrison for being my adviser once removed. Thank you all for helping me retain some sanity through this long educative journey.

ACKNOWLEDGMENTS

I would like to acknowledge the invaluable trust, enforced autonomy, and indestructible patience of Dr. Tammo Steenhuis and my extended committee advisers Dr. Leonard W. Lion, Dr. Bin Gao, Dr. James J. Jr. Bisogni, and Dr. Jean-Yves Parlange. I would also like to thank the Alfred P. Sloan Foundation, USDA-NRI, the National Science Foundation, the Binational Agricultural Research and Development fund, the N.G. Kaul Foundation, and the Teresa and H. John Heinz III Foundation for their financial support.

TABLE OF CONTENTS

LIST OF FIGURES

LIST OF TABLES

CHAPTER 1

INTRODUCTION: PATHOGEN TRANSPORT AND FATE: THE PROBLEM OF SCALE FRAGMENTATION

Scale Dependent Transport Behavior -The Pore Scale

A significant amount of work has been done to elucidate the physical, chemical, and biological factors that control the transport and survival of pathogenic microorganisms in an effort to improve the protection of drinking water supplies. Because current transport models inadequately describe microbial transport in either engineered nor more complex natural environments, a wide range of biological and abiotic processes have been studied in increasing detail with the aim of finding universally applicable mathematical expressions that will account for the unresolved discrepancies. In this section the processes studied at the pore scale are presented and the links and gaps leading to the next scale up are discussed.

Mass transfer: Diffusion, Sedimentation, and Interception

The pore scale consists of a set of solid grains (i.e., collectors) with multiple solid-water interfaces or air-water interfaces and contact points of adjacent grains or converging interfaces that dictate the pore space geometry [*Bradford and Torkzaban*, 2008]. The classic colloid filtration theory (CFT) from Yao et al. [1971] and the correlation equation of Rajagopalan and Tien [1976] for Happel's [1958] sphere-in-cell type models (such that the thickness of the fluid surrounding the solid sphere is equivalent to unit porosity of the packed bed) are used extensively to predict the single-collector efficiency term η_o, which is defined as the total collisions of suspended particles (e.g., inorganic colloids and microorganisms) against a porous medium grain. The correlation is obtained from the assumption that the components of

colloid transport by diffusion (η_D), interception (η_I), and sedimentation (η_G) are additive. As such, the governing equation for single-collector efficiency is written as:

$$\eta_o = \eta_D + \eta_I + \eta_G \qquad [1.1]$$

Recently, a new correlation equation for η_o was proposed by Tufenkji and Elimelech [2004a] to individually determine the contribution of each transport mechanism to the overall collector contact efficiency, taking into account hydrodynamic and van der Waals interactions. Regression analysis results indicate that the correlation equation for $\eta_{D,}$ $\eta_{I,}$ and η_G can be written as:

$$\eta_D = 2.4 A_S^{1/3} N_R^{-0.081} N_{Pe}^{-0.715} N_{vdW}^{0.052}, \qquad [1.2]$$

$$\eta_I = 0.55 A_S N_R^{1.675} N_A^{0.125},$$

$$\eta_G = 0.22 N_R^{-0.24} N_G^{1.11} N_{vdW}^{0.053}$$

A_s is defined by the relationship:

$$A_s = \frac{2(1-\gamma^5)}{2-3\gamma+3\gamma^5-2\gamma^6} \qquad [1.3]$$

Where γ is $(1-\varepsilon)^{1/3}$, and ε is the medium's porosity. The overall single-collector contact efficiency for deposition in saturated porous media is thus a function of a set of dimensionless transport parameters (summarized in Table 1.1) with the form [*Tufenkji and Elimelech*, 2004a]:

$$\eta_o = 2.4 A_s^{1/3} N_R^{-0.081} N_{Pe}^{-0.715} N_{vdw}^{0.052} + 0.55 A_s N_R^{1.675} N_A^{0.125} + 0.22 N_R^{-0.24} N_G^{1.11} N_{vdw}^{0.053} \qquad [1.4]$$

Table 1.1 Summary of dimensionless parameters governing particle filtration (from Tufenkji and Elimelech [2004a]).

Parameter	definition[a]	physical interpretation
N_R	$\frac{d_p}{d_c}$	Aspect ratio
N_{Pe}	$\frac{Ud_c}{D_\infty}$	Peclet number characterization ratio of convective transport to diffusive transport
N_{vdw}	$\frac{A_H}{kT}$	Van der Waals number characterization ratio of van der Waals interaction energy to the particle's thermal energy
N_A	$\frac{A_H}{12\pi\mu a_p{}^2 U}$	Attraction number; represents combined influence of van der Waals attraction forces and fluid velocity on particle deposition rate due to interception
N_G	$\frac{2}{9}\frac{a_p{}^2(\rho_p-\rho_f)g}{\mu U}$	Gravity number; ratio of Stokes particle settling velocity to approach velocity of the fluid

[a] The parameters in the various dimensionless groups are as follows: d_p is the particle diameter, d_c is the mean collector diameter, U is the approach velocity, D_∞ is the bulk diffusion coefficient (described by Stokes-Einstein equation), A_H is the Hamaker constant, k is the Boltzmann constant, T is fluid absolute temperature, a_p is particle radius, ρ_p is the particle density, ρ_f is the fluid density, μ is the absolute fluid viscosity, g is the gravitational acceleration.

Although this newly proposed correlation for η_o takes into account the effect of hydrodynamic and van der Waals interactions, it does not address the inadequacy of colloid filtration theory in the presence of an energy barrier. In addition, the correlation only applies to saturated systems, leaving the need for a mathematical expression to describe colloid filtration in unsaturated media unresolved. In unsaturated systems two complications must be dealt with: (i) the presence of an air phase changes and complicates the fluid shell geometry and [*Ishii, et al.*] air-associated interfaces like the air-water and air-water-solid interfaces can act, in addition to the solid-water interface (i.e., collector surface), as sinks for colliding colloids [*Crist, et al.*, 2005; *Gao, et al.*, 2008; *Morales, et al.*, 2009; *Zevi, et al.*, 2009; *Zhang, et al.*, 2010].

Interactions - DLVO and Extended-DLVO

The interaction energy approach developed by Derjaguin, Landau, Verwey and Overbeek (DLVO) to describe colloid stability [*Derjaguin and Landau*, 1941; *Verwey and Overbeek*, 1946] is typically employed to elucidate the shortcomings of CFT. DLVO theory provides information on the interaction energy profile of a colloid-spherical collector system as a function of separation distance, as illustrated in Figure 1. The total interaction energy of two particles or of a particle interacting with a surface is calculated as the sum of Lifshitz-van der Waals attraction and electrical double layer repulsion as a function of the particle separation distance. A central assumption to the theory pertains to the interacting component geometries, which are considered to be spherical and perfectly smooth. Because this assumption is inadequate when considering naturally heterogeneous systems, extensions to the classic DLVO theory have been proposed. More recently, additional primary forces to van der Waals and electrostatic have been incorporated in colloidal stability calculations to include short range Lewis acid-base interactions [*van Oss, et al.*, 1987; *van Oss, et al.*, 1986] and steric interactions. Lewis acid-base interactions are based on the hydrogen-bonding repulsion of hydration shells of interacting particles with opposing layers of well oriented water molecules. Steric interactions result from the sorption of chains and/or chain elements onto particle surfaces [*Rijnaarts, et al.*, 1999]. The magnitude of steric forces depends on the inter-chain strand changes in osmotic pressure, chain length, charge, and elasticity [*Bowen and Williams*, 1995; *Ohshima*, 1995]. As is discussed in later sections, surface biomolecules in protozoa have been recently associated with steric repulsion, as experimental observations reported a decrease in deposition rates under favorable conditions in their presence and an improvement in filter efficiency post biomolecule denaturing [*Considine, et al.*, 2001; *Kuznar and Elimelech*, 2005].

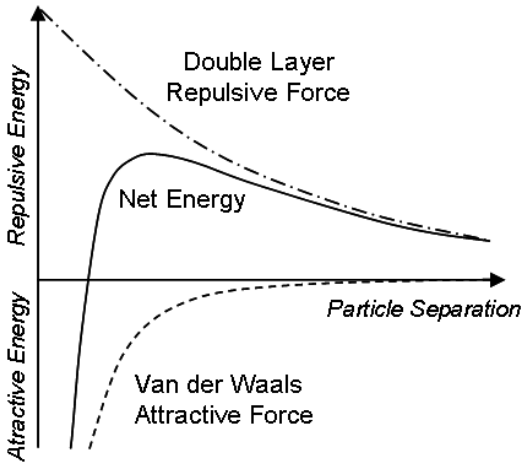

Figure 1.1 Schematic diagram of the DLVO energy potential of two approaching colloidal particles.

Favorable / unfavorable conditions: DLVO energy profiles are used to determine if suspension conditions are *unfavorable* (presence of high energy barriers, with net positive energy potential) or *favorable* for deposition (absence of energy barriers and/or presence of primary and secondary minima, with net negative energy potential at near zero and other positive separation distances, respectively). Transitions between favorable and unfavorable conditions are most commonly induced by changes in solution chemistry, which alter both the solution properties and particle charge. Typical systematic conditions that create unfavorable conditions in natural environments include low solution ionic strength and high pH.

Suspension stability: The stability of colloidal dispersions is commonly expressed in terms of the stability ratio (*W)*, which is the ratio of rapid rate of aggregation (at high ionic strength solutions) to the actual slower rate. The quantitative prediction of colloid stability incorporates DLVO interaction energy terms

into each kinetic aggregation rate, such that the fast aggregation rate is defined by entirely attractive DLVO interactions. Thus, the expression for W according to McGown and Parfitt [1967] is written as:

$$W = \frac{\int_2^\infty \frac{\exp(V/kT)}{s^2} ds}{\int_2^\infty \frac{\exp(V_A/kT)}{s^2} ds} \qquad [1.5]$$

Where V is the energy of interaction of two spherical particles of radius a_p, $s = x/a_p$, x is the distance between particle centers, V_A is the attractive potential energy, k is the Boltzmann constant, and T is the absolute temperature.

Surface Roughness

Deviations of DLVO classification of conditions that should be unfavorable, yet exhibit aggregation and deposition are often attributed to the natural inhomogeneities of the particle and collector surfaces. Work by Hoek and Agarwal [2006] and Shellenberger and Logan [2002] indicate that surfaces that are on average unfavorable for colloid deposition can be effective collectors of particles due to surface asperities that create localized favorable sites. In this work, the authors propose that the magnitude of DLVO repulsive potential is reduced because the particle-rough surface collector separation is increased to a distance where long range van der Waals attraction is stronger than electrostatic repulsion.

Bacterial extracellular appendages or surface structures such as flagella, pili, curli, and polysaccharides are suspected to also play a key role in bacterial transport and retention through soils [*Stevik, et al.*, 2004]. Some extracellular structures like lipopolysaccharides, curli and pili are typically associated with strains that are easily retained in soils, as it is hypothesized that the small appendages are used as "sticky arms" that help cells hold on to surfaces [*van Houdt and Michiels*, 2005; *Walker, et al.*, 2004]. In contrast, extracellular structures like flagella and cilia are typically

implicated in cell motility, thus are usually associated with mobile strains that favor nomadic lifestyles [*Kolter and Greenberg*, 2006].

Chemical Heterogeneity

Like the effect of surface roughness on enhanced colloid deposition, intrinsic surface impurities of the porous medium (e.g., metal oxides, organic matter coatings) can also generate localized regions where deposition is favorable in spite of the medium's average unfavorable properties [*Kim, et al.*, 2008; *Metge, et al.*, 2010]. Specifically for biological systems, it is well recognized that microbial surfaces are intrinsically chemically and structurally more complex than inorganic particles, and dynamically adjust to the changes in the surrounding microenvironment. As Foppen and Schijven [2006] describe, bacterial cells are typically non-uniform in charge, may possess hydrophilic cell walls, are characteristic of cell surface heterogeneity, and often have the capability for biomolecule production (e.g., proteins, lipopolysaccharides, extracellular polysaccharides). An increasing number of studies have found that extracellular macromolecules impact the electrophoretic mobility and surface hydrophobicity of certain microbial cells (e.g., *Escherichia coli* O157:H7, *Cryptosporidium parvum* oocysts, and *Rhodococcus rhodochrous*), thus also affecting cell adhesion and transport [*Gargiulo, et al.*, 2007; *Gargiulo, et al.*, 2008; *Kim, et al.*, 2009a; *Kim, et al.*, 2009b; *Kim, et al.*, 2010; *Liu, et al.*, 2010]. Although significant efforts have been made to improve the understanding on the effect of biomolecule presence on microbial transport, reported results indicate that biomolecules can enhance [*Burks, et al.*, 2003; *Rijnaarts, et al.*, 1996; *Rijnaarts, et al.*, 1999; *Salvucci, et al.*, 2009; *Walker, et al.*, 2004], and also hinder transport [*Burks, et al.*, 2003; *Kim, et al.*, 2010; *Rijnaarts, et al.*, 1996; *Rijnaarts, et al.*, 1999; *Salvucci, et al.*, 2009].

The heterogeneity of microbial surfaces poses a problem when characterizing the surface charge with zeta potential values. Zeta potential is a macroscopic

parameter used to represent the charge of hard and impermeable particles. However, biological cells are soft, permeable, and typically have a wide range of surface structures. Moreover, zeta potential values of microbial particles at best reflect the net electrokinetic properties of the cell [*Foppen and Schijven*, 2006], neglecting the small scale variations of the cell surface charge that may allow cells to be deposited on like net charged soil particles.

Pore Structure

Pore scale investigations of particle transport address the overly simplified pore geometry in CFT, as experimental observations and mathematical simulations corroborate that colloid retention is highly dependent on the medium's pore structure. In addition, pore scale observations have been useful to identify dominant retention mechanisms besides solid-water interface sorption. The most noted retention mechanisms pertaining to particle transport and retention at the pore scale include: straining of particles that are physically too large to pass through certain pores [*Bradford and Bettahar*, 2005; *Bradford, et al.*, 2006; *Shen, et al.*, 2008; *Xu and Saiers*, 2009], film straining in water films enveloping soil grains [*Lenhart and Saiers*, 2002; *Wan and Tokunaga*, 1997], attachment at grain-grain contacts [*Johnson, et al.*, 2007; *Ma and Johnson*, 2010], retention at the air-water interface [*Sirivithayapakorn and Keller*, 2003; *Wan and Wilson*, 1994], as well as immobilization at the junction of all three phases i.e., the air-water-solid interface [*Crist, et al.*, 2005; *Morales, et al.*, 2009; *Zevi, et al.*, 2009; *Zhang, et al.*, 2010].

In order to refine the terminology of the newly proposed colloid retention terms, Bradford and Torkzaban [2008] have proposed to classify as *straining* those processes involving multiple interfaces, while reserving the classification of *attachment* to retention processes concerning a single interface. The two-class organization differentiates new retention mechanisms by forces and torques acting on

a single versus a multi-interfacial site. Colloid removal by straining is generally considered as a process for irreversible removal and described mathematically with a first-order term. Bradford et al. [2005] account for straining (E_{sw}^{str}) in a saturated porous medium in their colloid mass balance equation, viz:

$$\frac{\partial(\theta_w C)}{\partial t} = -\nabla \cdot J_T - E_{sw}^{att} - E_{sw}^{str} \qquad [1.6]$$

Where C is the colloid concentration in the aqueous phase, t is time, θ_w is the volumetric water content, J_T is the total colloid flux, E_{sw}^{att} and E_{sw}^{str} are the colloid mass transfer terms between the aqueous and solid phases due to colloid attachment/detachment and straining, respectively. The straining term, E_{sw}^{str}, is calculated from an additional mass balance equation of strained particles as a function of depth, given by the following equation:

$$E_{sw}^{str} = \rho_b \frac{\partial S_{str}}{\partial t} = \theta_w k_{str} \psi_{str} C \qquad [1.7]$$

where S_{str} is the solid phase concentration of strained colloids, ρ_b is the soil bulk density, k_{str} is the straining coefficient, and ψ_{str} is a dimensionless colloid straining function for discrete layers of distance z from the inlet give by:

$$\psi_{str} = H(z - z_o)\left(1 - \frac{S_{str}}{S_{str}^{\max}}\right)\left(\frac{d_{50} + z - z_o}{d_{50}}\right)^{-\beta} \qquad [1.8]$$

Here, $H(z\text{-}z_o)$ is the Heaviside function, z is depth, z_o denotes the depth of the column inlet or textural interface, $S_{str}^{\max}$ is the maximum solid phase concentration of strained colloids, d_{50} is the median grain diameter, and β is a parameter that controls the shape of the colloid spatial distribution.

More simply, soil grain size is used to evaluate the probability that straining processes will occur in natural porous media. Real soils are characteristic of having a

broad distribution of grain sizes that produce a wide range of pore sizes. Some studies have reported that the susceptibility of colloids to physical straining is increased if the pore throat to particle ratio is smaller than 2.5 [*Auset and Keller*, 2006], and that the physical factors that affect straining may be magnified in unsaturated systems where the water flow occurs in smaller pore spaces [*Bradford, et al.*, 2002]. A factor that has received little attention with respect to straining is the shape/aspect ratio of both grains and microorganisms, as soil particles within the same grain diameter can greatly differ in aspect ratio, and real bacteria exist in various sizes and shapes (e.g., cocci, rod, and spiral) [*Weiss, et al.*, 1995].

Biofilm

Biofilms are the prevailing habitat of most soil bacteria and undoubtedly play an important role in the retention of bacteria in the subsurface. It has been reported that biofilms promote biocolloid retention by anchoring cells to soil surfaces [*Or, et al.*, 2007] and often act as a nucleation site for suspended biocolloids [*Keller and Auset*, 2007]. However, little research has been conducted on biofilm sloughing in porous media and the effect this process could have on detachment and reentry of active pathogen organisms back to the mobile liquid phase.

Motility

Although motility is a process that is often neglected in biocolloid transport models, it is well recognized that certain microorganisms are capable of moving (with maximum measured motility rates of 70-85 μm s^{-1} [*Camper, et al.*, 1993; *Schneide.Wr and Doetsch*, 1974]) by numerous mechanisms. It is important to note that in the presence of a porous medium the effective motility is reduced due to the longer paths required to move around impenetrable solids (i.e., tortuosity). Harshey [2003] describes the mechanisms used for motility as follows: *swimming* (single cell) and *swarming* (colonial) are dependent on the presence of flagella to propel cells through

the liquid medium, *twitching* and some forms of *gliding* require active extension and retraction of type IV pili, and *sliding* and *spreading* are passive forms of movement that play a significant role in bacterial surface colonization. Moreover, colony growth and production of surfactants are strongly correlated to the *sliding/spreading* phenomenon, while *tumbling*, is often observed in flagellated bacteria that move chaotically. Those studies that have investigated motility with respect to bacterial transport reported that motility did not speed up the breakthrough of biocolloids [*Camper, et al.*, 1993], that the attachment rates of motile bacteria are greater than non-motile bacteria [*McClaine and Ford*, 2002; *Mueller*, 1996], and yet others only report inconclusive results [*Becker, et al.*, 2004].

Chemotaxis

Chemotaxis is the self-generated displacement of motile microbes in the direction of an increasing concentration gradient of a chemo-attractant or a decreasing concentration gradient of a chemo-repellent. Physical and chemical signals that initiate motility toward more favorable micro-environments include: moisture availability, nutrients, slime, and temperature. Chemotactic migration toward or away from chemical gradients has been integrated into bacterial transport models [*Nelson and Ginn*, 2001] by including cellular dynamics simulations with CFT particle trajectory analysis. As such, chemotaxis induced cell motility is theoretically shown to significantly affect surface association of cells to the porous medium and near-grain surface transport processes, which consequently affects the value for the collector efficiency, η.

Issues Identified at Pore Scale

At the pore scale our understanding of the physico-chemical colloid transport processes in saturated porous media is relatively good. However, knowledge of the mechanisms that drive transport in unsaturated systems is much less robust. The

intricate flow fields and diverse interactions with air-associated interfaces in unsaturated systems have encumbered the progress of a mass transfer equation that can suitably describe unsaturated transport processes. Incorporation of biological activity into transport models in both saturated and unsaturated conditions is yet to be addressed.

Scale Dependent Transport Behavior –The Soil Core

Microbial transport is traditionally studied in packed columns with well-characterized porous media, where data are collected as measurements of biocolloid breakthrough as a function of time. The data recovered from such studies is thus used to evaluate deposition kinetics, which can be integrated into mathematical models that help improve currently available deterministic predictive capabilities for microbial transport.

Saturated and Unsaturated

Much of the work done to date and generally used theories concern particle transport in saturated porous media. Less is understood about unsaturated porous media transport due to the systematic complexities that arise with the presence of an air phase. Firstly, the liquid phase in unsaturated systems is restricted, as both water and air must occupy the porous medium's void space. Secondly, the coexistence of solid, water and air phases gives rise to interfaces that individually or together can act as retention sites.

Transport - Convective Dispersion Equation

The processes that control fate of microorganisms are typically broken down into one of three categories: (i) transport (advection and dispersion), (ii) physico-chemical filtration (attachment and detachment from immobile phases), and (iii) biological activity (growth and death/inactivation). The fundamental equation for

colloid filtration is a one-dimensional function of particle advection, hydrodynamic dispersion, and a reaction term to represent attachment/detachment, as follows:

$$\frac{\partial C}{\partial t}+\frac{\rho_b}{\varepsilon}\frac{\partial S}{\partial t}=D\frac{\partial^2 C}{\partial z^2}-v\frac{\partial C}{\partial z} \qquad [1.9]$$

Here, C is the concentration of suspended particles, t is time, ρ_b is the porous medium bulk density, ε is the bed porosity, S is the concentration of attached particles, D is the hydrodynamic dispersion coefficient, z is the depth distance, and v is the interstitial particle velocity. As is discussed in later sections the term $\frac{\rho_b}{\varepsilon}\frac{\partial S}{\partial t}$ is often modified to account for the various physico-chemical and biological processes that can change the concentration of attached particles as sink and source terms with respect to C.

Retention

The removal of microorganisms from the liquid phase can be considered an irreversible or reversible process that can further be modeled as an equilibrium or kinetic process.

$k_{att}/k_{det:}$ The most common representation of filtration is by irreversible attachment onto the surface of immobile phases, chiefly the solid-water interface. This process is assumed to occur instantaneously at a rate k_{att}, which is generally of first-order. Deposition profiles from this type of attachment—in a clean bed—predict exponential decreases in retained colloids with depth and k_{att} is typically calculated from breakthrough curve regression or by relation with the experimental value of η_o, the attachment efficiency which is discussed next (α), the bed porosity (ε), and the mean grain size (d_c) by:

$$k_{att}=\frac{3(1-\varepsilon)v}{2d_c}\eta_o\alpha \qquad [1.10]$$

However, the profiles of retained particles in filters characterized with repulsive electrostatic interactions (as are most real filters) are hyper-exponential. To address this discrepancy, Tufenkji and Elimelech [2004b] proposed a bimodal deposition mode model that would better capture the profile with a distribution of *fast* and *slow* deposition rates. Plots of the semi-log profiles exhibit two distinct slopes, which the authors attribute to fast deposition in locations characterized by favorable chemical-colloid interactions, and slow deposition in locations where interactions are unfavorable.

Filtration can also be considered to be reversible in equilibrium or kinetic with paired attachment and detachment rates. Reversible filtration at equilibrium implies that the concentration of microbes adsorbed is at equilibrium with the concentration of cells in the aqueous phase. Thus, equilibrium adsorption can only result in elution retardation of a traveling pulse of suspended cells and does not contribute to the true sinks responsible for removal of organisms from the liquid phase. Reversible kinetic filtration is requires separate kinetic rates for attachment (k_{att}) and detachment (k_{det}) to be established and are expressed in the attached particle rate term of the governing equation as:

$$\frac{\rho_b}{\varepsilon}\frac{\partial S}{\partial t} = k_{att} C - \frac{\rho_b}{\varepsilon} k_{\det} S \qquad [1.11]$$

An integrated mass balance that combines equilibrium sorption, kinetic sorption, straining and a simple biological activity term was proposed by Foppen and Schijven [2006] in the following equation (1.12). Here, the mass balance equation for bacteria retained in a soil matrix includes a fraction of retained cells by each equilibrium sorption (S_1), kinetic sorption (S_2), and straining (S_3), as well as a first-order term for bacterial die-off on the soil matrix (k_{is}) as:

$$\frac{\partial S}{\partial t} = \frac{\partial S_1}{\partial t} + \frac{\partial S_2}{\partial t} + \frac{\partial S_3}{\partial t} - k_{is} S \,, \qquad [1.12]$$

$$S_1 = \pi a_p^2 K_D C \,,$$

$$\frac{\partial S_2}{\partial t} = \pi a_p^2 k_{att} C B(S_2) - k_{\det} S_2 \,,$$

$$\frac{\partial S_3}{\partial t} = \pi a_p^2 k_{str} C$$

S is the dimensionless fractional surface coverage (i.e., total cross-section area of deposited bacteria per interstitial surface area of the solid matrix), a_p is the radius[1] of the bacteria, K_D is an empirical distribution coefficient, C is the number concentration of suspended bacteria in the aqueous phase, k_{att} is the attachment rate coefficient, $B(S_2)$ is the dimensionless dynamic blocking function (discussed in greater detail in later sections), k_{det} is the detachment rate coefficient, and k_{str} is the straining rate coefficient.

Yao et al.'s [1971] filtration theory predicts that the amount of colloid retention experienced by particles traveling through a porous medium—and therefore the mass transfer of colloids from the liquid phase onto the solid phase—will depend on the collector efficiency (η) and the sticking efficiency (α). The term α represents the fraction of collisions between suspended particles and the collector grains that result in attachment.

It is common to use column experiments to determine α from fitted k_{att} and predetermined η_o values, or from experimentally measured values where particles move across a packed bed of homogenized collectors as:

$$\alpha = -\frac{2}{3}\frac{d_c}{(1-\varepsilon) L \eta_o} \ln(C / C_o) \qquad [1.13]$$

[1] Foppen and Schijven (2006) define a_p mistakenly as the *diameter* rather than the *radius* of the bacterial cells.

Here, L is the porous medium packed length, C/Co is the column outlet normalized particle concentration at the initial stage of the particle breakthrough curve, and η_o can be calculated from previously discussed expressions (e.g., equation 1.4). Under unfavorable attachment conditions, several investigators have estimated the value of α from energy calculations of the depth of the secondary minimum and the frequency of kinetic energies [*Hahn, et al.*, 2004; *Shen, et al.*, 2007; *Simoni, et al.*, 1998]. Shen et al. [2007] have proposed to separate the sticking coefficients due to primary and secondary minima as they are dominant in the deposition of large (micron sized) and small (nano sized) colloids, respectively. In this study, the fraction of successful collisions that result in deposition in the secondary minimum (α_{sec}) and at the primary minimum (α_{pri}) were analytically derived as follows:

$$\alpha_{\text{sec}} = \int_0^{\sqrt{\Phi_{\text{sec}}}} \frac{4}{\pi^{1/2}} E^2 \exp(-E^2) dE \qquad [1.14]$$

$$\alpha_{pri} = \int_{\sqrt{\Delta\Phi}}^{\infty} \frac{4}{\pi^{1/2}} E^2 \exp(-E^2) dE \qquad [1.15]$$

Here, Φ_{sec} is the depth of the secondary minimum, E is the kinetic energy of the colloids, and $\Delta\Phi$ is the sum of the energy barrier and the depth of the secondary minimum well.

The kinetic energy method assumes that a particle's kinetic energy can be described by from Maxwell distribution functions (probability of the particle's velocity) and that DLVO energy profiles accurately predict the interaction energies between particle and collector. The kinetic energy, E, of a particle can be estimated from its Maxwellian velocity (v_M) and its mass (m_p) with the expression [*Shen, et al.*, 2007] viz:

$$E = \frac{m_p {v_M}^2}{2kT} \qquad [1.16]$$

Where the velocity distribution of the particles follows the function:

$$f(v_M) = 4\pi\left(\frac{m_p}{2\pi kT}\right)^{(3/2)} v^2 \exp\left(-\frac{m_p {v_M}^2}{2kT}\right) \quad [1.17]$$

Such that:

$$\int_0^\infty f(v_M)dv_M = 1 \quad [1.18]$$

The kinetic energy method is of particular importance in the mathematical justification of colloid retention in secondary energy minima. As equation 1.14 indicates, attachment efficiencies for deposition in the secondary minimum are equivalent to the probability that a particle does not have sufficient kinetic energy to escape from the energy well. Similarly, equation 1.15 predicts attachment efficiencies for deposition in the primary minimum to be directly related to the fraction of particles with sufficient kinetic energy to overcome the energy barrier and escape retention at the secondary minimum. It is important to note that an overestimation of α_{pri} is recognized as colloids with sufficient kinetic energy to escape the secondary minimum trap and the energy barrier may also escape primary minimum retention and re-enter the bulk suspension.

Two-site / two-region models: Because pathogen interaction with the solid phase during transport cannot be associated with a single category, the two-site or two-region models are often used to include multiple sorption processes to the pathogen-solid phase reaction in the porous medium. The non-equilibrium sorption kinetics transport models for two-site and two-region are mathematically identical [*Toride, et al.*, 1995] though the significance of the terms are different and represent different processes. The two-site transport model makes a distinction between equilibrium adsorption in the first site and first-order kinetic adsorption in the second

site. The two-region transport model assumes that the liquid phase is divided into two regions, the first which is mobile (flowing) and the second that is immobile (stagnant). A first-order mass transfer factor connects the two regions, but transport is limited to the mobile region.

Blocking / ripening: Investigations of non-clean filters indicate that retention processes not only depend on the interaction between the approaching colloid and the collector surface, but are also affected by interactions with pre-attached particles. Approaching particles have been observed to experience a decline in deposition rates as a result of *blocking,* which refers to the occlusion of collector surface by already attached particles [*Adamczyk, et al.*, 1994; *Bradford and Torkzaban*, 2008; *Johnson and Elimelech*, 1995]. This phenomenon assumes that a finite amount of chemically favorable attachment locations are already filled so incoming particles only see the most chemically unfavorable sites and thus fail to be retained. Conversely, approaching particles may experience an increase in deposition rates as a result of *ripening*, as attractive colloid-colloid interactions enhance attachment to the collector surface [*Bradford and Torkzaban*, 2008; *Zhang, et al.*, 2010]. As is discussed in later sections, biological activity is suspected to highly influence these two phenomena [*Tufenkji*, 2007].

Transients in chemistry and moisture content: Two key factors that affect the collision/sticking efficiency and therefore the filter performance of a porous medium are the solution chemistry and the porous medium's moisture content.

It is well accepted that changes in solution chemistry in the form of ionic strength, pH, and concentration of organic matter have the greatest impact on particle and collector surface charge. The most evident physical parameter that these factors change is the electric double layer thickness that is responsible for electrostatic interactions. Chemical perturbations are often used to shift the interaction energies

between colloids and retention site surfaces between net attractive and net repulsive in order to induce particle attachment [*Jenkins, et al.*, 1973; *NocitoGobel and Tobiason*, 1996; *Shiratori, et al.*, 2007; *Tosco, et al.*, 2009] or detachment [*Bales, et al.*, 1991; *Grolimund, et al.*, 2001; *Lenhart and Saiers*, 2003; *McDowellboyer*, 1992; *NocitoGobel and Tobiason*, 1996; *Roy and Dzombak*, 1996; *Ryan and Gschwend*, 1994; *Shiratori, et al.*, 2007; *Tosco, et al.*, 2009]. Ryan and Gschwend [1994] reported that changes in solution chemistry must be great enough to eliminate the detachment energy barrier in order to successfully achieve detachment. Tosco [2009] reported from mathematical simulations the linear dependence of attachment coefficients on ionic strength, and that upon chemical perturbations, increases in detachment rates are well correlated to disappearance of secondary minima wells.

Several studies have investigated the effects of sudden changes in moisture content on particle fate by affecting draining and imbibing events [*Auset, et al.*, 2005; *Cheng and Saiers*, 2009; *Gao, et al.*, 2006; *Saiers, et al.*, 2003; *Saiers and Lenhart*, 2003; *Zhuang, et al.*, 2007; *Zhuang, et al.*, 2009]. The reported results appear inconsistent, as some studies attribute increased retention to drainage events [*Zhuang, et al.*, 2009], others ascribe mobilization to drainage [*Saiers, et al.*, 2003], and another set have reported mobilization during imbibition [*Auset, et al.*, 2005; *Gao, et al.*, 2006; *Saiers and Lenhart*, 2003]. A more recent study indicates that mobilization can occur during imbibing or draining events because of the pore-scale changes in the air-water configuration that can scour colloids loosely trapped at the SWI [*Cheng and Saiers*, 2009]. The contending reports indicate a lack of thorough understanding of the processes driving particle fate with advancing drying/wetting fronts. Moreover, transients in moisture content that increase the pore water velocity may reduce the liquid phase areas that are hydrodynamically stagnant and expand the air-water-solid interface, thus mobilizing more colloids in the streamlines.

Factors that hamper the prediction of retention and release: A number of factors intrinsic to real systems often conflict with the underlying assumptions of the above described mathematical methods designed to describe particle transport, thus encumbering the applicability of such models to dynamic and heterogeneous systems.

As discussed in the retention section earlier, adsorption/attachment can be modeled as equilibrium or kinetic (i.e., non-equilibrium) processes and classified as physical, chemical, or exchange in origin [*Corapcioglu and Haridas*, 1984]. Physical adsorption refers to sorption resulting from non-surface site specific van der Waals attractive forces acting at sub-micron separation distances. Chemical adsorption requires chemical interaction between the particle and the adsorbent. Exchange adsorption involves ion-exchange and electrokinetic attractive forces. In this third type of adsorption, ions of one substance (either the particle or the collector) concentrate at a surface as a result of electrostatic attraction of charged sites at the other surface.

Based on the criterion that the transport of biocolloids is strongly controlled by size and electrostatic interactions, it is expected that the transport of viruses should be greatest, then bacteria, and lastly protozoa [*Jin*, 2002]. Often, viruses are considered the pathogen of greatest threat to groundwater quality due to their small size and negative charge, which—at least in theory—make them less likely to become retained by straining processes. Bacteria of smaller size and coccus shape are typically expected to be more mobile than larger strains or those that are rod or spiral in shape [*Weiss, et al.*, 1995]. The capability of production of extracellular polymeric substances is often an indicator for expectations of reduced biocolloid transport [*Salvucci, et al.*, 2009]. Characteristics unique to protozoa that control their transport (beyond the size factor) are not yet clear as studies on protozoa transport are hindered by the difficulties of quantifying cysts.

Microorganisms commonly modify their microenvironments by synthesizing extracellular polymeric substances (EPS) to generate a shelter from temporal and chemical variations in the soil matrix [*Or, et al.*, 2007]. Abundant secretion of EPS will inevitably alter the pore geometry, leading to a reduction of the soil's hydraulic conductivity [*Baveye, et al.*, 1998; *Cunningham, et al.*, 1991] and optimization for conditions that trigger preferential flow [*Morales, et al.*, 2010].

In addition to the physico-chemical parameters described above that affect colloid attachment, surface biomolecules (e.g., proteins, lipopolysaccharides, and extracellular polysaccharides) and growth phase stage are two additional factors suspected to strongly contribute to biocolloid induced attachment. As researchers have attempted to advance the current understanding of biomolecules with respect to microbial adhesion, numerous studies report that the presence of biomolecules can both promote [*Abu-Lail and Camesano*, 2003; *Burks, et al.*, 2003; *Rijnaarts, et al.*, 1996; *Rijnaarts, et al.*, 1999], and hinder [*Burks, et al.*, 2003; *Kuznar and Elimelech*, 2005; *Rijnaarts, et al.*, 1996] cell adhesion in aqueous media. The apparent conflicting results from these studies warrants attention to the types of biomolecules considered, and the conditions under which the same biomolecule may reverse its effect on attachment. Investigations on the role of growth-phase stage on attachment/adhesion indicate that cells undergoing starvation (i.e., death phase) were observed to have decreased attachment capabilities [*Sanin*, 2003; *Sanin, et al.*, 2003], while studies comparing bacterial transport in the stationary and mid-exponential phases reported that deposition in the former phase was significantly higher than that in the latter [*Boonaert, et al.*, 2001; *Dufrene and Rouxhet*, 1996; *Walker, et al.*, 2005]. Walker et al. [2005] attributes this trend to the more heterogeneous distribution of charged functional groups on stationary phase cell surfaces that supports greater deposition kinetics.

Survival

The process of die-off, after retention, is the second most important sink responsible for removal of viable pathogens moving through a porous medium [*Tufenkji*, 2007]. Biocolloid die-off can occur as a result of environmental changes that inactivate viruses or lyse cells, or from biotic antagonistic activity in the form of parasitism or predation [*Lang, et al.*, 2007; *Molin and Cvetkovic*, 2010].

First order inactivation: Environmentally induced die-off is often modeled as a first-order decay rate process [*Corapcioglu and Haridas*, 1985] typically associated to with changes in temperature, soil type, pH, presence of toxic substances, dissolved oxygen, salinity, moisture content, and nutrient availability [*Foppen and Schijven*, 2006; *Tufenkji*, 2007]. Although biocolloid death can occur while suspended in the liquid phase and/or while sorbed onto the soil matrix, many predictive models for bacteria assume that inactivation is significant only for the sorbed phase, as is the case in equation 1.12. Some experimental observations and stochastic analysis of virus indicate that the rate of inactivation is smaller for soil sorbed viruses [*Rehmann, et al.*, 1999; *Schijven and Hassanizadeh*, 2000] than for those in suspension or attached to the air-water interface [*Chu, et al.*, 2001; *Jin, et al.*, 2000; *Thompson and Yates*, 1999], suggesting different inactivation rates for the liquid-phase and the sorbed phase [*Sim and Chrysikopoulos*, 2000]. However, others have found inactivation to be virus-specific and nearly independent of adsorption [*Schijven and Hassanizadeh*, 2000].

Time dependent inactivation: Viruses in the environment are present in subpopulations that can become inactivated sequentially at different rates [*Chrysikopoulos and Vogler*, 2004; *Molin and Cvetkovic*, 2010]. The mathematical complexities of representing sequential inactivation by a set of discrete first-order rate coefficients, each governing a different inactivation phase, have been managed by

approximating sequential inactivation by a time dependent pseudo first-order rate coefficient based on experimental data [*Sim and Chrysikopoulos*, 1996].

Dependency of survival on abiotic factors: Specific physical (e.g., temperature and water content) and chemical (abiotic stresses) are known to affect the viability of microorganisms. Temperature has been regarded as the most critical factor affecting oocyst [*Peng, et al.*, 2008] and virus survival with thresholds for viral inactivation at temperatures greater than 20^{o} C [*John and Rose*, 2005]. Although the thermal influence of bacterial die-off is not as strong as that of viruses, studies that have investigated the effect of temperature on survival often use variations of the Arrhenius equation, which is written as:

$$\mu = A \cdot \exp^{-E_a / RT} \qquad [1.19]$$

where A is a constant, R is the universal gas constant, E_a is the activation energy. At freezing temperatures, bacteria are protected from inactivation and become "incubated" [*Vidovic, et al.*, 2007]. Analysis of a large number of reported die-off studies of *E. coli* reveal that the increase in die-off rate per degree Celsius rise is comparable in most experiments [*Foppen and Schijven*, 2006; *Lang, et al.*, 2007] where, for example, the average die-off at 10^{o} C is 15 d^{-1} and drops to 0.50 d^{-1} at 20^{o} C. Other studies propose that the effect of temperature fluctuations on die-off may be dampened by finer soil textures [*Cools, et al.*, 2001] or by the presence and type of organic carbon [*Garzio-Hadzick, et al.*, 2010; *Ishii, et al.*, 2010; *Vidovic, et al.*, 2007].

It is well accepted that prolonged dry periods or exceptionally low moisture contents may lead to desiccation, which consequently affects the viability of biocolloids [*Berry and Miller*, 2005; *Gomoryova, et al.*, 2009; *Habteselassie, et al.*, 2008; *Ishii, et al.*, 2010; *Peng, et al.*, 2008; *Vidovic, et al.*, 2007]. A monotonically

increasing relationship between water potential and bacterial respiration rate (as a surrogate measurement for viability) was reported by Bazin et al. [1976]. Conversely, a study by Halverson et al. [2000] reported that, although sudden increases in soil water potential did not cause significant cells lysis, observed dilution stress responses varied in amounts of intracellular solutes released and culturability. Numerous studies have confirmed the nonlinear correlation between viral persistence and soil moisture [*Hurst, et al.*, 1980; *Song, et al.*, 2005; *Straub, et al.*, 1993; *Williamson, et al.*, 2005; *Zhao, et al.*, 2008].

The effect of ionic strength and pH on survival are dependent on the microbial species considered. For instance, halophiles and some salt tolerant bacteria thrive in saline environments because they have the capability to osmoregulate [*Essendoubi, et al.*, 2007; *Zahran*, 1997], while other non-halophilic species typically experience growth arrest and may even go into osmotic shock [*Wood and Sorensen*, 1998]. An early study by Singleton et al. [1982] determined that in the presence of saline conditions the growth of all the species and strains of *Rhizobium* decreased when the electric conductivity of the medium was raised from 1.2 mS to 6.7 mS cm and several strains were completely growth hindered at 13.1 mS cm. Perhaps more importantly, this study indicates that the saline effects on viable count reduction can be delayed for multiple weeks. The effect of pH on bacterial inactivation is lowest at pH levels between 6 and 8 [*Foppen and Schijven*, 2006], greatest in both acidic [*Inglis and Sagripanti*, 2006] and alkaline conditions [*Stimson, et al.*, 2010].

Although significant progress has been made to qualitatively understand the physical and chemical stresses described with respect to pathogen survival, the often reported quantitative description of these effects is antiquated and indifferent to the range of stress factors considered. To date, the most common model used to simulate

inactivation is Chick's [1908] equation for first-order exponential inactivation, which follows the form:

$$C(t) = C_o \exp^{-\lambda t} \qquad [1.20]$$

Where C is the concentration of cells at time t, C_o is the initial concentration of cells, and λ is the inactivation rate constant. An early model for *E. coli* survival proposed by Cerf et al. [1996] combines the effects of temperature (T), pH, and water activity (a_w) on inactivation rate (λ) with the following empirical expression:

$$\ln(\lambda) = 86.49 - \frac{0.3028 \times 10^5}{T} - 0.5470\,pH + 0.0494\,pH^2 + 3.067\,a_w^2 \qquad [1.21]$$

Dependency of survival on biotic factors: The survival of microorganisms in soil is due to a complex combination of abiotic (as listed above) and biotic factors (e.g., population density, dissolved oxygen, substrate/product inhibition and activation) that may not be independent. In order to work around this mathematical complexity, a first-order *net decay* term is used to model survival as the difference between decay rate and rate of growth with the following expression:

$$\lambda = K_i C \qquad [1.22]$$

C is the pathogen concentration at time t and K_i is the first-order inactivation constant that expresses the sum total of all the factors that contribute to the inactivation of the pathogen being modeled.

Biofilm: Soil bacteria have developed survival strategies, such as biofilm formation, to cope with abrupt environmental changes in soil moisture and temperature. Biofilms buffer the colony against detrimental pH changes, protect cells

against predation, and serve as a carbon source when nutrients are scarce [*Winfield and Groisman*, 2003].

Growth

Incorporation of biological factors that influence the fate and transport of microorganisms into predictive mathematical models remains a challenge. Growth of microbial populations is typically modeled with Monod, Tessier, Contois, or Andrews expressions or their extended versions. These models describe the correlation between substrate concentration and specific growth rates with the assumption that saturation kinetics for the cellular population can be reached.

Classic Monod kinetics [*Monod*, 1942] relates the specific growth rate (G) of a particular microbial population to the concentration of a limiting nutrient (N) in the environment as:

$$G = \frac{G_{\max} N}{K_N + N} \qquad [1.23]$$

where G_{max} is the maximum specific growth rate when $N >> K_N$ and K_N is the half-maximum concentration. A modified Monod expression to account for utilization of electron donors, *ed*, and electron acceptors, *ea*, as presented by Mohamed et al. [2007] and Bailey and Ollis [1977] is written as:

$$G = G_{\max}\left(\frac{A_{ea}}{K_{ea} + A_{ea}}\right)\left(\frac{A_{ed}}{K_{ed} + A_{ed}}\right) \qquad [1.24]$$

Here, K_{ea} is the half saturation coefficient for the electron acceptor of the microbial species, K_{ed} is the half saturation coefficient for the electron donor of the microbial species, A_{ed} is the aqueous phase concentration for electron donor, and A_{ea} is the aqueous phase concentration of electron acceptor.

Tessier's equation [1942] uses an alternative expression to model growth rate as a function of the saturation constant (Y), by:

$$G = G_{\max}\left(1 - \exp^{-N/Y}\right) \qquad [1.25]$$

Contois's approach [1959] sets the specific growth rate as a function of the population density and concentration of the limiting nutrient. Contois kinetics best describes the macroscopic behavior of attached biomass as a function of the ratio of substrate to biomass. Moreover, the specific growth rate from this model restricts the kinetic growth process to the available surface area, which limits the mass-transfer of substrate to the biomass, viz:

$$G = G_{\max}\left(\frac{N/X}{K_N + N/X}\right) \qquad [1.26]$$

Where X is the concentration of microorganisms.

Andrews's model [1968] predicts specific growth rate as inhibited by substrate or product constituents as:

$$G = \frac{G_{\max} N}{K_N + N + N^2/K_i} \qquad [1.27]$$

Where K_i is the substrate inhibition constant.

Several limitations to the above listed growth kinetic models make predictions of the dynamic behavior of soil ecosystems subjected to environmental perturbations a difficult task. The first limitation to the models above is that G_{max} must be determined independently from saturation constants, which is commonly measured from batch cultures. Second, additional equations must be developed to account for the limiting nutrient or substrate in the growth equation. Third, conditions that cultures experience in batch test are assumed to be at steady-state and may not translate well to the

dynamic system of the porous medium being modeled. Fourth, responses to transient conditions (even if they are well defined) are difficult to capture as they are usually delayed. Fifth, multiple correlated parameters may give similar fits to the measured data, resulting in the problem of parameter "identifiability" [*Beck and Arnold*, 1977; *Liu and Zachara*, 2001].

Growth can be neglected for virus and protozoa: Growth kinetics of viruses and protozoa are typically not modeled. Unlike cellular microorganisms, viruses and pathogenic protozoa are obligate intracellular parasites, and thus remain biochemically inert if found to be free in an extracellular environment.

Persistent low levels of survival: Physico-chemical sorption/filtration of pathogen transport through a porous medium provides a fair understanding of the processes responsible for short-term elution of colloidal pathogens from a porous medium. After initial breakthrough, however, a porous medium with retained biological particles capable of surviving and growing in the midst of harsh environmental stresses can in itself become a significant source of pathogens long-term and low-level elution.

REFERENCES

Abu-Lail, N. I., and T. A. Camesano (2003), Role of lipopolysaccharides in the adhesion, retention, and transport of Escherichia coli JM109, *Environmental Science & Technology*, *37*, 2173-2183.

Adamczyk, Z., et al. (1994), Kinetics of localized adsorption of colloid particles, *Advances in Colloid and Interface Science*, *48*, 151-280.

Andrews, J. F. (1968), Mathematical model for the continuous culture of microorganisms utilizing inhibitory substrates., *Biotechnol. Bioeng.*, *10*, 707-723.

Auset, M., and A. A. Keller (2006), Pore-scale visualization of colloid straining and filtration in saturated porous media using micromodels, *Water Resources Research*, *42*, 9.

Auset, M., et al. (2005), Intermittent filtration of bacteria and colloids in porous media, *Water Resources Research*, *41*, 14.

Bailey, J. E., and D. F. Ollis (1977), *Biochemical engineering fundamentals*, McGraw Hill, New York.

Bales, R. C., et al. (1991), Bacteriophage adsorption during transport through porous media - Chemical perturbations and reversibility, *Environmental Science & Technology*, *25*, 2088-2095.

Baveye, P., et al. (1998), Environmental impact and mechanisms of the biological clogging of saturated soils and aquifer materials, *Critical Reviews in Environmental Science and Technology*, *28*, 123-191.

Bazin, M. J., et al. (1976), Models of microbial interactions in the soil, *Critical Reviews in Microbiology*, *4*, 463-498.

Beck, J. V., and K. J. Arnold (1977), *Parameter Estimation in Engineering and Science*, John Wiley & Sons, New York.

Becker, M. W., et al. (2004), Effect of cell physicochemical characteristics and motility on bacterial transport in groundwater, *Journal of Contaminant Hydrology*, *69*, 195-213.

Berry, E. D., and D. N. Miller (2005), Cattle feedlot soil moisture and manure content: II. Impact on Escherichia coli O157, *Journal of Environmental Quality*, *34*, 656-663.

Boonaert, C. J. P., et al. (2001), Adhesion of Lactococcus lactis to model substrata: direct study of the interface, *Colloids and Surfaces B-Biointerfaces*, *22*, 171-182.

Bowen, W. R., and P. M. Williams (1995), The osmotic pressure of electrostatically stabilized colloidal dispersions, *Advances in Colloid and Interface Science*, *56*, 201-243.

Bradford, S. A., and M. Bettahar (2005), Straining, attachment, and detachment of Cryptosporidium oocysts in saturated porous media, *Journal of Environmental Quality*, *34*, 469-478.

Bradford, S. A., et al. (2005), Straining of colloids at textural interfaces, *Water Resources Research*, *41*, 18.

Bradford, S. A., et al. (2006), Significance of straining in colloid deposition: Evidence and implications, *Water Resources Research*, *42*.

Bradford, S. A., and S. Torkzaban (2008), Colloid transport and retention in unsaturated porous media: A review of interface-, collector-, and pore-scale processes and models, *Vadose Zone Journal*, *7*, 667-681.

Bradford, S. A., et al. (2002), Physical factors affecting the transport and fate of colloids in saturated porous media, *Water Resources Research*, *38*, 12.

Burks, G. A., et al. (2003), Macroscopic and nanoscale measurements of the adhesion of bacteria with varying outer layer surface composition, *Langmuir*, *19*, 2366-2371.

Camper, A. K., et al. (1993), Effects of motility and adsorption rate coefficient on transport of bacteria through saturated porous-media, *Applied and Environmental Microbiology*, *59*, 3455-3462.

Cerf, O., et al. (1996), Thermal inactivation of bacteria - A new predictive model for the combined effect of three environmental factors: Temperature, pH and water activity, *Food Research International*, *29*, 219-226.

Cheng, T., and J. E. Saiers (2009), Mobilization and transport of in situ colloids during drainage and imbibition of partially saturated sediments, *Water Resources Research*, *45*.

Chick, H. (1908), An investigation of the law of disinfection, *Journal of Hygiene*, *8*, 92-158.

Chrysikopoulos, C. V., and E. T. Vogler (2004), Estimation of time dependent virus inactivation rates by geostatistical and resampling techniques: application to virus transport in porous media, *Stochastic Environmental Research and Risk Assessment*, *18*, 67-78.

Chu, Y., et al. (2001), Mechanisms of virus removal during transport in unsaturated porous media, *Water Resources Research*, *37*, 253-263.

Considine, R. F., et al. (2001), Force of interaction between a biocolloid and an inorganic oxide: Complexity of surface deformation, roughness, and brushlike behavior, *Langmuir*, *17*, 6325-6335.

Contois, D. E. (1959), Kinetics of bacterial growth - Relationship between population density and specific growth rate of continuous cultures, *Journal of General Microbiology*, *21*, 40-50.

Cools, D., et al. (2001), Survival of E. coli and Enterococcus spp. derived from pig slurry in soils of different texture, *Applied Soil Ecology*, *17*, 53-62.

Corapcioglu, M. Y., and A. Haridas (1984), Transport and fate of microorganisms in porous-media - A theoretical investigation, *Journal of Hydrology*, *72*, 149-169.

Corapcioglu, M. Y., and A. Haridas (1985), Microbial transport in soils and groundwater - A numerical model, *Advances in Water Resources*, *8*, 188-200.

Crist, J. T., et al. (2005), Transport and retention mechanisms of colloids in partially saturated porous media, *Vadose Zone Journal*, *4*, 184-195.

Cunningham, A. B., et al. (1991), Influence of biofilm accumulation on porous-media hydrodynamics, *Environmental Science & Technology*, *25*, 1305-1311.

Derjaguin, B., and L. Landau (1941), A theory of the stability of strongly charged lyophobic sols and adhesion of highly charged particles in solution of electrolytes., *Acta Phys.-Chim. URSS*, *14*, 2178.

Dufrene, Y. F., and P. G. Rouxhet (1996), Surface composition, surface properties, and adhesiveness of Azospirillum brasilense - Variation during growth, *Canadian Journal of Microbiology*, *42*, 548-556.

Essendoubi, M., et al. (2007), Osmoadaptative responses in the rhizobia nodulating Acacia isolated from south-eastern Moroccan Sahara, *Environmental Microbiology*, *9*, 603-611.

Foppen, J. W. A., and J. F. Schijven (2006), Evaluation of data from the literature on the transport and survival of Escherichia coli and thermotolerant coliforms in aquifers under saturated conditions, *Water Research*, *40*, 401-426.

Gao, B., et al. (2006), Pore-scale mechanisms of colloid deposition and mobilization during steady and transient flow through unsaturated granular media, *Water Resources Research*, *42*.

Gao, B., et al. (2008), Capillary retention of colloids in unsaturated porous media, *Water Resources Research*, *44*.

Gargiulo, G., et al. (2007), Bacteria transport and deposition under unsaturated conditions: The role of the matrix grain size and the bacteria surface protein, *Journal of Contaminant Hydrology*, *92*, 255-273.

Gargiulo, G., et al. (2008), Bacteria transport and deposition under unsaturated flow conditions: The role of water content and bacteria surface hydrophobicity, *Vadose Zone Journal*, *7*, 406-419.

Garzio-Hadzick, A., et al. (2010), Survival of manure-borne E. coil in streambed sediment: Effects of temperature and sediment properties, *Water Research*, *44*, 2753-2762.

Gomoryova, E., et al. (2009), Effect of alginite amendment on microbial activity and soil water content in forest soils, *Biologia*, *64*, 585-588.

Grolimund, D., et al. (2001), Release and transport of colloidal particles in natural porous media 2. Experimental results and effects of ligands, *Water Resources Research*, *37*, 571-582.

Habteselassie, M., et al. (2008), Environmental Controls on the Fate of Escherichia coli in Soil, *Water Air and Soil Pollution*, *190*, 143-155.

Hahn, M. W., et al. (2004), Aquasols: On the role of secondary minima, *Environmental Science & Technology*, *38*, 5915-5924.

Halverson, L. J., et al. (2000), Release of intracellular solutes by four soil bacteria exposed to dilution stress, *Soil Science Society of America Journal*, *64*, 1630-1637.

Happel, J. (1958), Viscous flow in multiparticle systems - Slow motion of fluids relative to beds of spherical particles, *Aiche Journal*, *4*, 197-201.

Harshey, R. M. (2003), Bacterial motility on a surface: Many ways to a common goal, *Annual Review of Microbiology*, *57*, 249-273.

Hoek, E. M. V., and G. K. Agarwal (2006), Extended DLVO interactions between spherical particles and rough surfaces, *Journal of Colloid and Interface Science*, *298*, 50-58.

Hurst, C. J., et al. (1980), Effects of environmental variables and soil characteristics on virus survival in soil, *Applied and Environmental Microbiology*, *40*, 1067-1079.

Inglis, T. J. J., and J. L. Sagripanti (2006), Environmental factors that affect the survival and persistence of Burkholderia pseudomallei, *Applied and Environmental Microbiology*, *72*, 6865-6875.

Ishii, S., et al. (2010), Factors Controlling Long-Term Survival and Growth of Naturalized Escherichia coli Populations in Temperate Field Soils, *Microbes and Environments*, *25*, 8-14.

Jenkins, S. H., et al. (1973), *Effects of dissolved salts on the filtration of coliform bacteria in sand dunes*, Pergamon Press, New York.

Jin, Y. (2002), Virus retention and transport in porous media, paper presented at International Workshop on colloids and colloid-facilitated transport of contaminants in soils and sediments, Tjele, Denmark, 19-20 September 2002., Danmarks JordbrugsForskning.

Jin, Y., et al. (2000), Virus removal and transport in saturated and unsaturated sand columns, *Journal of Contaminant Hydrology*, *43*, 111-128.

John, D. E., and J. B. Rose (2005), Review of factors affecting microbial survival in groundwater, *Environmental Science & Technology*, *39*, 7345-7356.

Johnson, P. R., and M. Elimelech (1995), Dynamics of colloid deposition in porous-media - Blocking based on random sequential adsorption, *Langmuir*, *11*, 801-812.

Johnson, W. P., et al. (2007), Colloid retention in porous media: Mechanistic confirmation of wedging and retention in zones of flow stagnation, *Environmental Science & Technology*, *41*, 1279-1287.

Keller, A. A., and M. Auset (2007), A review of visualization techniques of biocolloid transport processes at the pore scale under saturated and unsaturated conditions, *Advances in Water Resources*, *30*, 1392-1407.

Kim, H. N., et al. (2009a), Escherichia coli O157:H7 Transport in Saturated Porous Media: Role of Solution Chemistry and Surface Macromolecules, *Environmental Science & Technology*, *43*, 4340-4347.

Kim, H. N., et al. (2009b), Surface Characteristics and Adhesion Behavior of Escherichia coli O157:H7: Role of Extracellular Macromolecules, *Biomacromolecules*, *10*, 2556-2564.

Kim, H. N., et al. (2010), Macromolecule mediated transport and retention of Escherichia coli O157:H7 in saturated porous media, *Water Research*, *44*, 1082-1093.

Kim, S. B., et al. (2008), Transport and retention of Escherichia coli in a mixture of quartz, Al-coated and Fe-coated sands, *Hydrological Processes*, *22*, 3856-3863.

Kolter, R., and E. P. Greenberg (2006), Microbial sciences - The superficial life of microbes, *Nature*, *441*, 300-302.

Kuznar, Z. A., and M. Elimelech (2005), Role of surface proteins in the deposition kinetics of Cryptosporidium parvum oocysts, *Langmuir*, *21*, 710-716.

Lang, N. L., et al. (2007), Field investigations on the survival of Escherichia coli and presence of other enteric micro-organisms in biosolids-amended agricultural soil, *Journal of Applied Microbiology*, *103*, 1868-1882.

Lenhart, J. J., and J. E. Saiers (2002), Transport of silica colloids through unsaturated porous media: Experimental results and model comparisons, *Environmental Science & Technology*, *36*, 769-777.

Lenhart, J. J., and J. E. Saiers (2003), Colloid mobilization in water-saturated porous media under transient chemical conditions, *Environmental Science & Technology*, *37*, 2780-2787.

Liu, C. X., and J. M. Zachara (2001), Uncertainties of monod kinetic parameters nonlinearly estimated from batch experiments, *Environmental Science & Technology*, *35*, 133-141.

Liu, Y., et al. (2010), Composition and Conformation of Cryptosporidium parvum Oocyst Wall Surface Macromolecules and Their Effect on Adhesion Kinetics of Oocysts on Quartz Surface, *Biomacromolecules*, *11*, 2109-2115.

Ma, H. L., and W. P. Johnson (2010), Colloid Retention in Porous Media of Various Porosities: Predictions by the Hemispheres-in-Cell Model, *Langmuir*, *26*, 1680-1687.

McClaine, J. W., and R. M. Ford (2002), Characterizing the adhesion of motile and nonmotile Escherichia coli to a glass surface using a parallel-plate flow chamber, *Biotechnology and Bioengineering*, *78*, 179-189.

McDowellboyer, L. M. (1992), Chemical mobilization of micron-sized particles in saturated porous-media under steady flow conditions, *Environmental Science & Technology*, *26*, 586-593.

McGown, D. N. L., and G. D. Parfitt (1967), Improved theoretical calculation of stability ratio for colloid systems, *Journal of Physical Chemistry*, *71*, 449-&.

Metge, D. W., et al. (2010), Influence of organic carbon loading, sediment associated metal oxide content and sediment grain size distributions upon Cryptosporidium parvum removal during riverbank filtration operations, Sonoma County, CA, *Water Research*, *44*, 1126-1137.

Mohamed, M., et al. (2007), Evaluation of Monod kinetic parameters in the subsurface using moment analysis: Theory and numerical testing, *Advances in Water Resources*, *30*, 2034-2050.

Molin, S., and V. Cvetkovic (2010), Microbial risk assessment in heterogeneous aquifers: 1. Pathogen transport, *Water Resources Research*, *46*, 16.

Monod, J. (1942), Recherches sur la croissance des cultures bactériennes., edited, Hermann, Paris.

Morales, V. L., et al. (2009), Grain Surface-Roughness Effects on Colloidal Retention in the Vadose Zone, *Vadose Zone Journal*, *8*, 11-20.

Morales, V. L., et al. (2010), Are prefrential flow paths perpetuated by microbial activity in the soil matrix? A review, *Journal of Hydrology*.

Mueller, R. F. (1996), Bacterial transport and colonization in low nutrient environments, *Water Research*, *30*, 2681-2690.

Nelson, K. E., and T. R. Ginn (2001), Theoretical investigation of bacterial chemotaxis in porous media, *Langmuir*, *17*, 5636-5645.

NocitoGobel, J., and J. E. Tobiason (1996), Effects of ionic strength on colloid deposition and release, *Colloids and Surfaces a-Physicochemical and Engineering Aspects*, *107*, 223-231.

Ohshima, H. (1995), Electrophoresis of soft particles, *Advances in Colloid and Interface Science*, *62*, 189-235.

Or, D., et al. (2007), Physical constraints affecting bacterial habitats and activity in unsaturated porous media - a review, *Advances in Water Resources*, *30*, 1505-1527.

Peng, X., et al. (2008), Evaluation of the Effect of Temperature on the Die-Off Rate for Cryptosporidium parvum Oocysts in Water, Soils, and Feces, *Applied and Environmental Microbiology*, *74*, 7101-7107.

Rajagopalan, R., and C. Tien (1976), Trajectory analysis of deep-bed filtration with sphere-in-cell porous-media model, *AIChE Journal*, *22*, 523-533.

Rehmann, L. L. C., et al. (1999), Stochastic analysis of virus transport in aquifers, *Water Resources Research*, *35*, 1987-2006.

Rijnaarts, H. H. M., et al. (1996), Bacterial deposition in porous media: Effects of cell-coating, substratum hydrophobicity, and electrolyte concentration, *Environmental Science & Technology*, *30*, 2877-2883.

Rijnaarts, H. H. M., et al. (1999), DLVO and steric contributions to bacterial deposition in media of different ionic strengths, *Colloids and Surfaces B: Biointerfaces*, *14*, 179-195.

Roy, S. B., and D. A. Dzombak (1996), Colloid release and transport processes in natural and model porous media, *Colloids and Surfaces a-Physicochemical and Engineering Aspects*, *107*, 245-262.

Ryan, J. N., and P. M. Gschwend (1994), Effects of ionic-strength and flow-rate on colloid release - Relating kinetics to intersurface potential-energy, *Journal of Colloid and Interface Science*, *164*, 21-34.

Saiers, J. E., et al. (2003), The role of moving air-water interfaces in colloid mobilization within the vadose zone, *Geophysical Research Letters*, *30*.

Saiers, J. E., and J. J. Lenhart (2003), Colloid mobilization and transport within unsaturated porous media under transient-flow conditions, *Water Resources Research*, *39*.

Salvucci, A. E., et al. (2009), The impact of biofilm-forming potential and tafi production on transport of environmental Salmonella through unsaturated porous media, *Biologia*, *64*, 460-464.

Sanin, S. L. (2003), Effect of starvation on resuscitation and the surface characteristics of bacteria, *Journal of Environmental Science and Health Part a-Toxic/Hazardous Substances & Environmental Engineering*, *38*, 1517-1528.

Sanin, S. L., et al. (2003), Effect of starvation on the adhesive properties of xenobiotic degrading bacteria, *Process Biochemistry*, *38*, 909-914.

Schijven, J. F., and S. M. Hassanizadeh (2000), Removal of viruses by soil passage: Overview of modeling, processes, and parameters, *Critical Reviews in Environmental Science and Technology*, *30*, 49-127.

Schneide.Wr, and R. N. Doetsch (1974), Effect of viscosity on bacterial motility, *Journal of Bacteriology*, *117*, 696-701.

Shellenberger, K., and B. E. Logan (2002), Effect of molecular scale roughness of glass beads on colloidal and bacterial deposition, *Environmental Science & Technology*, *36*, 184-189.

Shen, C. Y., et al. (2008), Effects of solution chemistry on straining of colloids in porous media under unfavorable conditions, *Water Resources Research*, *44*.

Shen, C. Y., et al. (2007), Kinetics of coupled primary- and secondary-minimum deposition of colloids under unfavorable chemical conditions, *Environmental Science & Technology*, *41*, 6976-6982.

Shiratori, K., et al. (2007), Deposition and subsequent release of Na-kaolinite particles by adjusting pH in the column packed with Toyoura sand, *Colloids and Surfaces a-Physicochemical and Engineering Aspects*, *306*, 137-141.

Sim, Y., and C. V. Chrysikopoulos (1996), One-dimensional virus transport in porous media with time-dependent inactivation rate coefficients, *Water Resources Research*, *32*, 2607-2611.

Sim, Y., and C. V. Chrysikopoulos (2000), Virus transport in unsaturated porous media, *Water Resources Research*, *36*, 173-179.

Simoni, S. F., et al. (1998), Population heterogeneity affects transport of bacteria through sand columns at low flow rates, *Environmental Science & Technology*, *32*, 2100-2105.

Singleton, P. W., et al. (1982), Effect of salinity on rhizobium growth and survival, *Applied and Environmental Microbiology*, *44*, 884-890.

Sirivithayapakorn, S., and A. Keller (2003), Transport of colloids in unsaturated porous media: A pore-scale observation of processes during the dissolution of air-water interface, *Water Resources Research*, *39*.

Song, I., et al. (2005), Effects of temperature and moisture on coliphage PRD-1 survival in soil, *Journal of Food Protection*, *68*, 2118-2122.

Stevik, T. K., et al. (2004), Retention and removal of pathogenic bacteria in wastewater percolating through porous media: a review, *Water Research*, *38*, 1355-1367.

Stimson, J., et al. (2010), Basic oxygen furnace slag as a treatment material for pathogens: Contribution of inactivation and attachment in virus attenuation, *Water Research*, *44*, 1150-1157.

Straub, T. M., et al. (1993), Virus survival in sewagesludge amended desert soil, *Water Sci. Technol.*, *27*, 421-424.

Tessier, G. (1942), Croissance des populations bactériennes et quantité d'aliment disponible., edited, pp. 80-209, Rev. Sci., Paris.

Thompson, S. S., and M. V. Yates (1999), Bacteriophage inactivation at the air-water-solid interface in dynamic batch systems, *Applied and Environmental Microbiology*, *65*, 1186-1190.

Toride, N., et al. (1995), The CXTFIT code for estimating transport parameters from laboratory or field tracer experiments, Version 2.0, in *Research Report No. 137*, edited, U.S. Salinity Laboratory, USDA, ARS, Riverside, CA.

Tosco, T., et al. (2009), Ionic Strength Dependent Transport of Microparticles in Saturated Porous Media: Modeling Mobilization and Immobilization Phenomena under Transient Chemical Conditions, *Environmental Science & Technology*, *43*, 4425-4431.

Tufenkji, N. (2007), Modeling microbial transport in porous media: Traditional approaches and recent developments, *Advances in Water Resources*, *30*, 1455-1469.

Tufenkji, N., and M. Elimelech (2004a), Correlation equation for predicting single-collector efficiency in physicochemical filtration in saturated porous media, *Environmental Science & Technology*, *38*, 529-536.

Tufenkji, N., and M. Elimelech (2004b), Deviation from the classical colloid filtration theory in the presence of repulsive DLVO interactions, *Langmuir*, *20*, 10818-10828.

van Houdt, R., and C. W. Michiels (2005), Role of bacterial cell surface structures in *Escherichia coli* biofilm formation, *Research in Microbiology*, *156*, 626-633.

van Oss, C. J., et al. (1987), MONOPOLAR SURFACES, *Advances in Colloid and Interface Science*, *28*, 35-64.

van Oss, C. J., et al. (1986), The role of van der Waals forces and hydrogen bonds in "hydrophobic interactions" between biopolymers and low energy surfaces, *Journal of Colloid and Interface Science*, *111*, 378-390.

Verwey, E. J. W., and J. T. G. Overbeek (1946), Long distance forces acting between colloidal particles, *Trans. Faraday Soc.*, *42*, B117-B123.

Vidovic, S., et al. (2007), Effect of soil composition, temperature, indigenous microflora, and environmental conditions on the survival of Escherichia coli O157 : H7, *Canadian Journal of Microbiology*, *53*, 822-829.

Walker, S. L., et al. (2004), Role of cell surface lipopolysaccharides in Escherichia coli K12 adhesion and transport, *Langmuir*, *20*, 7736-7746.

Walker, S. L., et al. (2005), Influence of growth phase on bacterial deposition: Interaction mechanisms in packed-bed column and radial stagnation point flow systems, *Environmental Science & Technology*, *39*, 6405-6411.

Wan, J. M., and T. K. Tokunaga (1997), Film straining of colloids in unsaturated porous media: Conceptual model and experimental testing, *Environmental Science & Technology*, *31*, 2413-2420.

Wan, J. M., and J. L. Wilson (1994), Colloid transport in unsaturated porous-media, *Water Resources Research*, *30*, 857-864.

Weiss, T. H., et al. (1995), Effect of bacterial cell shape on transport of bacterial in porous media, *Environmental Science and Technology*, *29*, 1737-1740.

Williamson, K. E., et al. (2005), Abundance and diversity of viruses in six Delaware soils, *Applied and Environmental Microbiology*, *71*, 3119-3125.

Winfield, M. D., and E. A. Groisman (2003), Role of nonhost environments in the lifestyles of Salmonella and Escherichia coli, *Applied and Environmental Microbiology*, *69*, 3687-3694.

Wood, N. J., and J. Sorensen (1998), Osmotic stimulation of microcolony development by Nitrosomonas europaea, *Fems Microbiology Ecology*, *27*, 175-183.

Xu, S. P., and J. E. Saiers (2009), Colloid straining within water-saturated porous media: effects of colloid size nonuniformity, *Water Resources Research*, *45*, W05501.

Yao, K. M., et al. (1971), Water and Wastewater Filtration: Concepts and Applications, *Environmental Science and Technology*, *5*, 1105-1112.

Zahran, H. H. (1997), Diversity, adaptation and activity of the bacterial flora in saline environments, *Biology and Fertility of Soils*, *25*, 211-223.

Zevi, Y., et al. (2009), Transport and retention of colloidal particles in partially saturated porous media: Effect of ionic strength, *Water Resources Research*, *45*, 10.

Zhang, W., et al. (2010), Colloid Transport and Retention in Unsaturated Porous Media: Effect of Colloid Input Concentration, *Environmental Science & Technology*, *44*, 4965-4972.

Zhao, B. Z., et al. (2008), Virus adsorption and inactivation in soil as influenced by autochthonous microorganisms and water content, *Soil Biology & Biochemistry*, *40*, 649-659.

Zhuang, J., et al. (2007), In situ colloid mobilization in hanford sediments under unsaturated transient flow conditions: Effect of irrigation pattern, *Environmental Science & Technology*, *41*, 3199-3204.

Zhuang, J., et al. (2009), Colloid transport and remobilization in porous media during infiltration and drainage, *Journal of Hydrology*, *377*, 112-119.

CHAPTER 2

IMPACT OF DISSOLVED ORGANIC MATTER ON COLLOID TRANSPORT IN THE VADOSE ZONE: DETERMINISTIC APPROXIMATION OF TRANSPORT DEPOSITION COEFFICIENTS FROM POLYMERIC COATING CHARACTERISTICS[1]

Abstract

Although numerous studies have been conducted to discern colloid transport and stability processes, the mechanistic understanding of how dissolved organic matter (DOM) affects colloid fate in unsaturated soils (i.e., the vadose zone) remains unclear. This study aims to bridge the gap between the physicochemical responses of colloid complexes and porous media interfaces to solution chemistry, and the effect these changes have on colloid transport and fate. Measurements of adsorbed layer thickness, density, and charge of DOM-colloid complexes and transport experiments with tandem internal visualization were conducted for key constituents of DOM, humic (HA) and fulvic acids (FA), at acidic, neutral and basic pH and two $CaCl_2$ concentrations. Polymeric characteristics reveal that of the two tested DOM constituents only HA electro*sterically* stabilizes colloids. This stabilization is highly dependent on solution pH which controls DOM polymer adsorption affinity, and on the presence of Ca^{+2} which promotes charge neutralization and inter-particle bridging. Transport experiments indicate that HA improved colloid transport significantly, while FA only marginally affected transport despite having a large effect on particle charge. A transport model with deposition and pore-exclusion parameters fit experimental

[1] This paper was published as Morales, V.L., et al. (2010), Impact of dissolved organic matter on colloid transport in the vadose zone: Deterministic approximation of transport coefficients from polymeric coating characteristics, *Water Research,* DOI:10.1016/j.watres.2010.10.030 (In print).

breakthrough curves well. Trends in deposition coefficients are correlated to the changes in colloid surface potential for bare colloids, but must include adsorbed layer thickness and density for sterically stabilized colloids. Additionally, internal process observations with bright field microscopy reveal that, under optimal conditions for retention, experiments with FA or no DOM promoted colloid retention at solid-water interfaces, while experiments with HA enhanced colloid retention at air-water interfaces, presumably due to partitioning of HA at the air-water interface and/or increased hydrophobic characteristics of HA-colloid complexes.

Introduction

Dissolved organic matter (DOM) plays a prominent role in many soil processes and is ubiquitous in soils; high concentrations are found in manure or wastewater sludge amended lands. Humic acid (HA) and fulvic acid (FA) are principal constituents of soil, aquatic, sewage sludge, and manure DOM [*Schnitzer*, 1972; *Thurman*, 1985]. The structural properties of the moieties that make up DOM in soil environments have been explored by several investigators; reporting (as general consensus) that DOM molecules behave as flexible entities that can swell and shrink in response to changes in pH and ionic strength [*Avena, et al.*, 1999; *Benedetti, et al.*, 1996; *Duval, et al.*, 2005; *Hosse and Wilkinson*, 2001]. The amphiphilic character (i.e., presence of hydrophobic and hydrophilic moieties) of DOM has been reported by a number of studies [*Guetzloff*, 1994; *Lenhart and Saiers*, 2004; *Ma, et al.*, 2007; *von Wandruszka*, 2000] and used to explain its high surface reactivity and adsorptive fractionation to solid-water and air-water interfaces [*Chi and Amy*, 2004; *Lenhart and Saiers*, 2004; *Ma, et al.*, 2007]. Greater affinity of larger, more hydrophobic DOM components for mineral surfaces and air-water interfaces is of primary importance for contaminant flux through the vadose zone [*Lenhart and Saiers*, 2004; *Meier, et al.*,

1999], as this unsaturated soil region is the critical connection that buffers deep groundwater from surface and shallow contaminants.

Physicochemical interactions between DOM and contaminants have received considerable attention in recent years. Numerous investigations have demonstrated that even small amounts of DOM greatly increase the mobility of colloid-associated contaminants (e.g., radionuclide plutonium, americium, thorium, and radium; phosphorus; hydrophobic organic compounds; uranium(IV)/(VI); carbon nanotubes; and lead) [*Flury and Qiu*, 2008; *Granger, et al.*, 2007; *Jaisi, et al.*, 2008; *Marley, et al.*, 1993; *Mibus, et al.*, 2007; *Sen and Khilar*, 2006; *Tang and Weisbrod*, 2009] and colloid-sized pathogens (e.g., *E. coli*, *Cryptosporidium parvum* oocysts, *Giardia*, and bacteriophage PRD1) [*Abudalo, et al.*, 2005; *Abudalo, et al.*, 2010; *Bradford, et al.*, 2006; *Foppen, et al.*, 2008] through hydrologic pathways. Laboratory batch kinetic and isotherm experiments have also been conducted to explore the interactions between DOM and colloidal particles. Results from these experiments indicate that DOM increases the stability of colloid and nanoparticle suspensions in the presence of electrolytes through electrostatic and/or steric stabilization by way of adsorption onto colloid surfaces [*Akbour, et al.*, 2002; *Chen and Elimelech*, 2007; *Heidmann, et al.*, 2005; *Kretzschmar, et al.*, 1998; *Pefferkorn*, 2006]. Moreover, complexation of surface functional groups with non-indifferent ions in solution is a widely recognized process [*Amirbahman and Olson*, 1995; *Chen and Elimelech*, 2007; *Chen, et al.*, 2006] that could significantly affect the stability and therefore the transport of colloids suspended in DOM rich solutions.

A number of investigations systematically examined the impact of DOM on colloid mobility in saturated porous media in terms of pore water velocity and deposition kinetics [*Akbour, et al.*, 2002; *Jaisi, et al.*, 2008; *Kretzschmar, et al.*, 1997]. The effects of mono- vs. divalent cation concentrations [*Jaisi, et al.*, 2008], and ionic

strength on attachment efficiency have been evaluated [*Franchi and O'Melia*, 2003; *Kretzschmar and Sticher*, 1997], as well as charge reversal by organic matter adsorption [*Kretzschmar and Sticher*, 1997]. Both natural and well characterized porous media have been used in research spanning acidic and neutral pore water pH ranges [*Akbour, et al.*, 2002; *Franchi and O'Melia*, 2003; *Jaisi, et al.*, 2008; *Kretzschmar, et al.*, 1997; *Kretzschmar and Sticher*, 1997]. However, only limited studies have explored the effect of DOM and pH on colloid transport in unsaturated porous media [*Tang and Weisbrod*, 2009] and the effect of colloid transport in alkaline DOM rich conditions [*Harvey, et al.*, 2010]. This range of solution chemistry is of high relevance for soils amended with lime-treated manure as a commonly used pathogen inactivation treatment. Two general consensuses about the presence of air phases are that interfaces with air in unsaturated porous media promote colloid retention, and that organic matter of hydrophobic character preferentially fractionates to the air-water interface. Thus, it is of critical importance to understand the effect that DOM has on colloid transport in unsaturated soils; particularly if adsorbed amphiphilic DOM may provide hydrophobic characteristics to the interfaces and colloid surfaces it adsorbs onto.

This study aims to experimentally bridge the gap between the physicochemical changes of DOM-colloid complexes and porous media interfaces and the effect that these systematic changes have on the transport of colloids in unsaturated soils. These objectives will be achieved by: (i) directly measuring the changes in surface charge, adsorbed layer thickness and density of organic matter–colloid complexes under acidic, neutral, and basic solution pH in the presence and absence of $CaCl_2$, (ii) assessing with column experiments the effects that HA and FA have on colloid transport at the solution chemistries listed above, (iii) simultaneous internal observation of the dominant pore scale retention sites for each set of conditions, and

(iv) mathematical modeling of the transport behavior of organic matter-colloid complexes to relate deposition coefficients with changes in solution composition.

Materials and Methods

Preparation of Materials: In order to meet the objective of discerning the specific steric characteristics that increase the stability of organic matter-colloid complexes (e.g., thickness of adsorbed organic matter layer and uniform adsorption of DOM onto colloid surfaces), the use of uniform and spherical colloids was essential. As such, calibration grade polystyrene and carboxylated spheres of 24 nm diameter (Bangs Laboratories Inc.; Fishers, IN) were used to measure the adsorbed layer thickness. These spheres were selected because of their exceptional size uniformity that allowed the measurement of changes in size at the nanometer scale. Similar surfactant-free, red-dyed, polystyrene and carboxylated spheres of 2.6 μm diameter (Magsphere, Pasadena, CA) were used for all other measurements. The larger red colloids were chosen because they permitted excellent visualization of individual colloids against the porous medium with Bright Field Microscopy (BFM).

Elliott Soil HA and FA standards purchased from the International Humic Substances Society were used for this study. The individual DOM solutions were prepared by dissolving 200 mg L^{-1} of HA and FA in deionized water, and adjusting the stock solution pH to 7 with NaOH. HA and FA stock solutions were further diluted to create solutions of 20 mg of total dissolved organic carbon L^{-1}, as measured by persulfate oxidation with an O-I-Analytical Total Organic Carbon Analyzer model 1010 (College Station, TX). Deionized water (DI) was used as the control for no DOM. Solution pH was adjusted to pre-established experimental values (e.g., 4, 6 and 9) with NaOH and HCl immediately prior to starting the experiments. For simplification, the changes in ionic strength (IS) by addition of acid and base to adjust

for pH are considered small (e.g., IS of 10^{-2} mM for pH 9 and IS of 10^{-1} mM for pH 4) relative to the change from addition of $CaCl_2$, so the solution's IS is referred to as 0 mM and 1 mM for solutions in the absence and presence of $CaCl_2$, respectively. Batch measurements of surface tension of DOM solutions were significantly similar, with a mean surface tension for all tested solution chemistries of 71.7±0.11 mN m^{-1}.

Translucent quartz sand (Unimin Corp., Vineland, NJ) of 0.4-0.59 mm diameter was used for the porous medium. Before use, the sand was washed according to the procedure in Morales et al. [2009] in order to remove soluble organic compounds from the surface, dissolved metal oxide coatings, and obtain a constant baseline for optical density measurements during breakthrough measurements.

Adsorbed Layer Characteristics: The amount of HA and FA adsorbed onto the sand, Γ_s (M M^{-1}), and colloid surfaces, Γ_c (M L^{-2}), was measured by solution depletion for each solution composition. Briefly, for Γ_s, the column was wet packed with 60 g of quartz sand, and 60 mL of solution were recycled through the cell with a peristaltic pump for 24 hours at a rate of 0.32 mL min^{-1}. Afterward, the equilibrium concentration of the solution was measured by spectrophotometry (λ = 350 nm) and the difference between the initial and the equilibrium DOM concentration was used to determine the mass of adsorbed organic matter mass per gram of sand medium. For Γ_c, two sets of 20 mL of each solution composition were prepared and $1x10^8$ colloids were added to the first. The suspensions and colloid-free solutions were agitated for 24 hrs, then centrifuged for 2 hrs at 8000 rpm to settle HA-colloid complexes. This centrifugation step was verified to not significantly alter the concentration of non-adsorbed HA and FA components. The supernatant equilibrium concentration was measured by spectrophotometry, and the difference between the colloid-free and the colloid equilibrated concentration was used to determine the mass of adsorbed organic matter per m^2 of colloid surface.

The thickness of the organic matter layer adsorbed onto the spherical colloidal particles, *d* (L), was directly measured (rather than fit with existing soft particle theory that is valid only for systems with symmetric and indifferent electrolytes) as the difference between the hydrodynamic radius (R_H) of particles exposed to the DOM solution and that of bare particles (i.e., suspended in DI), holding pH and ionic strength constant. For the measurement of this parameter exclusively, 24 nm microspheres were used as the core particles suspended in 18 different solution compositions of varying DOM type (DI, FA, and HA), at three different pHs (4, 6, and 9), and two different ionic strengths (0 and 1 mM). This down scaling of particle size was necessary to measure significant differences in R_H at the nanometer scale for colloids with and without a brush layer of adsorbed organic matter. The R_H of the colloids was determined by dynamic light scattering (DLS) at each characteristic solution composition using a BIC 200 SM DLS (Long Island, NY).

The density of adsorbed DOM layer, Φ, was estimated with equation 2.1 for colloids of radius *a* (L), using the DOM density value (ρ_{DOM}) of 1.45×10^{-18} mg nm^{-3} reported by Relan et al. [1984].

$$\Phi = \frac{3\Gamma_c a^2}{\rho_{DOM}[(d+a)^3 - a^3]} \qquad [2.1]$$

Electrophoretic Mobility: Electrophoretic measurements (EM) measurements were collected with a Malvern Zetasizer nano (Worcestershire, UK) for colloid suspensions in each solution composition. Eight measurements were collected for each treatment and the mean EM values were used to calculate the zeta (ζ) -potential of the particles via Smoluchowski's formula (using a measured viscosity value at 25^{o}C of $0.91 \times 10^{-4} \pm 0.01 \times 10^{-4}$ Pa·s and the dielectric constant of the water medium of 78.54).

Zeta potentials were converted to surface potential, ψ_o, in mV according to van Oss [2003]:

$$\psi_o = \zeta\left(1+\frac{z}{a}\right)\exp(\kappa z) \qquad [2.2]$$

where z is the distance from the particle's surface to the slipping plane (here taken to be 0.5 nm), and $1/\kappa$ is the is the thickness of the diffuse double layer.

Column Setup: The column apparatus consisted of a transparent vertical acrylic flow cell (inside dimensions: 10-cm length, 2-cm width, 2-cm depth) with inlet and outlet tubing connected to a two-chamber micropurge peristaltic pump (Masterflex, Barnat, Barrington, IL) to induce perfectly matched steady-state flow. The column apparatus is the same as that used by Morales et al. [2009] and is built with a thin acrylic front side (1.5-mm thickness) to allow tandem collection of visual data of internal processes during column breakthrough experiments.

Colloid transport data were collected in duplicate from 18 column experiments consisting of three background combinations of DOM (DI, 20 mg L^{-1} FA, and 20 mg L^{-1} HA) at three solution pHs (4, 6, 9) and two background ionic strengths. The column was wet packed with clean sand using gentle vibration to ensure uniform packing (porosity of 0.41). Then, the saturated column was conditioned by circulating colloid-free DOM background solution through the column for 24 hrs to allow the sand medium to equilibrate with adsorbable DOM prior to injection of the colloid pulse. Subsequently, the column was allowed to become unsaturated by increasing the outflow rate above the inflow rate until a volumetric moisture content, θ, of 0.24±0.03 (equivalent to 0.61±0.08 water saturation) was attained (measured gravimetrically). Upon reaching the target moisture content, the outflow and inflow rates were restored to identical and uninterrupted rates of 0.30 mL min^{-1} to ensure steady state flow.

The colloid suspension was prepared in a solution of the same composition as that of the background. It is important to note that the optical density of dissolved HA and FA was accounted for when establishing the standard curves for colloid concentration measurements with spectrophotometry. To inject a 10 mL colloid pulse the column influent was switched to the colloid suspension, after which the inflow was switched back to the colloid-free background solution to flush un-retained colloids out of the medium. The BTCs were constructed from effluent colloid concentrations assayed by spectrophotometry (λ = 350 nm) with a linear correlation for absorbance and colloid concentration over the concentration range tested. For mass balance comparisons, the fraction of colloids recovered (MR) from the pulse of injected colloids was calculated as:

$$MR = \frac{\Sigma J \Delta t_i \left(C_i + C_{i+1}\right)}{2 t_c J C_o} \qquad [2.3]$$

where J is the steady state flux ($L^3\ T^{-1}$), Δt_i is the time difference between collected effluent samples (T), C_i is the aqueous colloid concentration of the ith effluent sample ($M\ L^{-3}$), t_c is the duration of the colloid or tracer pulse (T), and C_o is the initial concentration of the injected pulse ($M\ L^{-3}$). In addition, colloid BTCs were compared to an independently run non-sorbing bromide tracer (Br^-), analyzed with a Dionex Ion Chromatography System-2000 (Sunnyvale, California) to determine the pore-water velocity, v ($L\ T^{-1}$) and dispersion coefficient, D ($L^2\ T^{-1}$).

Transport Model: An deterministic model including terms for first-order attachment kinetics and colloid-excluded volume (i.e., colloid accessible pore space responsible for early elution of colloids with respect to the conservative tracer) in homogeneous soil was utilized to determine each solution composition's effect on colloid deposition and pore-exclusion with the following governing equation:

$$\frac{\partial(\theta_c C)}{\partial t} = \frac{\partial}{\partial x}\left(\theta_c D \frac{\partial C}{\partial x} - JC\right) - \theta_c k_d C \qquad [2.4]$$

where k_d is the colloid deposition coefficient (T^{-1}), θ_c is the colloid accessible volumetric moisture content ($L^3\ L^{-3}$) (obtained from the product of E and θ), E is the pore-exclusion factor (unitless), C is the concentration of the colloids ($M\ L^{-3}$), x is the distance (L), and J is the specific water flux ($L^3\ T^{-1}$). The authors acknowledge the complexities of the system and the need to construct a more detailed model to discern the contribution from specific retention mechanisms involved in DOM-colloid complexes transported through unsaturated porous media. Nonetheless, the k_d term accounts for the loss of particles as the sum of all participating sinks, acceptably captures the BTC shape, and allows relationships to be interpreted between deposition of sterically stabilized colloid complexes and polymer characteristics (as discussed in the section titled *Mathematical Model*).

Internal Process Visualization: A horizontally mounted bright field microscope was used to visualize colloid transport in-situ from a lateral view of the vertical cell in a fashion similar to that used by Morales et al. [2009]. Briefly, observation of colloid transport and retention at the pore scale was achieved by selecting random pores at heights of 9 and 5 cm from the bottom of the column, and capturing still images at 250× magnification (resolution 0.8 μm $pixel^{-1}$). Wherever the pores remained in clear view for the duration of the experiment video recordings were also collected to observe the progressive retention of colloids.

Results

Adsorbed Layer Characteristics: A summary of the adsorbed layer characteristics determined by solution depletion, DLS, and EM is listed in Table 2.1 for all the conditions tested in this study. Data on the amount of DOM adsorbed onto

surfaces, Γ_s and Γ_c, suggest that HA has a superior affinity for solid surface sorption than FA because of its higher molecular weight, which is consistent with the literature [*Ko, et al.*, 2005]. The amount of HA adsorbed onto colloid surfaces was greatest at pH of 4 and decreased with increasing pH (see Γ_c values in Table 2.1), which is in agreement with previous reports [*Jada, et al.*, 2006; *Lenhart and Saiers*, 2004]. Moreover, the presence of $CaCl_2$ drastically increased Γ_c and Γ_s from 25 to 107%; particularly for adsorption of FA, which was undetectable in the absence of $CaCl_2$. The adsorption of organic matter onto sand generally followed the same trend as that for colloids (see Γ_s values in Table 2.1), with variations here attributed to the heterogeneity of the medium.

Table 2.1 Characteristics of adsorbed organic layer and transport parameters. Data is organized by pH, dissolved organic matter type (DOM), and ionic strength (IS). Characteristics and parameters include: mass of adsorbed DOM onto colloid (Γ_c) and sand (Γ_s) surfaces, thickness (d) and density of adsorbed layer (Φ), colloid electrophoretic mobility (EM) and surface potential (ψ_o), fraction of colloids recovered (MR), pore-exclusion factor (E), and deposition rate (k_d).

	DOM / IS	Γ_c	Γ_s	d	Φ	EM	ψ_o	MR	E	k_d
	(- /mM)	(mg m^{-2})	(mg g^{-1})	(nm)	(-)	(μm cm Vs^{-1})	(mV)	(-)	(cm^3 cm^{-3})	(hr^{-1})
pH 4	HA / 0	34.6±0.7	0.0024	32.0	0.73	-3.43±0.20	-43.9	60.7 ± 0.35	0.87	0.26
	HA / 1	43.3±0.2	0.0031	24.7	1.2	-1.60±0.24	-20.3	41.4 ± 0.29	0.79	0.43
	FA / 0	0.0	0.0	0.0	0.0	-2.04±0.43	-26.0	45.7 ± 1.8	0.91	0.40
	FA / 1	31.4±0.4	0.0031	0.0	0.0	-1.49±0.19	-19.0	5.20 ± 1.3	0.86	1.5
	DI / 0	0.0	0.0	0.0	0.0	-0.229±0.083	-2.92	20.2 ± 2.8	0.71	0.77
	DI / 1	0.0	0.0	0.0	0.0	0.273±0.080	3.48	3.00 ± 1.1	0.84	1.8
pH 6	HA /0	27.2±1	0.0008	52.8	0.34	-3.58±0.11	-45.7	85.7 ± 0.34	0.84	0.11
	HA / 1	38.4±1	0.0006	55.1	0.46	-1.62±0.14	-20.7	24.9 ± 1.3	0.71	0.70
	FA / 0	0.0	0.0	2.90	0.0	-3.33±0.14	-42.5	71.1 ± 3.1	0.82	0.19
	FA / 1	13.0±2	0.0004	2.90	2.5	-1.57±0.065	-20.0	5.00 ± 0.28	0.77	1.5
	DI / 0	0.0	0.0	0.0	0.0	-1.66±0.076	-21.2	75.6 ± 1.3	0.81	0.15
	DI / 1	0.0	0.0	0.0	0.0	-0.427±0.013	-5.59	2.60 ± 2.0	0.90	1.9
pH 9	HA / 0	16.0±0.2	0.0022	1.50	7.2	-3.95±0.19	-50.5	48.1 ± 3.2	0.82	0.40
	HA / 1	33.1±0.5	0.0025	11.9	1.9	-1.78±0.16	-22.7	20.6 ± 2.1	0.79	0.77
	FA / 0	0.0	0.0	0.0	0.0	-2.47±0.66	-31.5	70.2 ± 1.8	0.82	0.22
	FA / 1	35.7±1	0.004	0.0	0.0	-1.73±0.029	-22.1	4.50 ± 1.1	0.88	1.6
	DI / 0	0.0	0.0	0.0	0.0	-3.03±0.031	-38.8	78.9 ± 4.2	0.85	0.14
	DI / 1	0.0	0.0	0.0	0.0	-0.856±0.054	-11.0	4.00 ± 1.0	1.00	1.6

The DLS data indicate that a 'stabilizing shell' [*Fritz, et al.*, 2002] is developed on the colloids when they are exposed to HA. The adsorbed layer thickness, *d*, for HA-coated colloids *d* was intermediate at pH 4 (32.0-24.7 nm), greatest at pH 6 (52.8-55.1 nm), and lowest at pH 9 (1.5-11.9 nm); while *d* for FA-coated colloids was undetectable for all conditions except for pH 6 (see Table 2.1). Because the diffusivity of the colloids increased greatly with the addition of salts for suspensions of FA and DI, *d* could not be quantified accurately in the presence of $CaCl_2$. Consequently, already small *d* values for these samples ($0 < d < 2.9$ nm) were assumed to not be affected significantly by electrolyte addition and are reported as the same value as those measured at IS of 0 mM. Generally, *d* increased with IS for experiments with equal pH levels; particularly for HA suspensions. Moreover, the thickness of *d* for HA at pH 4 when IS is 0 mM (32.0 nm) and at pH 9 when IS is 1 mM (11.9 nm) were almost three fold different even though the mass of adsorbed HA is nearly the same (34.6 ± 0.7 mg m^{-2} and 33.1 ± 0.5 mg m^{-2}, respectively in Table 2.1). These results suggest that the HA adsorption conformation for pH 9 is in extended and tight multilayers, while that at pH 4 is in loose folds. Likewise, the *d* for HA at pH 6 for both IS levels (52.8 nm and 55.1 nm for IS at 0mM and 1mM, respectively) was very similar although the mass adsorbed experienced a 40% increase in the presence of $CaCl_2$ ($\Gamma_c = 27.2$ mg m^{-2} and $\Gamma_c = 38.4$ mg m^{-2} for IS at 0 mM and 1 mM, respectively) (see Table 2.1). This result indicates that the conformation of HA strands becomes more compact and therefore the adsorbed layer more dense with increasing IS.

Consistently, the density of adsorbed DOM layer, Φ, increased with IS, but also varied with pH such that the lightest layers formed in HA solutions at pH 6 (Φ = 0.34-0.46) and the most dense layers formed in HA at pH 9 (Φ = 1.9-7.2) (see Table 2.1). Because Φ is an encompassing parameter that accounts for the presence of a

steric layer on the surface of colloids, only those colloid complexes with Φ values greater than 0 were classified as being sterically stabilized.

It is important to note that Φ physically represents the normalized density of the adsorbed DOM layer with respect to the density of the dry DOM polymer. Although the boundary limits of Φ should in theory fall between 0 and 1, the measured density range of the DOM-colloid complexes was between 0 and 7.2. The authors suspect that calculated polymeric shell densities greater than 1 were an artifact of uneven coverage of the adsorbed polymer on the colloid surface due to low adsorption affinity, particularly for treatments with HA at pH 9 and the single treatment with FA at pH 6 that indicated presence of a polymeric shell.

Measurements of the particle charge are listed as raw electrophoretic mobility, EM, values along with their corresponding surface potential, ψ_o, value in Table 2.1. In general, our data indicate that for the conditions tested, colloids suspended in HA solutions have the most negative ψ_o, followed by those suspended in FA, and lastly by the bare suspensions in DI. As expected, addition of $CaCl_2$ screened the charge for all treatments, reflected in less negative EM and ψ_o values at higher IS treatments.

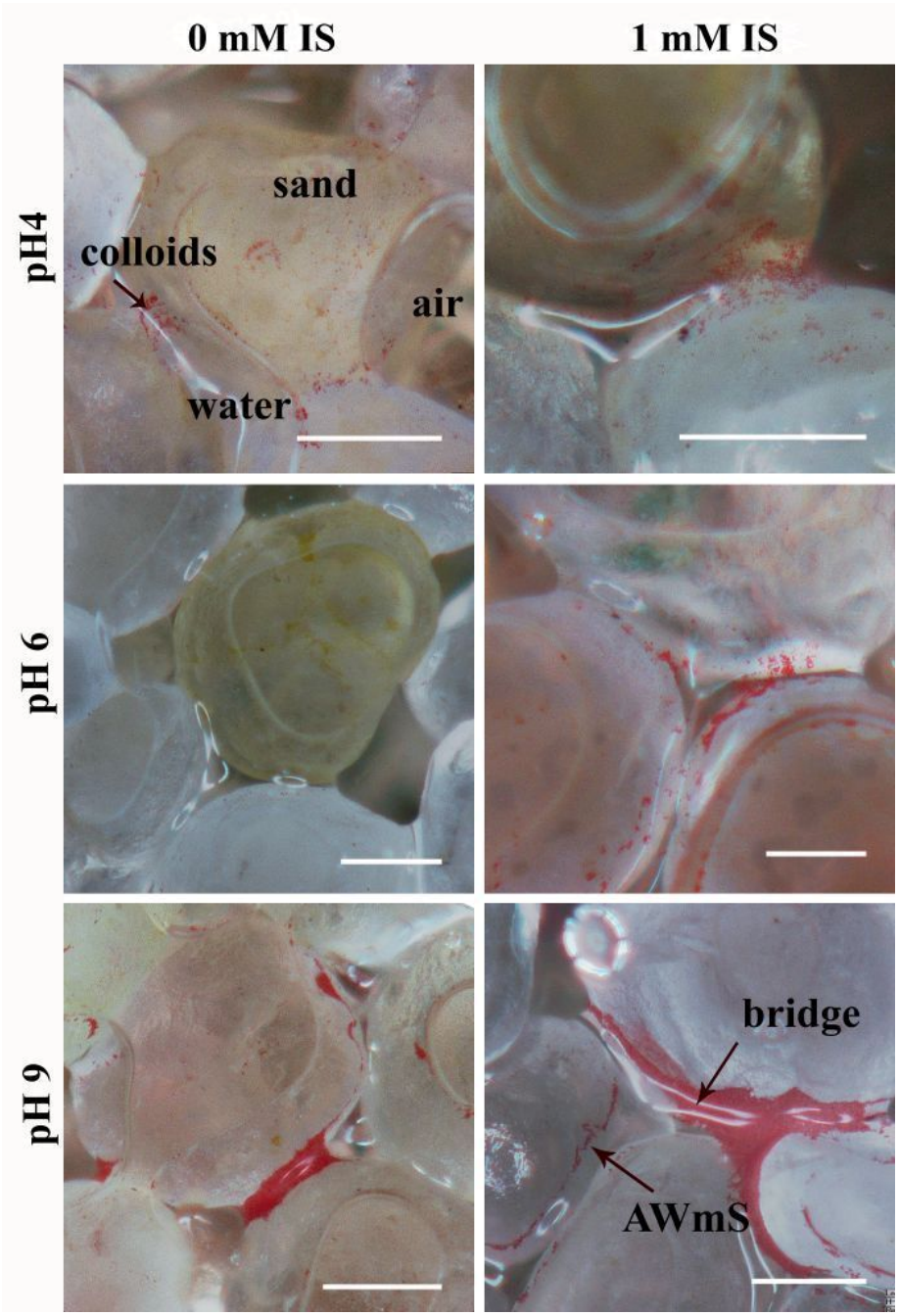

Figure 2.1 Colloid retention in bridge flocs when suspended in solutions of dissolved Humic Acid at different ionic strengths (IS) and pH levels. Left column 0 mM IS, right column 1 mM IS by $CaCl_2$ addition. Top row pH 4, middle row pH 6, bottom row pH 9. Scale bar length is 250 µm.

Colloid Retention Sites: Four distinct colloid retention sites were identified by visual observation during the column experiments (Figure A.1): (a) straining at grain-grain contact regions, (b) attachment to the solid-water interface (SWI), (c) straining at the air-water meniscus-solid interface (AWmSI), and (d) the accumulation/attachment of a continuous layer of enmeshed colloids along the air-water interface (AWI) (i.e., bridge flocculation at the AWI). Here, the distinction between straining and attachment processes is based on the definitions provided by Bradford and Torkzaban [2008]. Although the occurrence of colloid retention at the AWmSI was frequently observed in many of the treatments, it appeared to be unrelated to any particular set of solution conditions; especially to the type of DOM in solution. Retention at the SWI and grain-grain straining (i.e., multiple SWIs) (Figure A.1 a and b) were most common for experiments when the solution chemistry created optimal conditions for retention (i.e., higher ionic strength and/or low pH) in experiments with DI and FA. In contrast, retention at the AWI by bridge flocculation (Figure A.1 d) under similar conditions was the dominant retention site for experiments containing HA as is evident in Video 1 (http://soilandwater.bee.cornell.edu/colloids.html) at solution pH of 4 and IS of 1mM. Here, red colloids exhibit ripening-like behavior (defined as an increasing rate of colloid attachment with time due to colloid-colloid interactions on the collector surface [*Bradford and Torkzaban*, 2008]) at the AWI and become immobilized at close proximity to other previously retained colloids. It is evident that retained colloids are enmeshed in organic matter partitioned at the AWI, adsorbed on the surface of individual colloids, or both, given that the colloids in the aggregates are not in direct contact with each other but move as a floc unit with the pulsing flow. This behavior was consistently observed for experiments in HA, with denser flocs formed as pH and ionic strength levels increased (Figure 2.1).

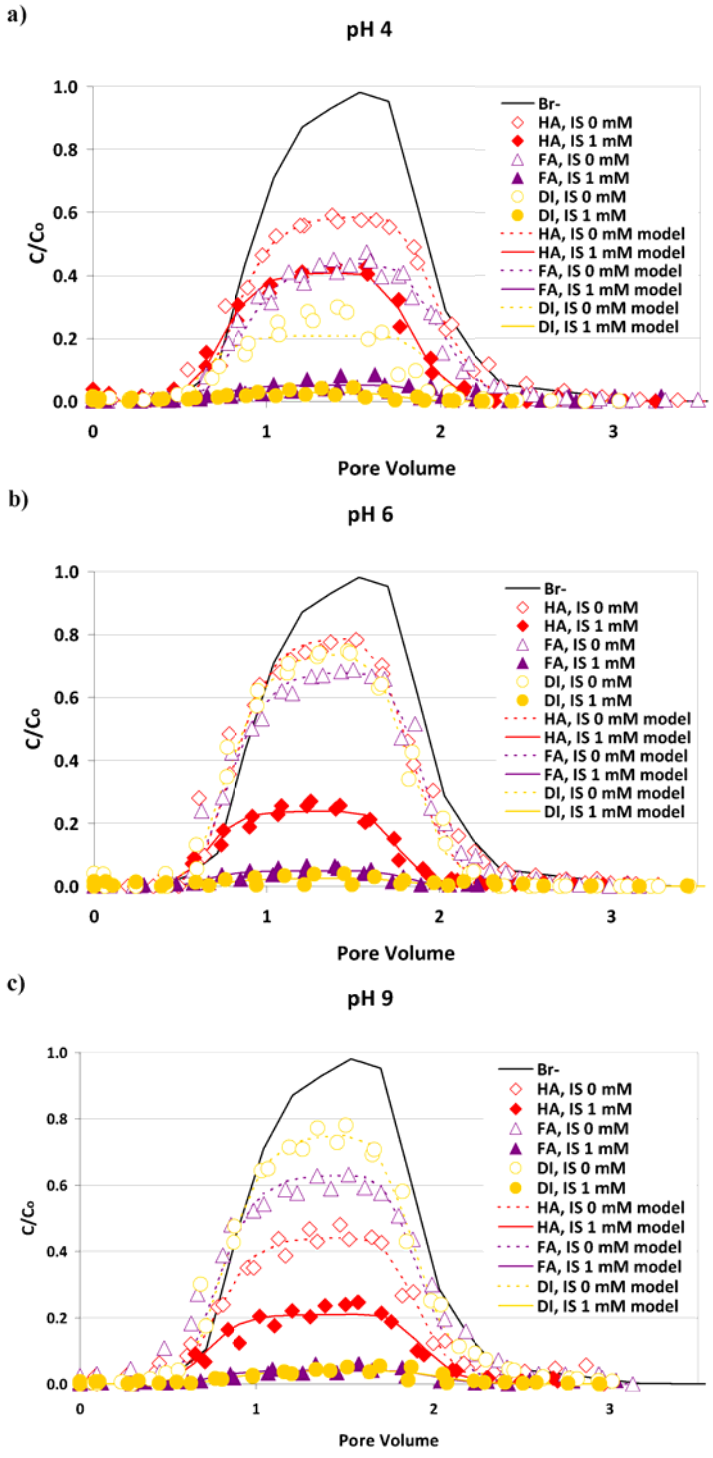

Figure 2.2 Breakthrough curves of column experiments and respective model fits for solutions containing dissolved HA, FA, and DI under ionic strength levels of 0 mM and 1 mM at: a) pH 4, b) pH 6, and c) pH 9.

Colloid Transport in Unsaturated Sand: The various solution treatments used to conduct the column studies are presented here and compared in terms of DOM type, changes in solution pH, and differences in $CaCl_2$ concentration.

The type of DOM in the solution of the column studies significantly affected the amount of colloids retained in the unsaturated quartz sand medium, as is evident in the HA (diamonds) vs. FA (triangles) vs. DI (circles) breakthrough curves in Figure 2.2a-c. In all but one solution (pH 9 and IS of 0 mM), experiments with HA displayed significantly greater elution (i.e., colloid mass recovery) (see MR values in Table 2.1) from the column than those treated with FA or DI with equal pH and ionic strength conditions. Figures 2.2a-c illustrate that experiments with FA behaved very similar to those treated with DI in all but one case (pH 4 and IS of 0 mM, open triangles in Figure 2.2a), in which colloid mobility was enhanced, although not as much in the presence of HA.

The transport of colloids in the sandy medium was considerably different at solution pH values of 4, 6 and 9 (compare like symbols from Figures 2.2a-c). For treatments of both DI and FA at lower IS, colloid transport varied directly with pH as the MR of colloids increased from 46-20% at pH 4, 71-76% at pH 6, and 70-79% at pH 9 (MR values for DI and FA in Table 2.1). For experiments where IS was raised to 1 mM, changes in colloid elution with solution pH for DI and FA treatments were insignificant, as the fraction of colloids recovered was low (solid circular and triangular symbols in Figures 2.2a-c), with MR values ranging from 3 to 5% (see Table 2.1). Conversely, experiments with HA exhibited distinct and significant changes in colloid mobility for the three pH values tested. For HA experiments conducted at lower IS, MR was 61% at pH 4, reached a maximum at pH 6 (86%), and experienced greatest retention at pH 9 (48%) (see Table 2.1). When the solution IS was raised to 1 mM, increases in pH resulted in a decrease in MR from 41 to 25 to

21% for pH changes from 4 to 6 to 9, respectively. The reduced mobility of HA-colloid complexes at high pH can be explained by the lack of steric hindrance evident in the thinnest adsorbed layer (smallest *d* values) and most densely packed adsorbed organic matter (largest Φ values from Table 2.1).

Increases in ionic strength through addition of $CaCl_2$ to the column study solution produced the expected reduction in colloid breakthrough (open vs. solid symbols in Figures 2.2a-c). For example, the MR of DI at lower IS ranged from 20 to 79%, but was reduced to less than 4% in the presence of $CaCl_2$ at IS of 1 mM (see MR values of DI in Table 2.1). The effect of $CaCl_2$ addition was similar in magnitude for experiments with FA, where the MR at lower IS ranged from 46 to 71%, and was reduced to less than 5% in the presence of $CaCl_2$ at IS of 1 mM (see MR values for FA in Table 2.1). While the addition of $CaCl_2$ to the system drastically reduced the mobility of colloids through the porous medium for all DOM types, the presence of dissolved HA resisted the destabilizing effect of $CaCl_2$, and permitted colloids to be eluted from the column in otherwise optimal conditions for retention. The addition of HA increased the amount of recovered colloids 5-13 fold over that observed in the same conditions but without the DOM addition (i.e., DI) (see MR values in Table 2.1).

Mathematical Model: The transport model was run in inverse mode to quantify the influence of solution composition on colloid transport and retention. Values for the colloid pore-exclusion, *E,* and deposition rate, k_d, were estimated from the BTC data using a least-squares algorithm and the best fit values corresponding to each solution composition presented in Table 2.1. Although the authors recognize that retention is likely due to more than one mechanism, quantitatively discerning the various components of retention from the breakthrough data is not feasible. We therefore approach retention with the nonspecific parameter, k_d, and shed light to the retention mechanism it represents with visual data. *D* and *v* were determined from separate

conservative tracer experiments where the terms for E and k_d equaled 0. Model fits are presented as solid and dashed lines in Figure 2.2 with R^2 values > 0.92 for experiments where MR was above 5%. This good fit shows that the simple transport model employed is capable of describing the conditions here tested. The average fitted value E was 0.83±0.07 (see Table 2.1), and accounted for the residence time reduction of 17% of colloids from that of the Br^- pulse. The values for k_d varied inversely with MR. k_d increased with IS, decreased with increasing pH for experiments in FA and DI, and was generally much lower for experiments in HA than for other DOM solutions under the same pH and IS conditions.

A positive linear correlation was found between k_d for non-sterically stabilized suspensions (i.e., suspensions with measured $\Phi = 0$) and their respective ψ_o when experiments were grouped into treatments of equal IS (see Figure 2.3a) with R^2 of 0.7 for both ionic strength groups, irrespective of DOM type and solution pH. As shown in Figure 2.3b, sterically stabilized suspensions (i.e., suspensions with measured $\Phi >$ 0) have a good positive linear correlation ($R^2 = 0.8$) with the product of the measured polymeric characteristics of sterically stabilized suspensions d/a, Φ, and ψ_o.

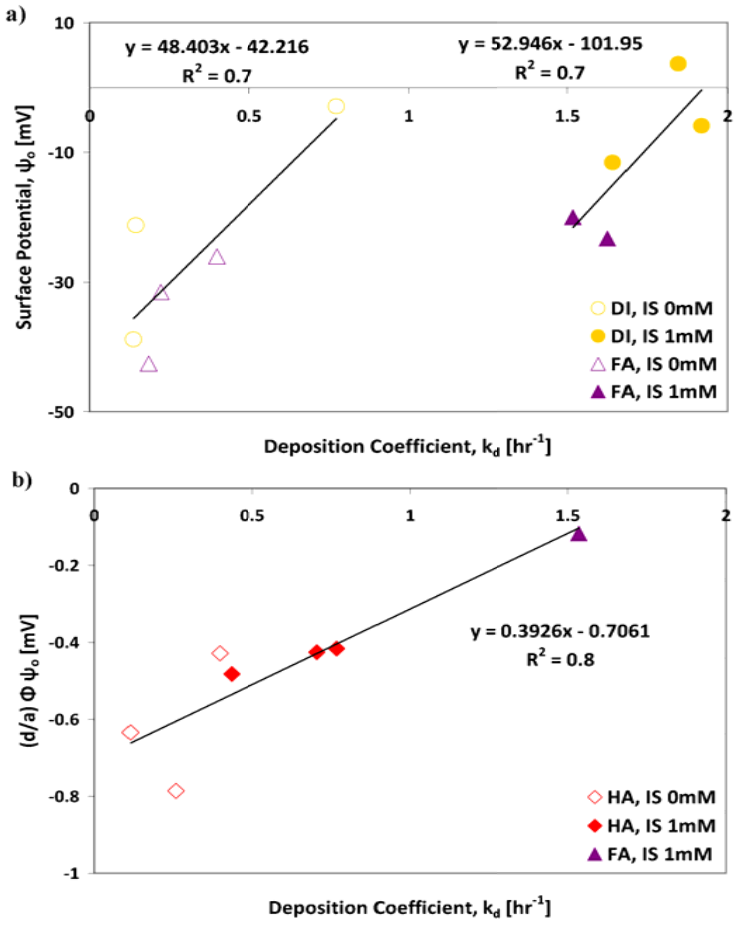

Figure 2.3 Correlation between deposition rate, k_d, of colloids traveling through an unsaturated porous medium and the particle's surface characteristics. a) Surface characteristic for non-sterically stabilized colloids is surface potential, ψ_o. Data included are for experiments in FA (triangles) and DI (circles) at ionic strengths of 0mM (open symbols) and 1mM (solid symbols). b) Surface characteristics for sterically stabilized colloids are represented by a value that includes ratio of adsorbed layer thickness to colloid radius, d/a, density of polymeric layer, Φ, and surface potential, ψ_o. Data included are for experiments in HA (diamonds) and FA (triangles) at ionic strengths of 0mM (open symbols) and 1 mM (solid symbols).

Discussion

Although the partitioning of DOM-colloid complexes at the AWI generally increases with the presence of HA, the overall breakthrough is still greater when HA is present than when it is not. The physicochemical characteristics of the colloids analyzed in this research indicate that, although the charge of colloids suspended in DOM was more negative than those suspended in DI (i.e., absence of DOM) (see EM and ψ_o values in Table 2.1), only HA had the capacity to electrosterically stabilize colloids. This was a result of the formation of a highly charged brush layer (of measured polymeric characteristics d, Γ_c, and $\Phi > 0$) on the colloid's surface that promoted colloid mobility in solutions with higher ionic strength. FA adsorption affinity onto surfaces was in most cases minor (see Γ_c values for FA in Table 2.1) and thus did not significantly improve the mobility of colloids despite its effect on colloid charge (see changes in EM and ψ_o for FA in Table 2.1). As has been recognized previously, the single effect of increasing a particle's negative charge is not sufficient to justify the increased colloid stability observed in certain treatments [*Elimelech, et al.*, 2000]. In this study disparate percentages of mass recovered colloids were observed for solution compositions that yielded comparable colloid surface charges. Hence, an additional physicochemical characteristic (to electrostatic charge) responsible for improving the suspension's stability was suspected to play a prominent role in enhancing the transport of DOM-colloid complexes. Various studies have suggested that the development of steric surface structures by adsorbed DOM may be implicated in the unsubstantiated repulsive forces of colloid suspensions, as these have been observed to remain stable even under conditions of high ionic strength [*Chen and Elimelech*, 2007; 2008; *Franchi and O'Melia*, 2003; *Phenrat, et al.*, 2010].

The adsorbed layer characteristics data demonstrate that the magnitude and range of steric repulsion depend on three factors: (i) density of adsorbed DOM layer,

Φ, (ii) the extension of the adsorbed layer, d, and (iii) the particle charge here presented as surface potential, ψ_o. Evidently, the eletrosterically stabilized particles with most negative surface potential, large adsorbed mass, and thickest brush layer experience the best transport enhancement, and the presence of all three polymeric characteristics is required to provide a suspension with steric stability. When either d is absent or Φ is very large, the colloids behave like hard colloidal particles and are sensitive to aggregation with changes in solution chemistry. These results reveal that structural hindrance, in addition to electrostatic repulsion, are the mechanisms by which HA, and in one extreme case FA, increases the stability of colloids in the bulk fluid. Clearly, the development of the organic matter brush layer grants soft particle functionalities to the otherwise chemically sensitive suspension, which, to the authors' knowledge, has only been visualized by Chen and Elimelech [2007] and physically characterized with indirect measurements by Phenrat et al. [2010]. This information explains the reduced particle-particle interaction that results in greater mobility of HA-colloid complexes through porous media, and can be assumed to be analogous to the interactions between the particles and the porous medium through which they move.

Internal observations of colloid transport demonstrate that for experiments in DI and FA with solution conditions conducive for high retention (e.g., higher ionic strength and/or low pH), colloid retention occurs at sites involving single or multiple SWI interfaces (Figures A.1a-d) and have high deposition rate values ranging from 0.4 to 2 hr^{-1} (see k_d for FA and DI at IS of 1 mM and both IS values at pH 4 in Table 2.1). This relation suggests that retention of hard particles, such as the colloid suspensions in DI and FA, experience retention with higher mass transfer toward the SWI when the medium's solution composition hinders transport. For experiments in HA with solution conditions that favor attachment, the dominant retention sites were along the AWI in bridge flocs (Figure 2.1), which were characterized with lower deposition

rates ranging from 0.3 to 0.8 hr^{-1} (see k_d for HA at ionic strength solutions of 1 mM and both ionic strength solutions at pH 4 in Table 2.1). This relation suggests that irreversible retention of soft particles, such as HA-colloid complexes, at the AWI is slower than the retention of hard particles, such as most FA-colloid complexes or colloids in the absence of DOM, at the SWI. Moreover, colloids retained at the AWI may be more susceptible for being remobilized with transient flow conditions than the colloids predominantly retained at the SWI. The dominant retention at AWIs suggests that: (i) HA partitioning to the AWI (as has been demonstrated previously [*Lenhart and Saiers*, 2004; *Ma, et al.*, 2007]) creates a rough surface or gelatinous layer that enhances colloid retention; (ii) HA-colloid complexation occurs in the bulk solution, where the amphiphilic character of HA augments the hydrophobic properties of the colloids resulting in hydrophobic expulsion toward the AWI (i.e., strong attractive non-electrostatic interactions); or (iii) both processes are occurring. Although the visual data in Figure 2.1 and Video 1 suggests that hydrophobic interactions significantly influence retention mechanisms in HA-colloid systems, these types of interactions do not occur in isolation from other interaction effects, warranting future work on hydrophobic alterations of surfaces by DOM.

Changes in pH affect colloid transport for suspensions in DI and FA by altering the level of functional group deprotonation on the surfaces of both colloids and the porous medium, which consequently affects the thickness of their respective electric double layers and resulting electrostatic interactions. For conditions where the system's IS was raised to 1 mM, it is evident that neutralization of the colloid's charge (from less negative ψ_o values in Table 2.1) dominated over any effect that pH had for experiments with DI and FA, as the colloid mass recovery (MR in Table 2.1) did not exceed 5% at any pH value. Alternatively, experiments conducted with HA demonstrate that pH is a critical factor for determining colloid transport, as the

thickness of the polymeric layer and adsorption affinity of HA onto colloid and medium surfaces was dictated by the solution's pH (see d and Γ_c values for HA in Table 2.1).

The addition of $CaCl_2$ affected the colloidal system by: (i) neutralizing the charge of deprotonated HA functional groups, (ii) forming multidentate complexes between available functional groups of the HA macromolecules and Ca cations (as demonstrated by the increase in Γ_c with $CaCl_2$ addition), and (iii) compressing the electric double layer of all charged surfaces (as is evident from ψ_o data in Table 2.1). Although chemical bonding of HA with Ca^{2+} promoted greater adsorption of organic matter onto the colloid surfaces, the chemical reaction at the Ca^{2+} and HA concentration tested weakened the ability of HA to mobilize colloids (observed in decreases in MR with increasing IS in Table 2.1) by neutralizing charged functional groups of adsorbed HA strands (apparent in the less negative ψ_o with increasing ionic strength in Table 2.1), and by bridging together HA-colloid complexes forming large flocs that can experience straining in the porous medium (apparent in visual data of internal colloid processes in Figure 2.1, A.1, and Video 1). The effects of charge neutralization and EDL compression are well known to stimulate colloid retention by reducing electrostatic energy barriers that otherwise prevent colloid aggregation and colloid attachment to immobile sites within the porous medium [*Kretzschmar and Sticher*, 1997].

The environmental relevance of this research is most apparent in the solution compositions selected to represent natural subsurface environments rich in DOM as well as agricultural settings that practice land application of alkaline-treated manure. This waste management practice is often preferred for its practicality at the farm level to inactivate zoonotic pathogens [*Gerba and Smith*, 2005] and control odor [*Zhu*, 2000]. The findings of this study advance our current understanding of the governing

mechanisms of colloid transport in a broad range of organic rich subsurface environments; particularly those associated with agriculture. Moreover, our current ability to predict the transport and fate of colloid-adsorbed contaminants and pathogenic microorganisms in the natural subsurface is limited by the incomplete understanding of the physico-chemical processes responsible for abiotic porous media filtration. Thus, the use of microspheres as colloidal pathogen surrogates makes elucidation of porous-media transport processes possible without the complications of even less understood biotic processes (e.g., biologically induced attachment, inactivation, die off, growth, motility, chemotaxis, bioclogging, etc.).

Conclusion

In summary, the effect of DOM on colloid characteristics can be directly measured through changes in surface potential, adsorbed layer thickness, and mass of adsorbed organic matter. Solution pH and $CaCl_2$ presence strongly affected the polymeric characteristics by varying the adsorption affinity of DOM onto surfaces and protonation of functional groups, and by neutralizing surface charge and chemically bridging DOM strands together, respectively. The presence of all three parameters (surface potential, adsorbed layer thickness, and mass of adsorbed organic matter by way of density of adsorbed DOM) was established to be a requirement for particles to be endowed with electrostatic and structural stability. Failure to possess all three polymeric characteristics resulted in one of three scenarios: (i) weakened electrostatic repulsion if surface potential were neutralized, (ii) lack of steric hindrance if adsorbed layer thickness were smaller than the separation distance where van der Waals forces are in effect, or (iii) polymer-colloid complexes approach hard particles if adsorbed layer densities were too high. Thus, of the two types of DOM examined, it was established that only HA can consistently electrosterically stabilize colloids. HA was

determined to enhance colloid mobility better than FA, even under the most chemically conducive conditions for retention. Retention of HA-colloid complexes along the AWI indicates that partitioning of DOM at the AWI may create a rough or gelatinous surface for colloids to become immobilized and/or that the amphiphilic character of adsorbed HA may encourage colloidal hydrophobic expulsion. Mathematical simulations of column transport data indicate that a simple convective dispersive model with a deposition term and colloid pore-exclusion correction is suitable to describe the fate and transport of organic matter-colloid complexes in the conditions here tested. A positive linear strong correlation was found between deposition coefficients of electro-sterically stabilized suspensions and the product of three polymeric characteristics: adsorbed layer thickness, density, and surface potential. As such, measurements of these specific polymeric characteristics can effectively be used to improve deterministic predictions of colloid transport in a wide range of DOM-rich solution compositions and assess the filtering function that the vadose zone serves to protect groundwater resources.

Acknowledgements

This study was financed by the National Science Foundation, Project No. 0635954; the Binational Agricultural Research and Development Fund, Project No. IS-3962-07; and the Teresa Heinz Foundation for Environmental Research. The authors thank Dr. John F. McCarthy for helpful discussions and Dr. Yuanming Zhang and Dr. Claude Cohen for assistance with light scattering techniques. We also thank Mr. Doug Caveney for constructing the flow cell used for this study.

APPENDIX A

Colloid Retention Sites in Unsaturated Porous Media

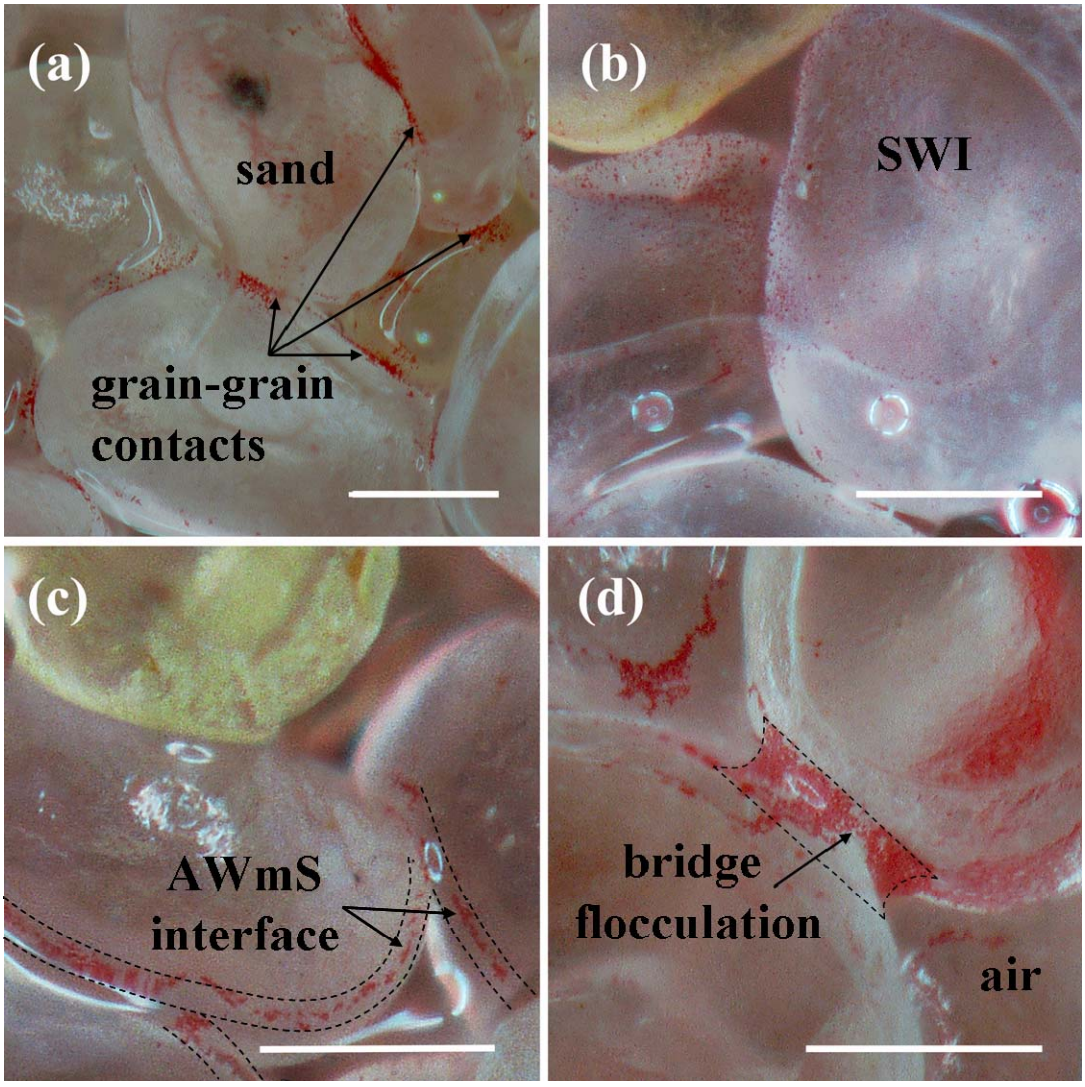

Figure A.1 Retention of red colloids in unsaturated quartz sand media in: a) grain-grain contact regions, b) soil-water interface, c) air-water meniscus-solid interface, d) bridge flocculation at the air-water interface. Scale bar length is 250 µm.

REFERENCES

Abudalo, R. A., et al. (2005), Effect of ferric oxyhydroxide grain coatings on the transport of bacteriophage PRD1 and Cryptosporidium parvum oocysts in saturated porous media, *Environmental Science & Technology*, *39*, 6412-6419.

Abudalo, R. A., et al. (2010), Influence of organic matter on the transport of Cryptosporidium parvum oocysts in a ferric oxyhydroxide-coated quartz sand saturated porous medium, *Water Research*, *44*, 1104-1113.

Akbour, R. A., et al. (2002), Transport of kaolinite colloids through quartz sand: Influence of humic acid, Ca2+, and trace metals, *Journal of Colloid and Interface Science*, *253*, 1-8.

Amirbahman, A., and T. M. Olson (1995), Deposition kinetics of humic matter-coated hematite in porous-media in the presence of Ca^{2+}, *Colloids and Surfaces a-Physicochemical and Engineering Aspects*, *99*, 1-10.

Avena, M. J., et al. (1999), Volume and structure of humic acids studied by viscometry pH and electrolyte concentration effects, *Colloids and Surfaces a-Physicochemical and Engineering Aspects*, *151*, 213-224.

Benedetti, M. F., et al. (1996), Humic substances considered as a heterogeneous donnan gel phase, *Environmental Science & Technology*, *30*, 1805-1813.

Bradford, S. A., et al. (2006), Transport of Giardia and manure suspensions in saturated porous media, *Journal of Environmental Quality*, *35*, 749-757.

Bradford, S. A., and S. Torkzaban (2008), Colloid transport and retention in unsaturated porous media: A review of interface-, collector-, and pore-scale processes and models, *Vadose Zone Journal*, *7*, 667-681.

Chen, K. L., and M. Elimelech (2007), Influence of humic acid on the aggregation kinetics of fullerene (C-60) nanoparticles in monovalent and divalent electrolyte solutions, *Journal of Colloid and Interface Science*, *309*, 126-134.

Chen, K. L., and M. Elimelech (2008), Interaction of Fullerene (C-60) Nanoparticles with Humic Acid and Alginate Coated Silica Surfaces: Measurements, Mechanisms, and Environmental Implications, *Environmental Science & Technology*, *42*, 7607-7614.

Chen, K. L., et al. (2006), Aggregation kinetics of alginate-coated hematite nanoparticles in monovalent and divalent electrolytes, *Environmental Science & Technology*, *40*, 1516-1523.

Chi, F. H., and G. L. Amy (2004), Kinetic study on the sorption of dissolved natural organic matter onto different aquifer materials: the effects of hydrophobicity and functional groups, *Journal of Colloid and Interface Science*, *274*, 380-391.

Duval, J. F. L., et al. (2005), Humic substances are soft and permeable: Evidence from their electrophoretic mobilities, *Environmental Science & Technology*, *39*, 6435-6445.

Elimelech, M., et al. (2000), Relative insignificance of mineral grain zeta potential to colloid transport in geochemically heterogeneous porous media, *Environmental Science & Technology*, *34*, 2143-2148.

Flury, M., and H. X. Qiu (2008), Modeling colloid-facilitated contaminant transport in the vadose zone, *Vadose Zone Journal*, *7*, 682-697.

Foppen, J. W., et al. (2008), Effect of humic acid on the attachment of Escherichia coli in columns of goethite-coated sand, *Water Research*, *42*, 211-219.

Franchi, A., and C. R. O'Melia (2003), Effects of natural organic matter and solution chemistry on the deposition and reentrainment of colloids in porous media, *Environmental Science & Technology*, *37*, 1122-1129.

Fritz, G., et al. (2002), Electrosteric stabilization of colloidal dispersions, *Langmuir*, *18*, 6381-6390.

Gerba, C. P., and J. E. Smith (2005), Sources of pathogenic microorganisms and their fate during land application of wastes, *Journal of Environmental Quality*, *34*, 42-48.

Granger, S. J., et al. (2007), Processes affecting transfer of sediment and colloids, with associated phosphorus, from intensively farmed grasslands: tracing sediment and organic matter, *Hydrological Processes*, *21*, 417-422.

Guetzloff, T. F. (1994), Does humic acid form a micelle?, *152*, 31-35.

Harvey, R. W., et al. (2010), Effects of altered groundwater chemistry upon the pH-dependency and magnitude of bacterial attachment during transport within an organically contaminated sandy aquifer, *Water Research*, *44*, 1062-1071.

Heidmann, I., et al. (2005), Aggregation kinetics of kaolinite-fulvic acid colloids as affected by the sorption of Cu and Pb, *Environmental Science & Technology*, *39*, 807-813.

Hosse, M., and K. J. Wilkinson (2001), Determination of electrophoretic mobilities and hydrodynamic radii of three humic substances as a function of pH and ionic strength, *Environmental Science & Technology*, *35*, 4301-4306.

Jada, A., et al. (2006), Surface charge and adsorption from water onto quartz sand of humic acid, *Chemosphere*, *64*, 1287-1295.

Jaisi, D. P., et al. (2008), Transport of Single-Walled Carbon Nanotubes in Porous Media: Filtration Mechanisms and Reversibility, *Environmental Science & Technology*, *42*, 8317-8323.

Ko, I., et al. (2005), Adsorption properties of soil humic and fulvic acids by hematite, *Chemical Speciation and Bioavailability*, *17*, 41-48.

Kretzschmar, R., et al. (1997), Experimental determination of colloid deposition rates and collision efficiencies in natural porous media, *Water Resources Research*, *33*, 1129-1137.

Kretzschmar, R., et al. (1998), Influence of pH and humic acid on coagulation kinetics of kaolinite: A dynamic light scattering study, *Journal of Colloid and Interface Science*, *202*, 95-103.

Kretzschmar, R., and H. Sticher (1997), Transport of humic-coated iron oxide colloids in a sandy soil: Influence of Ca2+ and trace metals, *Environmental Science & Technology*, *31*, 3497-3504.

Lenhart, J. J., and J. E. Saiers (2004), Adsorption of natural organic matter to air-water interfaces during transport through unsaturated porous media, *Environmental Science & Technology*, *38*, 120-126.

Ma, J., et al. (2007), Adsorptive fractionation of humic acid at air-water interfaces, *Environmental Science & Technology*, *41*, 4959-4964.

Marley, N. A., et al. (1993), Evidence for radionuclide transport and mobilization in a shallow, sandy aquifer, *Environmental Science & Technology*, *27*, 2456-2461.

Meier, M., et al. (1999), Fractionation of aquatic natural organic matter upon sorption to goethite and kaolinite, *Chemical Geology*, *157*, 275-284.

Mibus, J., et al. (2007), Migration of uranium (IV)/(VI)in the presence of humic acids in quartz sand: A laboratory column study, *Journal of Contaminant Hydrology*, *89*, 199-217.

Morales, V. L., et al. (2009), Grain Surface-Roughness Effects on Colloidal Retention in the Vadose Zone, *Vadose Zone Journal*, *8*, 11-20.

Pefferkorn, E. (2006), Clay and oxide destabilization induced by mixed alum/macromolecular flocculation aids, *Advances in Colloid and Interface Science*, *120*, 33-45.

Phenrat, T., et al. (2010), Estimating attachment of nano- and submicrometer-particles coated with organic macromolecules in porous media: Development of an empirical model, *Environmental Science & Technology*, *44*, 4531-4538.

Relan, P. S., et al. (1984), Molecular-configuration of composts humic-acid by viscometric studies, *Plant and Soil*, *81*, 203-208.

Schnitzer, M. (1972), *Humic substances in the environment*, 327 pp., Dekker, New York.

Sen, T. K., and K. C. Khilar (2006), Review on subsurface colloids and colloid-associated contaminant transport in saturated porous media, *Advances in Colloid and Interface Science*, *119*, 71-96.

Tang, X. Y., and N. Weisbrod (2009), Colloid-facilitated transport of lead in natural discrete fractures, *Environmental Pollution*, *157*, 2266-2274.

Thurman, E. M. (1985), *Organic Geochemistry of Natural Waters*, Kluwer Academic, Boston.

van Oss, C. J. (2003), Long-range and short-range mechanisms of hydrophobic attraction and hydrophilic repulsion in specific and aspecific interactions, *Journal of Molecular Recognition*, *16*, 177-190.

von Wandruszka, R. (2000), Humic acids: Their detergent qualities and potential uses in pollution remediation, *1*, 10-15.

Zhu, J. (2000), A review of microbiology in swine manure odor control, *Agriculture Ecosystems & Environment*, *78*, 93-106.

CHAPTER 3

CORRELATION EQUATION FOR PREDICTING ATTACHMENT COEFFICIENT (α) OF ORGANIC MATTER-COLLOID COMPLEXES IN POROUS MEDIA

Abstract

A semi-empirical approach is used to improve an existing model that predicts attachment efficiency (α) of electrosterically stabilized suspensions moving through a porous medium using direct measurements of polymeric characteristics.

Introduction

Predictive models to effectively determine the fate and transport of microparticles and nanoparticulate material or 'nano-enabled' products [*Scown, et al.*, 2010] in aqueous environments are of great interest due the growing concern regarding the threat that some particles have on environmental and public health. Recurrent outbreaks of waterborne diseases from colloidal groundwater contaminants (e.g., *Giardia*, *E. coli O157:H7*, *Cryptosporidium oocysts, Cryptosporidium parvum*, and chemical poisons [*Curriero, et al.*, 2001; *Lee, et al.*, 2002]) and the growing incorporation of under investigated engineered nanoparticles into consumer products (e.g., nano silver, TiO_2, and nanotubes [*Benn and Westerhoff*, 2008; *Kaegi, et al.*, 2008; *Mueller and Nowack*, 2008]) has raised the pressure for investigators to improve predictive models that can effectively determine fate of these particles once they enter the environment via deliberate or unintentional pathways.

It is well accepted that enhanced mobility of particles is often achieved by addition of anionic surface coatings. Such coatings are often engineered to improve the stability of suspensions [*Phenrat, et al.*, 2008; *Saleh, et al.*, 2005], though attention

has been growing on the similar role that sorbed natural organic matter (NOM) can play when particles enter soil environments [*Chen and Elimelech*, 2008; *Morales, et al.*, 2010; *Phenrat, et al.*, 2010], as soils are typically rich in NOM. The mechanisms by which NOM enhances particle mobility is via a combination of electrostatic and steric repulsion from surface adsorbed and highly charged macromolecules that increase the net charge of the particle and add steric hindrance to aggregation, as schematically illustrated in Figure 3.1. It is generally accepted that in addition to the classic colloid forces, van der Waals (V_{vdw}) and electrostatic double layer potentials (V_{EDL}), the electrosteric component (V_{ST}) generated from adsorbed NOM plays a significant role in maintaining the stability of a suspension even under the most favorable solution compositions (i.e., chemistry that promotes coagulation). It has been observed experimentally that organic matter-coated colloids have attachment efficiency values, α_{exp}, less than 1 at ionic strengths where the electrostatic repulsion is nearly completely screened [*Amirbahman and Olson*, 1995].

A recent study by Morales et al. [2010] investigated the effect of adsorbed NOM macromolecules on colloid transport through a porous medium under a broad range of solution compositions. The authors demonstrated that the criterion required to endow a suspension with electrostatic stability is that the density of the adsorbed NOM layer (as a function of the mass of NOM adsorbed, density of dry NOM, thickness of the NOM adsorbed, and radius of the colloidal particle) should be greater than 0. This parameter incorporates the significant sorption of NOM mass onto the surface of the colloid, as well as the formation of a polymeric shell of thickness d_M. For this criterion, an upper limit to the critical polymeric shell density must exist where the soft/rigid particle transition is. That is, if the stabilizing shell becomes is exceedingly high, then the particle may lose steric stability and resume to the electrostatic double layer as the only type of repulsion.

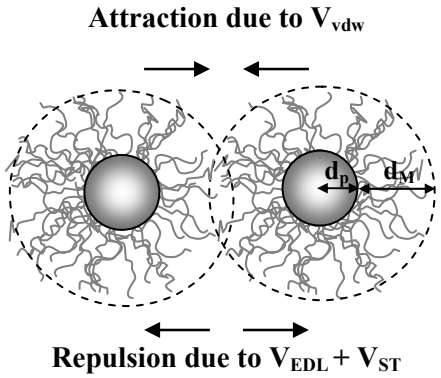

Figure 3.1 Schematic representation of the forces acting on two electrosterically stabilized organic matter-colloid complexes. The particles are represented by the spheres of radius d_p; adsorbed organic matter are the strands extending from the surface of the particle, which make up the stabilizing shell of thickness d_M; and the Debye-length is represented by the dashed line. Interacting forces include: van der Waals attraction (Vvdw), electrostatic double layer repulsion (V_{EDL}), and steric repulsion (V_{ST}).

Available semiempirical correlations for attachment efficiencies, such as those proposed by Elimelech [1992] and the more comprehensive form from Bai and Tien [1999] reasonably capture deposition trends under unfavorable surface interactions. However, as Phenrat et al. [2010] have demonstrated, these correlations break down when applied to suspensions characterized by electrosteric stability. In the light of the shortcomings of these mathematical correlations, Phenrat et al. [2010] proposed an empirical model that integrates a dimensionless parameter for steric repulsion to more closely predict the generally smaller attachment efficiency of soft particles. The proposed empirical correlation is based on polymeric characteristics values that were estimated with Ohshima's soft particle theory [1995]. Ohshima's approximation calculates the thickness of the adsorbed polymeric layer from electrophoretic mobility

measurements, but is only applicable for suspensions in symmetric and indifferent electrolyte solutions (e.g., NaCl). Moreover, Ohshima's analysis can often return multiple answers for a given set of conditions making it an unfitting technique to universally determine polymeric parameters, especially for asymmetric or non-indifferent electrolyte suspensions (e.g., $CaCl_2$). As Phenrat et al. note, a method to directly measure adsorbed layer thickness would likely improve the prediction of attachment efficiencies of surface-coated particles.

In this study, direct measurements of polymeric characteristics of soft particles and their corresponding experimental deposition data are used to refine Phenrat et al.'s attachment efficiency model for soft particles. The goodness of fit of Phenrat et al.'s model and a newly proposed model is presented for data from seven transport experiments that report direct measurements of particle polymeric characteristics and an additional fifteen experiments where the polymeric characteristics were obtained with Ohshima's approach.

Background

According to clean-bed filtration theory (CFT), the fate of particles moving through a porous medium can be estimated from the filter's attachment (i.e., collision) efficiency (α), which represents the probability that an approaching particle will become attached to the collector upon coming into contact with it [*Yao, et al.*, 1971]. α is defined as the fraction of collisions that result in attachment (single-collector collision efficiency, η) and the total collisions of suspended particles against the collector (i.e., i.e., single-collector contact efficiency, η_o) in the presence of repulsive interactions as:

$$\alpha = \frac{\eta}{\eta_o} \qquad [3.1]$$

Traditionally, column experiments are used to determine the attachment efficiency for a given set of physicochemical conditions by the following relationship:

$$\alpha_{\exp} = -\ln\left(\frac{C}{C_o}\right)\frac{2d_c}{3(1-n)\eta_o L} \qquad [3.2]$$

Where α_{exp} is the experimentally determined attachment efficiency, C/C_o is the normalized effluent concentration of particles when the breakthrough reached steady state, d_c is the is the average collector diameter, n is the bed porosity, L is the filter packed length, and η_o can be calculated from the equation proposed by Tufenkji and Elimelech (2004) as:

$$\eta_O = 2.4A_S^{1/3}N_R^{-0.715}N_{vdw}^{0.052} + 0.55A_S N_R^{1.675}N_A^{0.125} + 0.22N_R^{-0.24}N_G^{1.11}N_{vdw}^{0.0533} \qquad [3.3]$$

The semi-empirical correlation for predicted attachment efficiency, α_{pre}, proposed by Bai and Tien [1999] employs a comprehensive relation that incorporates dimensionless parameters (defined in Table 3.1) to account for the London number (N_{LO}), electrokinetic parameters (N_{E1} and N_{E2}), and a double-layer force parameter (N_{DL}) to predict the attachment efficiency of electrostatically stabilized particles with the form:

$$\alpha_{pre} = 2.527\times10^{-3}N_{LO}^{0.7031}N_{E1}^{-0.3121}N_{E2}^{3.5111}N_{DL}^{1.352} \qquad [3.4]$$

Nonetheless, because it has been shown in a number of studies that the single effect of changing a particle's charge or zeta-potential cannot always justify changes in stability and transport [*Elimelech, et al.*, 2000; *Morales, et al.*, 2010], additional repulsive parameters must be implicated in the prediction of attachment efficiencies of those suspensions (e.g., steric hindrance from adsorbed polymers). To the author's knowledge, Phenrat et al. [2010] are the first study to propose a correlation that takes

into account electrosteric repulsive forces (N_{LEK} defined in Table 3.1) to predict attachment efficiency, viz:

$$\alpha_{pre} = 10^{-1.35} N_{LO}^{\ 0.39} N_{E1}^{\ -1.17} N_{LEK}^{\ -0.10} \qquad [3.5]$$

Table 3.1 Summary of dimensionless parameters governing attachment efficiency.

Parameter	Definition	
N_{LO}	$\frac{4A}{9\pi\mu d_p^{\ 2} u_s}$	London number
N_{E1}	$\frac{\varepsilon\varepsilon_o(\zeta_p^{\ 2} + \zeta_g^{\ 2})}{3\pi\mu u_s d_p}$	First electrokinetic parameter
N_{E2}	$\frac{2\zeta_g\zeta_p}{(\zeta_p^{\ 2} + \zeta_g^{\ 2})}$	Second electrokinetic parameter
N_{DL}	κd_p	Double-layer force parameter
N_{LEK}	$\frac{d_p d_M^2 u_s \Gamma N_a \rho_p}{\mu M_W}$	Layer-electrokinetic parameter

A is the Hamaker constant, μ is the fluid viscosity, d_p is the particle diameter, u_s is the superficial velocity, ε is the relative permittivity of the fluid, ε_o is the permittivity in a vacuum, ζ_g and ζ_p are the zeta potential of the media grains and particles respectively, κ is the reciprocal of double layer thickness, d_M is the average adsorbed layer thickness, Γ is the mass of adsorbed polymer (i.e., surface excess), N_a is Avogadro's number, ρ_p is the macromolecule density, and M_W is the macromolecule molecular weight.

Materials and Methods

Experimentally determined attachment efficiencies and polymeric coating characteristics of organic matter-coated particles were obtained from the literature [*Amirbahman and Olson*, 1995; *Franchi and O'Melia*, 2003; *Morales, et al.*, 2010]. These studies were selected because they used NOM of various types (Georgetown Fulvic Acid (GFA), Swannee River Humic Acid (SRHA), Elliott Soil Humic Acid (ESHA), and Elliott Soil Fulvic Acid (ESHA)) as the adsorbed polymer and the

particles were all synthetic microspheres allowing presumably uniform sorption of the polymer. In addition, these studies reported experimental information on deposition coefficient, particle size, zeta potential of the particle and the collector, and porewater velocity (data details are listed in Table A.1 in the appendix). It is important to note that only the study by Morales et al. [2010] directly measured the thickness of adsorbed organic matter onto the microspheres. The d_M values for the other studies were reported by Phenrat et al. [2010] as polymeric layer thickness approximations from Ohshima's analysis. α_{exp} was calculated with equations 3.2 and 3.3.

Predicted attachment efficiency values, α_{pre}, were calculated with Bai and Tien's and Phenrat et al.'s approach (equations 3.4 and 3.5, respectively). The calculated α_{pre} were compared to the α_{exp} of all data, and separately to only those data with direct measurements of polymeric characteristics. This allowed us to evaluate the suitability of the existing models against a more precise data set, and suggest improvements that would refine the attachment efficiency model for soft particles. The existing, and most promising model from Phenrat et al., was taken through a step-wise method of least squares, where each dimensionless power coefficient term was adjusted to improve its relative contribution to the overall attachment efficiency based on observed and predicted values from directly measured polymeric data.

Results and Discussion

The model from Bai and Tien against all data yields a Nash-Sutcliffe E value of less than -100 (Figure 3.2a) and against data with only direct polymeric measurements yields E = -2.8×10^8 (Figure 3.2b). This indicates that the model fails to capture any trends in attachment efficiency for sterically stabilized particles as the efficiency for all conditions was predicted to be perfect, i.e., α_{pre} was constantly equal

to 1. The application of Phenrat et al.'s correlation against all data yields an E = 0.76 (Figure 3.2c), meaning that it fits the data generally well, but over-predicts attachment efficiencies for suspensions where $\alpha_{exp} \leq 1.74 \times 10^{-3}$ (see deviation from the 1:1 line at low α_{exp}). When testing Phenrat et al.'s correlation against only those data with direct polymeric measurements E was -6.5×10^{4} (Figure 3.2d), revealing that the model overestimated the data by a factor of 137, as indicated by the slope of the regression line. These comparisons indicate that Bai and Tien's correlation is fundamentally inadequate to predict α for soft particles. Although Phenrat et al.'s correlation is conceptually captures the effect that steric hindrance has on attachment efficiency, the proposed equation breaks down for suspensions that experience low retention. The authors suspect that employing Ohshima's approach to indirectly determine d_M underrates the polymeric properties of the stabilizing shell, forcing the model to inflate α_{pre}.

The application of either the Bai and Tien or Phenrat et al. models to suspensions of soft particles that are highly stable would result in the underprediction of the transport distances of the suspensions and accordingly overestimate the filtration efficiency of the porous medium.

The exponential coefficients of the dimensionless parameters in Phenrat's α_{pre} correlation equation were adjusted through a step-wise method of least squares to improve the predictive ability of the model using measured only those data of definite precision from Morales et al. [2010]. The new correlation based on data from direct polymeric characteristics measurements is:

$$\alpha = 10^{-3.52} N_{LO}^{\ 0.39} N_{E1}^{\ -1.17} N_{LEK}^{\ -0.11} \qquad [3.6]$$

In this revised correlation, the relative contribution from N_{LO} and N_{E1} parameters were not affected, indicating that the input from van der Waals and electrostatic forces are

adequately accounted for in the Phenrat et al. [2010] model. The common logarithm parameter had to be adjusted from $10^{-1.35}$ to $10^{-3.52}$ in order to reduce total attachment efficiency prediction, and the exponent for N_{LEK} to -0.11 to increase the weighed contribution of steric repulsion relative to the classic colloid forces.

The application of the correlation from equation 3.6 against all data yielded an E value of -0.31 (Figure 3.2e), indicating that the model and the mean of the observed data are nearly equally accurate. Here, the model captures low attachment efficiency trends, but underpredicts attachment efficiencies for suspensions where $\alpha_{exp} \geq 1.74 \times 10^{-3}$ (see deviation from the 1:1 line at high α_{exp}). However, when the new correlation was tested against only those data with direct polymeric measurements (Figure 3.2f) the attachment efficiency estimated α_{exp} well with an E = 0.83. These results indicate that that the conceptually accurate correlation from Phenrat et al. was a good base to improve α_{pre} based on a more precise data set with direct polymeric shell measurements.

Future improvements of equation 3.6 should include limits for the attachment efficiency correlation of soft particles to converge into an attachment efficiency correlation for electrostatically unfavorable interactions (e.g., of the format of equation 3.4) when the density of the adsorbed layer is large enough that the particles transition from supporting soft- to rigid- particle properties.

The results of existing and newly proposed α_{pre} correlations indicate that Ohshima's indirect approach for estimating polymeric characteristics yields a projected d_M that is smaller than its true value. Moreover, Ohshima's method is inadequate for determining the d_M of suspension in asymmetric and/or non-indifferent electrolyte solutions, such as those in $CaCl_2$. The non-indifferent properties of this divalent electrolyte are discussed in detail by Morales et al. [2010] and confirmed with salting out experiments (discussed in the appendix) of Elliott Soil Humic Acid

solutions at various concentrations of $CaCl_2$ and NaCl electrolyte. Briefly, the results confirmed that $CaCl_2$ has a high chemical affinity for NOM (i.e., is non-indifferent) as illustrated in Figure B.1a, while NaCl maintained its indifferent character even at high ionic strength levels as illustrated in Figure B.1b. Consequently, validation of Ohshima's estimation for d_M with directly measured values reported by Morales et al. [2010] was not possible, as the Ohshima's approach yielded multiple results (i.e., multiple minima answers with the least squares method) for the tested zeta-potential values (data not shown), making it difficult to use to determine α_{pre} as prescribed by Phenrat et al. [2010].

Engineering Applications and Implications

Currently, engineered polymers are being investigated to modify nanoparticles in order to inhibit aggregation (e.g., nanoscale zerovalent iron particles coated with poly-styrene sulfonate, polyaspartate, carboxymethyl cellulose, or block copolymers [*Phenrat, et al.*, 2008; *Saleh, et al.*, 2005]) and/or add specific functionality (e.g., biocompatibility, or providing functional groups for specific pollutant targeting [*Saleh, et al.*, 2005]). Given that for environmental applications colloidal and nanoparticles will inevitably acquire a layer of adsorbed DOM, it is worth while to investigate the transport of particles with such coatings to determine whether additional coatings are necessary to achieve the increased stability goal, or if the specific functionality of engineered polymer coatings is concealed by the inevitable coating of environmental NOM.

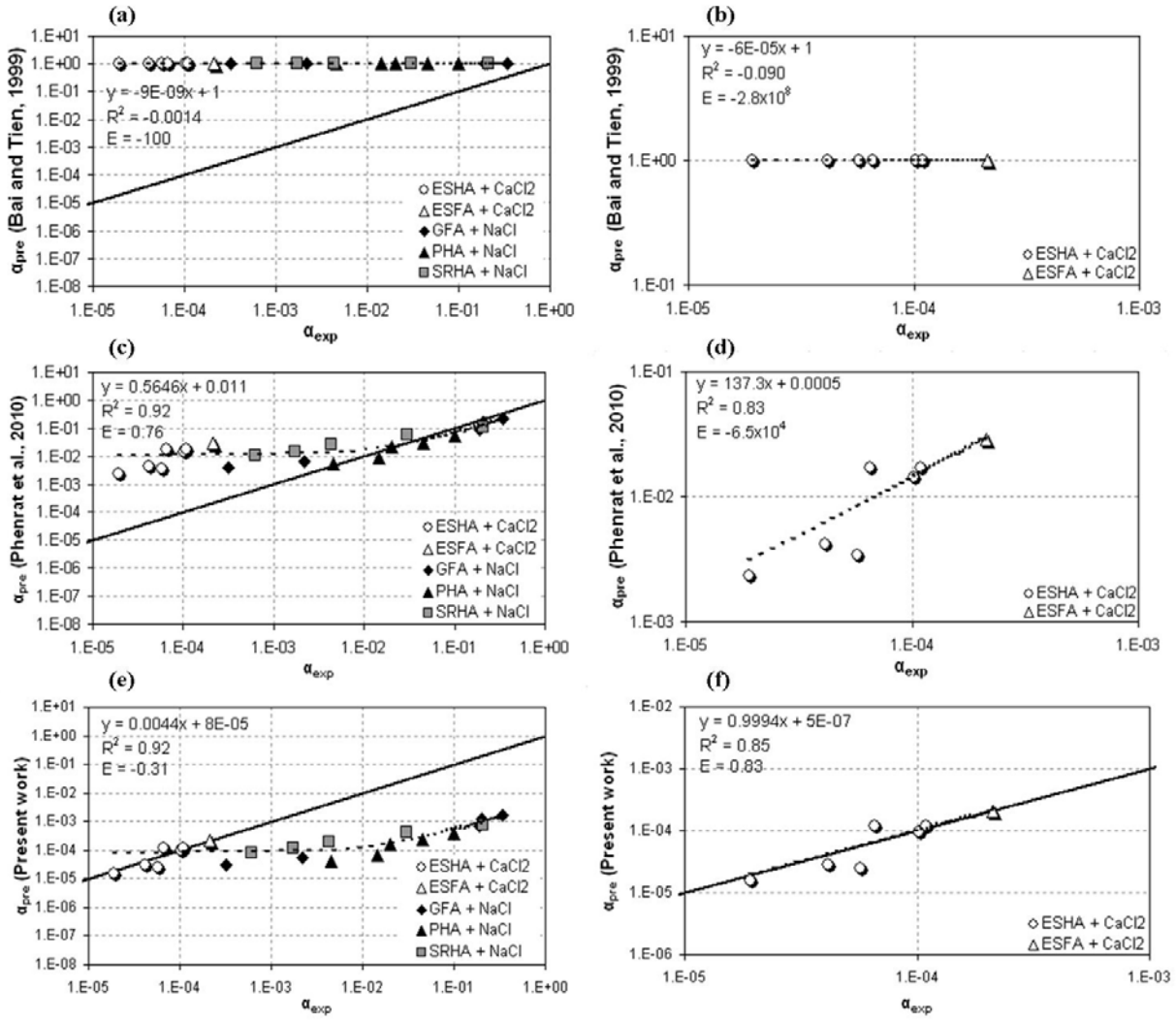

Figure 3.2 α_{exp} for polystyrene particles coated with ESHA and ESFA [*Morales, et al.*, 2010], latex particles coated with GFA and PHA [*Amirbahman and Olson*, 1995], and latex particles coated with SRHA [*Franchi and O'Melia*, 2003] vs. α_{pre} from Bai and Tien [1999] correlations (a and b), Phenrat et al. [2010] (c and d), and present study (e and f). Solid black line represents the 1:1 correlation for α_{exp} to α_{pre}. Plots b, d, and f contain α_{exp} data from those experiments that directly measured polymeric characteristics. Dashed line indicates the slope of the fit and slope of the regression.

Conclusion

Steric repulsion is a function of particle and adsorbed layer properties d_p, d_M, Γ, ρ_p, and M_w and is effectively represented by the dimensionless parameter N_{LEK}. Existing correlations between attachment efficiency and particle properties either entirely fail to capture decreased attachment efficiency caused by steric repulsion, or over-predict the attachment efficiencies of highly stable suspensions because they are based on a set of uncertain data that is biased by conditions that resulted in high deposition. In this study we adapted the soft-particle attachment efficiency correlation from Phenrat et al. [2010] and refined the relative contribution of the acting forces improve the model's predictive capabilities against a precise data set. The effective prediction of α with the proposed model for sterically stabilized suspensions in any type of electrolyte requires accurate means of obtaining information on the size of particle, its zeta potential as well as that of the stationary medium, mass of the adsorbed polymer, and most importantly, the thickness of the adsorbed polymer.

Aknowledgements

This study was financed by the National Science Foundation, Project No. 0635954; the Binational Agricultural Research and Development Fund, Project No. IS-3962-07; and the Teresa Heinz Foundation for Environmental Research. The authors thank Dr. Zachary M. Easton and Ms. Sheila M. Saia for helpful assistance with statistical methods.

APPENDIX B

Table B.1 Experimental conditions used to determine the attachment efficiency of natural organic matter coated particles from Amirbahman and Olson [1995], Franchi and O'Melia [2003], and Morales et al. [2010].

Ref.	Type of OM	Electrolyte	IS (mM)	pH	d_p (m)	d_M (m)	d_c (m)	ζ_p (V)	ζ_g (V)	u_s (m s^{-1})	Γ (kg m^{-2})
Amirbahman and Olson, 1995	GFA	NaCl	21	7.4	4.7E-07	7.0E-10	2.8E-04	-3.6E-02	-5.6E-02	4.2E-05	4.9E-07
	GFA	NaCl	49	7.4	4.7E-07	7.0E-10	2.8E-04	-3.0E-02	-4.4E-02	4.2E-05	4.9E-07
	GFA	NaCl	501	7.4	4.7E-07	7.0E-10	2.8E-04	-1.3E-02	-1.2E-02	4.2E-05	4.9E-07
	GFA	NaCl	681	7.4	4.7E-07	7.0E-10	2.8E-04	-1.1E-02	-8.0E-03	4.2E-05	4.9E-07
	GFA	NaCl	774	7.4	4.7E-07	7.0E-10	2.8E-04	-1.0E-02	-7.0E-03	4.2E-05	4.9E-07
	IHSS PHA	NaCl	50	7.4	4.7E-07	2.0E-09	2.8E-04	-2.6E-02	-4.7E-02	4.2E-05	7.9E-07
	IHSS PHA	NaCl	100	7.4	4.7E-07	2.0E-09	2.8E-04	-2.3E-02	-3.7E-02	4.2E-05	7.9E-07
	IHSS PHA	NaCl	251	7.4	4.7E-07	2.0E-09	2.8E-04	-1.7E-02	-2.4E-02	4.2E-05	7.9E-07
	IHSS PHA	NaCl	341	7.4	4.7E-07	2.0E-09	2.8E-04	-1.5E-02	-2.0E-02	4.2E-05	7.9E-07
	IHSS PHA	NaCl	464	7.4	4.7E-07	2.0E-09	2.8E-04	-1.3E-02	-1.5E-02	4.2E-05	7.9E-07
Franchi and O'Melia, 2003	SRHA	NaCl	1	7.2	9.8E-08	3.0E-09	2.0E-04	-6.8E-02	-5.3E-02	1.3E-03	3.5E-07
	SRHA	NaCl	3	7.2	9.8E-08	3.0E-09	2.0E-04	-6.1E-02	-4.4E-02	1.3E-03	3.5E-07
	SRHA	NaCl	10	7.2	9.8E-08	3.0E-09	2.0E-04	-4.3E-02	-4.0E-02	1.3E-03	3.5E-07
	SRHA	NaCl	55	7.2	9.8E-08	3.0E-09	2.0E-04	-3.3E-02	-2.6E-02	1.3E-03	3.5E-07
	SRHA	NaCl	500	7.2	9.8E-08	3.0E-09	2.0E-04	-2.6E-02	-2.0E-02	1.3E-03	3.5E-07
Morales et al., 2010	IHSS ESHA	$CaCl_2$	0	4	2.6E-06	3.2E-08	5.0E-04	-4.4E-02	-2.8E-02	5.3E-05	4.3E-05
	IHSS ESHA	$CaCl_2$	0	6	2.6E-06	5.3E-08	5.0E-04	-4.6E-02	-4.6E-02	5.3E-05	2.7E-05
	IHSS ESHA	$CaCl_2$	0	9	2.6E-06	1.5E-09	5.0E-04	-5.1E-02	-5.7E-02	5.3E-05	1.6E-05
	IHSS ESHA	$CaCl_2$	1	4	2.6E-06	2.5E-08	5.0E-04	-2.0E-02	-2.0E-02	5.3E-05	4.3E-05
	IHSS ESHA	$CaCl_2$	1	6	2.6E-06	5.5E-08	5.0E-04	-2.1E-02	-2.1E-02	5.3E-05	3.8E-05
	IHSS ESHA	$CaCl_2$	1	9	2.6E-06	1.2E-08	5.0E-04	-2.3E-02	-2.1E-02	5.3E-05	3.3E-05
	IHSS ESFA	$CaCl_2$	1	9	2.6E-06	2.9E-09	5.0E-04	-2.0E-02	-2.2E-02	5.3E-05	1.1E-05

Electrolyte Indifference Test

Salting out experiments of dissolved organic matter by NaCl and $CaCl_2$ electrolytes at various concentrations and solution pH were conducted to test the affinity of electrolytes toward dissolved organic matter (i.e., classify the electrolytes as indifferent or non-indifferent). Briefly, 30mL solutions of Elliott Soil HA (obtained from IHSS) at 20 mg of total dissolved organic carbon L^{-1} (measured by persulfate oxidation with an O-I-Analytical Total Organic Carbon Analyzer model 1010, College Station, TX) were prepared and adjusted to solution pH of 4, 5, 6, 7, 8, and 9 by addition of HCl or NaOH as well as ionic strength from 0-12mM by addition of NaCl for the first set and $CaCl_2$ for the second set. After thorough mixing with a vortex, the solutions were allowed to quiescently settle for 24 hours, after which an aliquot was collected and the dissolved organic concentration measured again.

The equilibrium dissolved HA concentrations after 24 hours of quiescent settling (Figure B.1a and b) demonstrate that the addition of $CaCl_2$ precipitates dissolved HA (possibly through complexation of metal cations, Ca^{2+}, with organic matter ligands, HA), while NaCl does not observably affect its solubility. Furthermore, these data demonstrate that pH plays an important role in the threshold calcium concentration at which HA becomes insoluble. Figure B.1a illustrates how, for solution pH levels 7-9, the concentration of soluble HA sharply drops to less than 13% the initial concentration when the ionic strength (by addition of $CaCl_2$) exceeds 2.25 mM. In contrast, for solution pH levels 4-6, the solubility of HA is more gradually reduced and reaches 18% the initial concentration at ionic strength levels exceeding 7.5 mM (by addition of $CaCl_2$). Figure B.1b illustrates that the solubility of HA does not change with the tested ionic strengths 0-12 mM by addition of NaCl at any pH level. This test confirms that while NaCl is an indifferent electrolyte in organic matter rich systems, $CaCl_2$ is not indifferent.

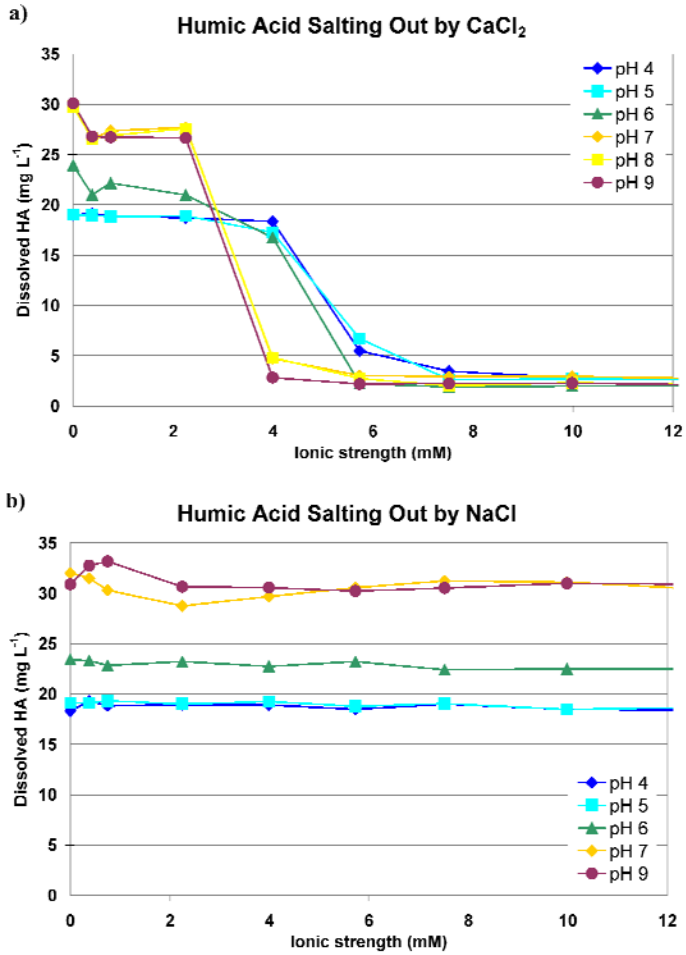

Figure B.1 Concentration of dissolved ESHA after 24 hr of quiescent salting out by addition of a) non-indifferent $CaCl_2$ and b) indifferent NaCl at equivalent ionic strengths.

REFERENCES

Amirbahman, A., and T. M. Olson (1995), The role of surface conformations in the deposition kinetics of humic matter-coated colloids in porous media, *Colloids and Surfaces a-Physicochemical and Engineering Aspects*, *95*, 249-259.

Bai, R. B., and C. Tien (1999), Particle deposition under unfavorable surface interactions, *Journal of Colloid and Interface Science*, *218*, 488-499.

Benn, T. M., and P. Westerhoff (2008), Nanoparticle silver release into water from commercially available sock fabrics, *Environmental Science & Technology*, *42*, 4133-4139.

Chen, K. L., and M. Elimelech (2008), Interaction of fullerene (C-60) nanoparticles with humic acid and alginate coated silica surfaces: Measurements, mechanisms, and environmental implications, *Environmental Science & Technology*, *42*, 7607-7614.

Curriero, F. C., et al. (2001), The association between extreme precipitation and waterborne disease outbreaks in the United States, 1948-1994, *American Journal of Public Health*, *91*, 1194-1199.

Elimelech, M. (1992), Predicting collision efficiencies of colloidal particles in porous-media, *Water Research*, *26*, 1-8.

Elimelech, M., et al. (2000), Relative insignificance of mineral grain zeta potential to colloid transport in geochemically heterogeneous porous media, *Environmental Science & Technology*, *34*, 2143-2148.

Franchi, A., and C. R. O'Melia (2003), Effects of natural organic matter and solution chemistry on the deposition and reentrainment of colloids in porous media, *Environmental Science & Technology*, *37*, 1122-1129.

Kaegi, R., et al. (2008), Synthetic TiO2 nanoparticle emission from exterior facades into the aquatic environment, *Environmental pollution*, *156*, 233-239.

Lee, S. H., et al. (2002), Surveillance for waterborne-disease outbreaks -- United States, 1999-2000, *MMWR Surveill Summ*, *51*, 1-47.

Morales, V. L., et al. (2010), Impact of dissolved organic matter on colloid transport in the vadose zone: Deterministic approximation of transport deposition coefficients from polymer coating characteristics, *Water Research*.

Mueller, N. C., and B. Nowack (2008), Exposure modeling of engineered nanoparticles in the environment, *Environmental Science & Technology*, *42*, 4447-4453.

Ohshima, H. (1995), Electrophoresis of soft particles, *Advances in Colloid and Interface Science*, *62*, 189-235.

Phenrat, T., et al. (2008), Stabilization of aqueous nanoscale zerovalent iron dispersions by anionic polyelectrolytes: adsorbed anionic polyelectrolyte layer properties and their effect on aggregation and sedimentation, *Journal of Nanoparticle Research*, *10*, 795-814.

Phenrat, T., et al. (2010), Estimating Attachment of Nano- and Submicrometer-particles Coated with Organic Macromolecules in Porous Media: Development of an Empirical Model, *Environmental Science & Technology*, *44*, 4531-4538.

Saleh, N., et al. (2005), Adsorbed triblock copolymers deliver reactive iron nanoparticles to the oil/water interface, *Nano Letters*, *5*, 2489-2494.

Scown, T. M., et al. (2010), Review: Do engineered nanoparticles pose a significant threat to the aquatic environment? , *Critical Reviews in Toxicology*, *40*, 653-670.

Yao, K. M., et al. (1971), Water and wastewater filtration: Concepts and applications, *Environmental Science & Technology*, *5*, 1105-1112.

CHAPTER 4

INTERACTION OF COLLOIDAL PARTICLES WITH THE AIR-WATER-SOLID INTERFACE OF A DRYING DROPLET

Abstract

Self-assembly of particles by controlled solvent evaporation is a simple and cost effective way for patterning surface at micro- and nano-meter scales. In this work, we manipulated the capillary forces acting on suspended colloids at the contact line of an evaporating sessile drop through the addition of a non-ionic surfactant. Three dynamic drying processes were identified: slipping contact line (at low surfactant concentrations), pinned contact line (at intermediate surfactant concentrations), and recurrent stick-slip (at surfactant concentrations near the critical micelle concentration). Each drying process produces distinct deposition patterns: amorphous stains, coffee-like stains, and concentric rings, respectively. The transition between the slipping and pinned contact line drying regimes is found to be governed by the force balance between the capillary forces pulling the colloids at the contact line inward and the friction force between the colloids and the substrate resisting the receding contact line. The transition between the pinned and the recurrent stick-slip drying regimes may be explained by the highly reduced surface tension that permits stretched thin films to rupture, thus forming concentric rings. Distinctive static friction coefficients (μ_s) were determined for particles at each surfactant concentration tested, with logarithmically decreasing μ_s values as the droplet's surfactant concentration increased. Attachment strength tests on deposition patterns for each regime indicate that attachment strength is proportional to droplet's respective static friction coefficient.

Introduction

Self-assembly of particles is a fundamental process with applications to a wide area of technology including: microfabrication (Kawase et al., 2003; Sirringhaus et al., 2000), nanowire production (Judai et al., 2006; Ondarcuhu and Joachim, 1998; Shi et al., 2006), crystal assembly (Velikov et al., 2002), and DNA/RNA mapping (Blossey and Bosio, 2002; Laurell et al., 2005). For these purposes, controlling the deposition of suspended particles is crucial to meet the goal of each industry.

Early investigations of evaporative self-assembly by Deegan et al. (2000; 1997; 2000) discovered the well known "coffee stain" phenomenon, where the evaporation rate of a sessile droplet is greatest near the contact line, producing a radially outward flow to replenish the lost liquid (coined in the literature as Deegan-type flow). This fluid drag, is in turn, able to carry suspended particles outward, where they are deposited and form a ring on the location of the original contact line. Picknett and Bexon (1977) identified two extreme modes of droplet behavior in response to evaporation: *constant contact angle mode* in which the contact area of the droplet decreases without changing the contact angle, and *constant contact area mode* in which the contact angle decreases without changing the contact area. In the same work, Picknett and Bexon (1977) note that it is not unusual to find evaporative systems that share qualities of both modes. Thus, for non-extreme systems, the evaporation process of a droplet on a solid surface occurs in two stages where, first, the contact line is pinned and the contact angle decreases to a critical contact angle, and second, the contact line recedes toward the center of the drop (Hu and Larson, 2005).

Deposition of particles onto a surface by evaporative self-assembly has often been considered a stochastic process (Byun et al., 2008). However, complex patterns,

such as the formation of stripes or concentric rings, with high regularity have been achieved by a number of researchers through restrictive geometry of the droplet and substrates that force the drying process to follow oscillatory motion of the shrinking contact line (Byun et al., 2008; Hong et al., 2008; Xu et al., 2006). This type of patterning mechanism was attributed by Adachi et al. (1995) to be a result of the competition between the surface tension of the bulk liquid, the surface tension of the thin film at the contact line, and the friction force exerted within a wetting-film region at the contact line. Shmuylovich et al. (2002) expanded on the contact line pinning mechanism proposed by Adachi et al. (1995) by studying in detail the structure of the film at the contact line during the drying process. They reported that the motion of the contact line was dependent on the intersection of the receding line with particles that are previously adhered onto the substrate surface.

A theoretical study by Gao et al. (2008) ascribed the retention of particles at air-water–solid interfaces (AWSI) to capillary forces of the deformed film as illustrated in Figure 4.1. The authors decomposed participating capillary forces into a lateral force (F_l) that can push the particle back to the bulk solution, and a vertical force (F_v) that can pin the colloid against the substrate. In the same study, the authors propose that a static friction force (F_f) generated between the colloid and the substrate must exist in order to immobilize colloids at the AWSI. For this scenario, F_f is proportional to the system's static friction coefficient, μ_s, and should be sufficiently large in magnitude to resist the lateral push by F_l.

Although the findings from the above described studies shed light on the mechanisms that may be responsible for interactions of particles with the triple interface, the systematic limitations responsible for colloids to slip or become pinned at dynamic air-water-solid interfaces are not yet well understood. Thus, the objective

of this paper is to investigate the role of capillary forces and limit of surface tension forces on the contact line dynamics of a drying droplet with colloidal suspension.

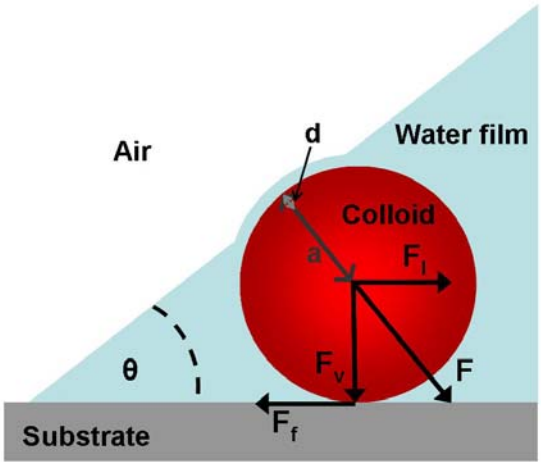

Figure 4.1 Schematic of capillary forces (*F*) acting on a colloid trapped at an air-water-solid interface. *F* is decomposed into lateral (F_l) and vertical (F_v) components. Friction force (F_f) between the slipping colloid and the substrate surface acts in the opposite direction as F_l.

Materials and Methods

The experimental setup consisted of visualizing in situ the evaporative processes of sessile water droplets of varying initial surfactant concentrations under ambient conditions in the presence and absence of suspended colloids. Visual data was collected from simultaneous overhead views to track particle interactions with the edge of the droplet, as well as from side views for contact angle goniometry.

Materials and preparation: Surfactant-free, carboxylated, and red polystyrene microspheres (Magsphere, Pasadena, California) of 5 μm in diameter were washed with deionized water (thermal conductivity of 0.609 W m^{-1} K^{-1}) to remove manufacturer added stabilizers. The stock suspension was subsequently adjusted to a concentration of 1.45×10^{9} colloids mL^{-1}. Particle zeta potential (ζ) was calculated to

be -51.4±4.8 mV from electrophoretic mobility measurements collected with a Malvern Zetasizer nano (Worcestershire, UK). Stock surfactant solutions of non-ionic and non-volatile Surfynol® 485 (Air Products, Allentown, Pennsylvania) were prepared at concentrations of 0, 0.03, 0.13, 0.64, 1.3, 2.6, 5.2, and 7.7 mg L^{-1} to which colloids were added until a concentration of 9×10^{6} colloids mL^{-1} was reached. Assigned experimental identification for each initial surfactant concentration is given in Table 4.1. The surface tension of each suspension was measured with a semiautomatic tensiometer (Model 21 Tensiomat, Fisher Scientific). Surface tension values are presented in Figure C.1 as a function of surfactant concentration. The non-ionic surfactant was selected to maintain the system's Coulombic forces unchanged. The surfactant concentrations were selected in the range where surface tension is most sensitive to surfactant concentration. Scratch-free sheets of Optix Polymethyl methacrylate (PMMA) (thermal conductivity of 0.13 W m^{-1} K^{-1}) (Plaskolite, Inc., Columbus, Ohio) were used as the pristine substrate. After removing the protective masking, the PMMA sheets were rinsed with distilled water, wiped dry with lens paper, and stored in a low humidity room for several days prior to use. The ζ-potential of PMMA used was that reported in the literature, -29 mV (Hogt et al., 1986).

Table 4.1 Experimental identification for droplets of various initial surfactant concentrations.

Experiment number	Initial Surfactant concentration (mg L^{-1})
1	0.00
2	0.03
3	0.13
4	0.64
5	1.3
6	2.6
7	5.2
8	7.7

Evaporation experimental setup: The suspensions were dispersed by sonication for 5 minutes prior to each experiment. 2 μL drops were set on the PMMA sheet and allowed to evaporate quiescently under ambient laboratory conditions devoid of sunlight. The drop shape was recorded concomitantly from overhead using bright field microscopy (BFM) (Hirox, model KH-7700) at 15 second intervals and from a side view with a macro lens camera (MiniVID) every 45 seconds. 2D measuring software (KH-7700Ver) integrated in the BFM unit was used to measure the diameter of the droplets. Contact angles were measured with the DropSnake plugin (Stalder et al., 2006) for ImageJ analysis software. Identical colloid-free experiments were conducted following the same protocol. Although the ambient conditions were not strictly regulated, the results were highly reproducible, thus demonstrating the consistency of the system.

Additional parameters needed to calculate the capillary forces were determined by indirect measurements. The volume of the droplet at time *i*, V_i, was calculated from the spherical cap approach relating drop radius to contact angle by (Thomas, 2003):

$$V_i = \frac{\pi\left(2 - 3\cos\theta_i + \cos^3\theta_i\right)}{3r_i^3 \sin^3\theta_i} \qquad [4.1]$$

where θ_i is the contact angle of the droplet and r_i is the radius of the droplet at time *i*. This information allowed us to calculate the evolution of droplet evaporation from the visual data, and determine the evolution of surface tension with evaporation knowing that surfactant evaporation was minimal; therefore the concentration of surfactant could be related back to the surface tension plot in Figure C.1. The protrusion distance of the colloids from the water film, *d*, was determined geometrically (as per Figure 4.1) from the measured contact angle, θ, and distance between the edge of the AWSI

and the center of the colloid. This distance was measured from overhead images collected at 1050× magnification, which allowed excellent contrast between the edge of the contact line, the colloids, and the substrate. The contact angle of water with colloids, β, was measured as per Zevi et al. (2005).

Capillary force estimation: The capillary force (F) acting on a spherical particle trapped at the air-water-solid interface is schematically illustrated in Figure 4.1, and defined with the following expression Laplace equation as per Gao, et al (2008):

$$F = \sigma 2\pi\sqrt{a^2 - (a-d)^2}\cos\left[\beta + \frac{\pi}{2} - \theta\right] \qquad [4.2]$$

Here, σ is the surface tension of the liquid, a is the radius of the colloid, d is the distance a colloid protrudes out of the deformed film, β is the contact angle of water surface with colloids, and θ is the contact angle between the water film and the substrate. The capillary force is further decomposed into a lateral force component (F_l) responsible for pushing the colloid toward the bulk of the liquid, and a vertical force component (F_v) responsible for pinning the particle on the substrate surface, viz:

$$\begin{aligned} F_l &= F\sin\theta \\ F_v &= F\cos\theta \end{aligned} \qquad [4.3]$$

In order to account for a force balance at the AWSI that will prevent the particles from being pushed into the bulk by F_l, a friction force, F_f, is required to act on the colloid and in the opposite direction. Thus, at the very instant before the particle starts sliding/rolling back into the bulk solution, F_f should act on the particle away from the center of the drop at a magnitude that is equal to or greater than F_l toward the center of the drop. For this condition, the friction force F_f is calculated as the product of the substrate's static friction coefficient, μ_s, and the normal force between the colloid and the substrate (i.e., F_v), as:

$$F_f = F_v \mu_s \quad [4.4]$$

This capillary force analysis defines conditions for the pinning or non-pinning of particles at the AWSI as: (i) when F_f is greater than or equal to F_l the colloids will remain pinned because there is sufficient friction to overcome the lateral push, and (ii) when F_f is smaller than F_l, the colloids will be pushed into the bulk solution because there is not enough friction between particle and substrate to negate this force.

Adhesion force between liquid and solid: Adhesive force indicating the affinity of the liquid to the solid (γ_{LS}) was estimated by the following surface tension expression:

$$\gamma_{LS} = \sigma \cos\theta \left(2\pi r\right) \quad [4.5]$$

Attachment strength test: A flow displacement system was used to measure the adhesion strength of dried colloid stains for three selected surfactant concentrations. This test was performed in quadruplicate for each surfactant concentration. The colloid stains were preserved under ambient conditions for 24 hrs prior to being washed with the flow displacement system. Briefly, an open channel with a cylindrical outlet of radius (R) of 2.7×10^{-4} m was set flush with the substrate such that deionized water could be discharged at a flow rate of 1.7×10^{-6} m^3 s^{-1} for a total of 120 seconds. Images were collected from overhead at 12 second intervals to track the particles that remained on the substrate throughout the washing procedure (see the example for three types of stains in Figure C.2 A-C). The applied shear stress (τ) and shear rate (σ) (8.2 kg m^{-2} and 8.2×10^4 s^{-1}, respectively) were calculated from the flow rate (Q) and dynamic viscosity (η) of the deionized water at 21^o C (9.9×10^{-5} kg s m^{-2}) viz:

$$\tau = \eta\sigma \qquad [4.6]$$

where σ for a cylindrical flow configuration is given by

$$\sigma = \frac{3Q}{\pi R^3} \qquad [4.7]$$

It is important to note, as Busscher and van der Mei (2006) indicate, that because the particles are spherical and the substrate smooth and homogeneous, under ideal conditions shear cannot cause detachment, but sliding or rolling instead. This continues until unfavorable conditions are encountered that permit the sliding/rolling particle to become detached. Thus, detachment was defined as the removal of particles from the field of view in the images captured. Detachment rates were estimated by quantification of binarized images collected during the shearing period. In this image analysis technique, the original picture was converted into a black and white image (i.e., binarized) portraying the colloids in black pixels and everything else in white pixels (see the example for three types of stains in Figure C.2 a-c). The percentage of black from total pixels in each image was taken (after calibration) as a direct measurement of the number of colloids in the deposited pattern. The rate of detached particles (k_{det}) is reported as:

$$k_{\text{det}} = \left(1 - \frac{B_t}{B_o}\right) t^{-1} \qquad [4.8]$$

Where B_t is the percent of black pixels in the image taken at the end of the attachment strength test, B_o is the percent of black pixels in the image taken at before the start of the attachment strength test, and t is the duration of the attachment strength test. The test duration was the time it took to detach 95% of the deposited colloids up to a maximum of 120 seconds.

Results

Effect of surfactant concentration on droplet shape: The effect of surfactant addition on sessile droplets is mainly the decrease in surface tension. This decreases the liquid-solid contact angle and consequently the droplet's aspect ratio (see droplet profiles in Figure 4.2).

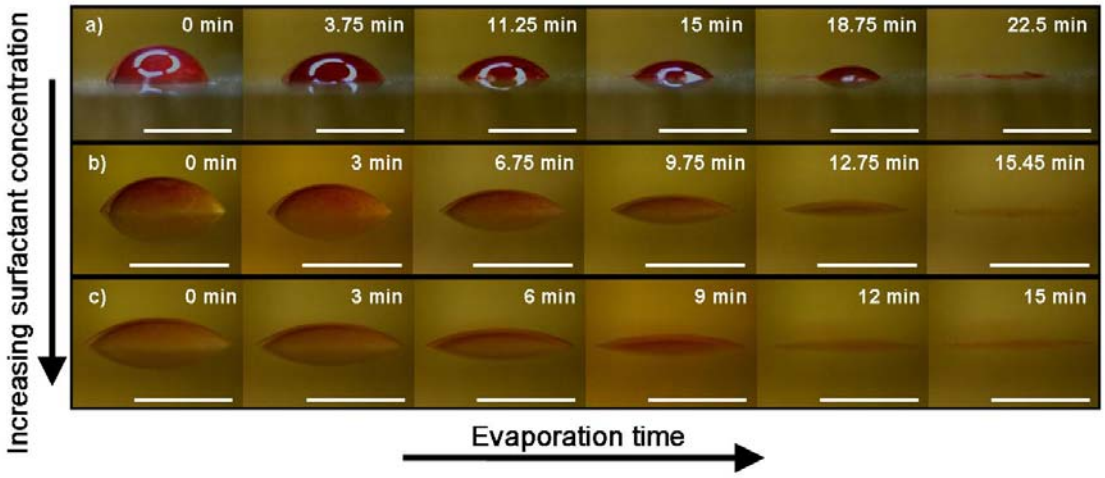

Figure 4.2 Side view of evaporating droplets at surfactant concentration of: a) Experiment 1 at 0 mg L^{-1} initial surfactant concentration, b) Experiment 4 at 0.64 mg L^{-1} initial surfactant concentration, and c) Experiment 8 at 7.7 mg L^{-1} initial surfactant concentration. Scale bar represents 2000µm.

Plots for droplet contact angle, θ, and diameter over normalized evaporation time (as real time (t) / final time for complete evaporation (t_f)) (Figure 4.3a and b, respectively) indicate that experiments 1 and 2 with droplets of low surfactant concentration, S, ($0.00 \leq S \leq 0.03$ mg L^{-1}, white symbols) are tightly confined, followed by experiments 3 and 4 with more dispersed droplets at medium surfactant concentration ($0.13 \leq S \leq 0.64$ mg L^{-1}, grey symbols), and lastly experiments 5 through 8 with droplets of high surfactant concentration ($1.3 \leq S \leq 7.7$ mg L^{-1}, black symbols) which are the most spread out. In general, the contact angle of the droplets

decreases with increasing surfactant concentration in spite of the stage of evaporation. For example, droplets of experiment 1 have contact angles that are on average more than 28^{o} larger than those for droplets of experiment 8 during the first 75% of the droplets' lifetime. Similarly, the initial droplet diameter increases from 2300 to 3000 μm for the same two experiments with the lowest and highest surfactant concentration, respectively. Data on the droplet diameter (here used as surrogates for contact line position) indicate that as evaporation progresses, droplets with low surfactant concentration (white symbols in Figure 4.3b) have a contact line that steadily contracts after a brief delay, droplets with medium surfactant concentration (gray symbols in Figure 4.3b) have an immobile contact line, and droplets with high surfactant concentration (black symbols in Figure 4.3b) initially have a stationary contact line and subsequently enter a recurrent cycle of fast contraction and a brief period of fixed contact line until evaporation is complete. In addition, parallel droplet experiments free of colloids for the same surfactant concentrations experienced diameter recession in a similar fashion as the droplets of low surfactant concentration (experiments 1 and 2), where the contact line would steadily contract after a delay period of increasing duration with surfactant concentration. This is discussed in detail in the section titled "Capillary force balance and particle pinning". Comparison of the contact line behavior between experiments in the presence and absence of colloids indicates that the presence of colloids in the drying droplet is the first requirement to pin the contact line in place.

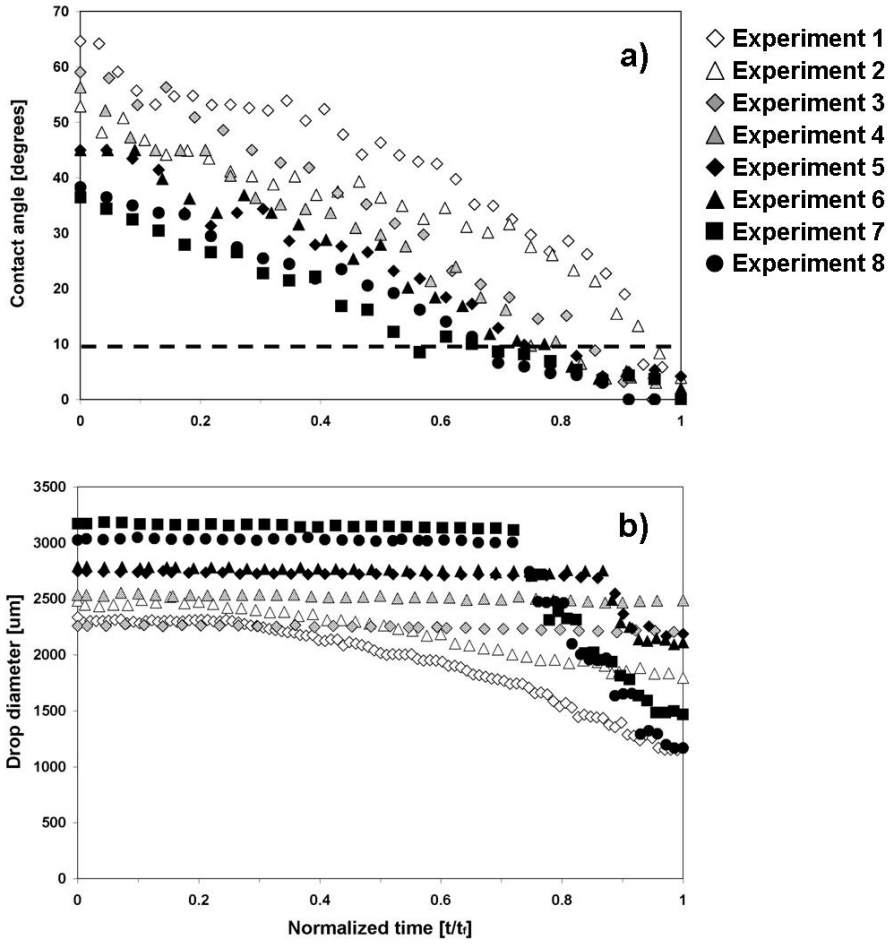

Figure 4.3 Change in shape over time of droplets of different initial surfactant concentrations: a) contact angle and b) diameter. Normalized time is presented as t/t_f indicating time, t, at an i^{th} interval per total duration of droplet evaporation, t_f.

Capillary force balance and particle pinning: Colloid-free evaporating droplet experiments were used to determine the time when the strength of attraction between the liquid molecules would overwhelm the attraction between the liquid and the solid at each surfactant concentration. This critical time was established as the time when the droplet contact line began to slip, t_s. As is evident in Figure 4.4a, t_s increases with

increasing surfactant concentration. Conversely, the contact angle at t_s decreases with increasing surfactant concentration, as is evident in Figure 4.4b. The increase in delay time concurs with the change in contact angle from the initial θ_o value to the contact angle when the line starts slipping, θ_c (as reported in Table 4.2). For example, droplets at low surfactant concentrations (experiments 1 and 2) have initially large θ_o, so a small change in contact angle results in a large change in cosine θ (the horizontal component of surface tension) at time t_s, which pulls the droplet toward the center. Droplets at high surfactant concentrations (experiments 5 through 8) have initially small θ_o, so they must experience a larger change in contact angle to experience the same magnitude change in cosine θ at time t_s to pull the droplet toward the center.

Additionally, the force between liquid molecules that pulls the droplet inward can also be thought of in terms of its competing force between liquid molecules and the solid, i.e., adhesion forces (γ_{LS}) as per equation 4.5. Here, γ_{LS} is taken to act along the circumference of the droplet, which makes it a function of the liquid's surface tension, the contact angle, and the radius of the droplet at time t_s. From the listed γ_{SLo} values in Table 4.2 no trend was observed to influence the initial adhesion forces with surfactant concentration. However, as is evident from Figure 4.4c (also reported as γ_{SLc} values in Table 4.2), adhesion of the liquid to the solid substrate increase with increasing surfactant concentration at the critical time when the contact line begins to slip. This corroborates the observation of droplets with low surfactant concentration (experiments 1 and 2) to evaporate in the slipping contact line mode, while droplets with higher surfactant concentration (experiments 5 through 8) evaporate in the pinned or stick-slip contact line mode. The values for γ_{LS} suggest that attachment affinity of the liquid to the solid (i.e., low contact angles and low surface tension) above 0.32 mN is the second requirement to pin the contact line in place.

Table 4.2 Droplet characteristics at the initial time of the experiment (indicated by the subscript 'o') and at the critical time when the contact line begins to slip (indicated by the subscript 'c'). Information for each experimental condition includes: initial surfactant concentration (S), droplet contact angle (θ), lateral capillary force (F_l), friction force (F_f), surface tension (σ), adhesion force (γ_{SL}), and static friction coefficient (μ_s).

	Initial values						Critical values when contact line begins to slip					
Exp No.	Initial S (mg L^{-1})	θ_o (degrees)	F_{lo} (mN)	F_{fo} (mN)	σ_o (mN m^{-1})	γ_{LSo} (mN)	θ_c (degrees)	F_{lc} (mN)	F_{fc} (mN)	σ_c (mN m^{-1})	γ_{LSc} (mN)	μ_s (-)
1	0.00	67 ± 3	0.00E+00	0.00E+00	72	0.23	51 ± 1	1.1E-04	1.0E-04	72	0.31	1.2
2	0.03	56 ± 3	3.5E-04	2.1E-04	63	0.30	38 ± 1	3.5E-04	3.4E-04	58	0.34	0.79
3	0.13	60 ± 0.6	0.00E+00	0.00E+00	53	0.20	34 ± 2	3.3E-05	3.1E-05	51	0.29	0.68
4	0.64	55 ± 1	0.00E+00	0.00E+00	48	0.21	9.1 ± 0.6	8.3E-05	8.9E-05	41	0.32	0.16
5	1.3	48 ± 3	1.4E-04	2.5E-05	45	0.28	10 ± 1	1.1E-04	1.0E-04	41	0.34	0.18
6	2.6	47 ± 2	1.9E-05	3.6E-06	42	0.23	13 ± 2	1.0E-04	9.1E-05	38	0.31	0.23
7	5.2	35 ± 1	0.00E+00	0.00E+00	42	0.34	9.0 ± 0.4	7.7E-05	7.4E-05	38	0.37	0.16
8	7.7	39 ± 1	0.00E+00	0.00E+00	40	0.30	8.0 ± 1	6.7E-05	8.1E-05	38	0.35	0.14

The capillary force balance at t_s requires that the lateral capillary force acting on the colloid (F_l) match the magnitude of the friction force between the substrate and the colloid (F_f) in the opposite direction. Therefore, taking the tangent of θ_c, which is the contact angle at time t_s produces the static friction coefficient value, μ_s, for colloids at each surfactant concentration, as reported in Figure 4.4d. In this figure, μ_s decreases with increasing surfactant concentration, indicating that for droplets at low surfactant concentration (experiments 1 and 2) the normal force F_v is small since θ_c is high, resulting in large total F_{fc} as reported in Table 4.2. Therefore μ_s must be large to compensate the lateral push by F_{lc} (reported in Table 4.2). In contrast, droplets at high surfactant concentration (experiments 5 through 8) have large F_v since θ_c are less than 13 degrees, resulting in small F_{fc}, as reported in Table 4.2. Therefore μ_s values do not have to be large to compensate for small F_{lc} values.

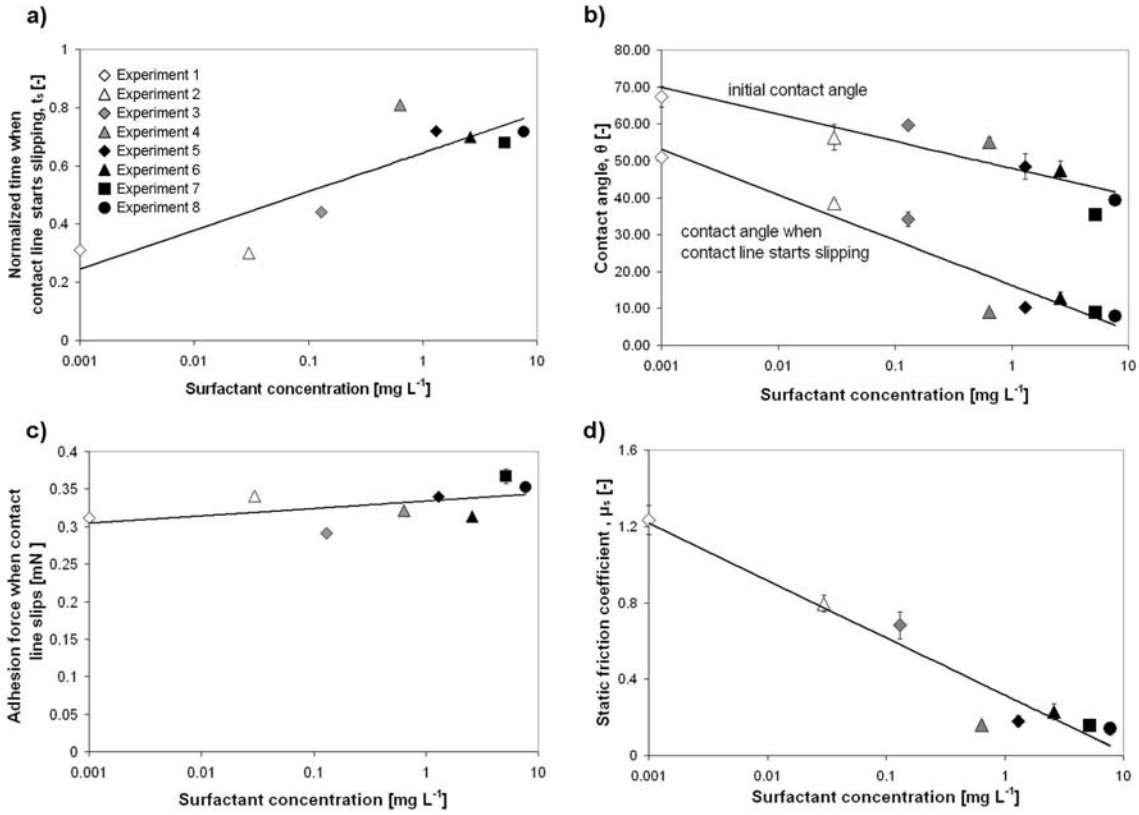

Figure 4.4 Droplet characteristics of sessile droplets with various initial surfactant concentrations: a) Normalized time when a droplet will begin contracting due to evaporation in the absence of colloids, b) Initial and critical contact angles when the droplet starts contracting, c) Adhesion force between the liquid and the substrate at the time when the droplet starts contracting, d) Static friction coefficient (μ_s) experienced by particles at the air-water-solid interface.

Final particle assembly of drying droplet: Three general particle assembly patterns were identified for the drying droplets at the various surfactant concentrations tested: amorphous stains produced by the low surfactant concentration droplet group (experiments 1 and 2 in Figure 4.5a and b), coffee-like stains produced by the medium surfactant concentration droplet group (experiments 3 and 4 in Figure 4.2c

and d), and concentric rings produced by the high surfactant concentration droplet group (experiments 5 through 8 in Figure 4.5e-h). The dashed white lines in Figure 4.5 indicate the initial contact line position. For the discrete surfactant concentrations tested, all but experiments 1 and 2 (droplets at the two lowest initial surfactant concentrations $S = 0$ and 0.03 mg L^{-1}) produced patterns with colloids deposited at the initial contact line position. Droplets that formed amorphous stains slowly contracted and carried the colloids with the receding contact line toward the center of the drop (as is indicated in the droplet diameter dynamics in Figure 4.3b, white symbols). In contrast, droplets that produced coffee-like stains (experiments 3 and 4 with respective S of 0.13 and 0.64 mg L^{-1}) and concentric rings (experiments 5 through 8 with $1.3 \geq S \leq 7.7$ mg L^{-1}) experienced constant nucleation growth at the original contact line position (as is indicated in the droplet diameter dynamics in Figure 4.3b, gray symbols for coffee-like stains and black symbols for concentric rings). For the latter scenario, particles were advected radially outward by Deegan-type flow, as discussed in the introduction, and became subsequently retained at the AWSI were the conditions for capillary force pinning were optimal (e.g., low droplet contact angle and low liquid surface tension).

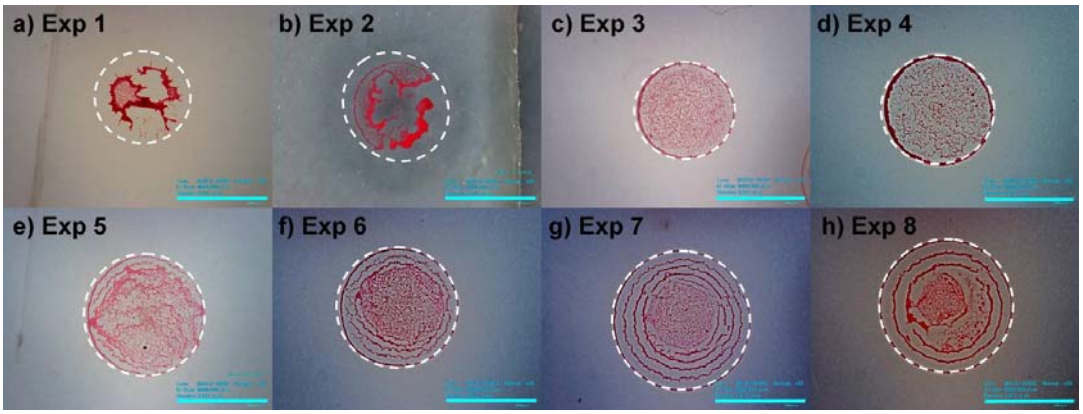

Figure 4.5 Self-assembly patterns of polystyrene particles produced after complete evaporation by droplets of various initial surfactant concentrations. Dashed white rings indicate the initial contact line location. Scale bar represents 2000μm.

Mode of droplet behavior: From information on the shape of the droplets and deposition patterns produced, a unique mode of droplet behavior was identified for each of the low, medium, and high surfactant concentration droplet groups. These modes are: slipping contact line, pinned contact line, and recurrent stick-slip, respectively. Droplets in the *slipping contact line* mode, schematically represented in Figure 4.6a, are characteristic for having: (i) large contact angles that remain relatively large (white symbols in Figure 4.3b) (i.e., θ at time i is approximately as large as θ_o) and push nearby colloids toward the center of the drop as the contact line slips (see Video 1 in the supporting information), and (ii) high surface tension, σ, ($47 < \sigma < 72$ mN m^{-1}, white symbols in Figure C.3) that hinders particles near the AWSI from protruding out of the water film. Droplets in the *pinned contact line* mode, schematically represented in Figure 4.6b, are characteristic for having: (i) contact angles that quickly decline (θ_i is smaller than θ_o) and pin the colloids against the substrate at the original contact line location (see Video 2 in the supporting

information), and (ii) lower surface tension ($53 < \sigma < 38$, grey symbols in Figure C.3) that permits protrusion of the colloid from the film. For droplets in the *recurrent stick-slip* mode, a pseudo-combination of the previous two evaporation modes takes place. Initially, the droplets share similar characteristics as those for the pinned contact line mode with small contact angles ($\theta \leq 49^{o}$) that decline down to a pinning angle, θ_p, of approximately 10^{o} (indicated by the dashed black line in Figure 4.3a), all while maintaining σ between 45 and 38 mN m^{-1} (black symbols in Figure C.3). This allows the colloids to protrude through the film and become pinned at the original contact line location. Evaporation following the decline of contact angle to the critical angle θ_p ensued the rupture of the water film (then at or very near the lower limit of σ) from the pinned colloids at the original contact line, followed by contraction of the droplet diameter by 200-500 μm. As the contact line slips inward, new particles are caught at the AWSI (schematically depicted in Figure 4.6c), which continues to slip until 78% of the linear contact line length is filled with particles. Additional particles will become nucleated at the newly established contact line, and the droplet will continue to evaporate. After a short time, the water film will break again and a new ring will be formed, leaving a space devoid of colloids between rings (see Video 3 in the supporting information).

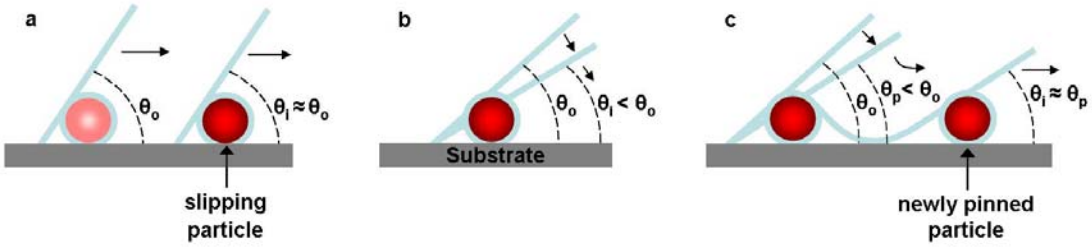

Figure 4.6 Schematic of contact line–colloid interactions at the air-water-solid interface during droplet evaporation. a) Slipping contact line mode; b) Pinned contact line mode; c) Recurrent stick-slip contact line mode.

Attachment strength test: Results from the flow displacement experiments indicated that for experiment 1 of initial $S = 0.0$ mg L^{-1}, representative of droplets in the slipping contact line mode, the applied shear stress detached deposited particles at a rate of 21±8 colloids s^{-1}. Experiment 3 of initial $S = 0.13$ mg L^{-1}, representative of droplets in the pinned contact line mode, had detachment rates of 44±7 colloids s^{-1}. And experiment 8 with initial $S = 7.7$ mg L^{-1}, representative of recurrent stick-slip contact line mode, had detachment rates of 140±75 colloids s^{-1}.

Discussion

In this paper, we investigated the systematic limitations responsible for colloids to slide or become pinned at the contact line of an evaporating droplet. Information regarding three modes for the range of surface tensions tested allowed us to explain the deposition patterns generated, as well as the necessary force required to remove the dried colloid stains.

The three modes of droplet behavior in response to evaporation identified exhibited distinct physical changes that are accountable for the transition of one mode to the next as a result of rising surfactant concentration. In the *recurrent stick-slip contact line mode* (experiments 1 and 2), the surface tension of the droplet is initially low and quickly approaches the lower limit of $\sigma_{min} = 38$ mN m^{-1}. For these droplets, even the slightest evaporation concentrates the initially added surfactant to a value above the critical micelle concentration (CMC). The reduced surface tension in turn produced small θ values that decrease as evaporation continues and more favorably pin colloids at the contact line. Pinning of the contact line causes the liquid of the droplet to become stretched with evaporation, such that when the droplet reaches a critical θ_c of 10^o the effect of lowered surface tension permits the thin liquid film to

break. The water film left behind after the break allows pinned colloids to stay in place, while a new contact line forms and recedes toward the center of the drop, sweeping particles inward with it. At this point the contact line becomes pinned again until more water is evaporated from the drop and the film is once again broken, the contact line recedes, and a new ring of colloids is left behind. Particles are permitted to slide with the broken contact line because of the low static friction coefficient, which prevents them from being pinned by the receding contact line until 78% of the linear contact line is filled with particles.

In the *pinned contact line mode* (experiments 3 and 4), surface tension is initially greater than in the recurrent stick-slip mode. In this mode, the surface tension slowly decreases during evaporation, but does not approach the CMC until the final 10% of the droplet's lifetime. The larger liquid surface tension allows droplets to maintain larger contact angles. In this mode, the effect of lowered surface tension is subdued as it is sufficiently low to decrease θ enough to pin particles at the contact line and form coffee-rings, but is also high enough to keep the liquid film from breaking. The droplet remains adhered to the substrate during the early stages of evaporation due to a weakened surface tension that prevents the drop from contracting immediately. As θ is reduced below 27^{o}, particles become pinned at the AWSI and fix the contact line in place for the remainder of the droplet's evaporation lifetime.

In the *slipping contact line mode* (experiments 5 through 8), the surface tension of the liquid is maintained above 48 mN m^{-1} at any given point. The high liquid surface tension results in θ values remaining well above 27^{o} for at least 80% of the droplet's lifetime. Because of the low initial surfactant concentration in these droplets, changes in surface tension are not large enough to strengthen the adhesion force between the liquid and the substrate. Consequently, the attraction between liquid molecules is strong enough to draw the contact line inward during evaporation as θ

remains large. The large θ values ensure that normal capillary forces remain weak, preventing F_f from overcoming F_l, and consequently promoting conditions for the contact line to slip and carry unpinned colloids inward.

The proportional decrease in static friction coefficient with increasing surfactant concentration illustrated in Figure 4.4d suggests that the surfactant sorbs onto the surfaces of the polystyrene colloids and/or the PMMA substrate, acting as a lubricant when the two materials come into contact. Flow displacement experiments further support this effect, as colloids in the slipping contact line mode were calculated to have large static friction coefficients and experienced low detachment rates (i.e., were difficult to wash off). Colloids in the pinned contact line mode were calculated to have lower static friction coefficients and experienced higher detachment rates, and colloids in the recurrent stick-slip mode were calculated to have lowest static friction coefficients and experienced the greatest detachment rates (i.e., were easily washed off).

Conclusion

In conclusion, different types of droplet behavior during evaporation are generated when the droplet's capillary forces are changed. For the range of surfactant concentrations tested here, droplet behavior transitioned from slipping contact line, to pinned contact line, to recurrent stick-slip contact line with decreasing surface tension; each producing a unique colloid pattern. The factors required to transition from one mode of droplet behavior to the next include the decrease of surface tension to weaken the forces pulling the liquid together during the course of droplet evaporation, and reduction of droplet contact angle below 27^o in order to pin particles at the contact line by capillary forces. In the absence of colloids, the contact line of an evaporating droplet will recede toward the center, indicating that in addition to

weakening the liquid surface tension and decreasing the droplet's contact angle, particles must be present to prevent the contact line from receding. The static friction coefficient for polystyrene particles and PMMA substrate was found to depend strongly on the concentration of surfactant in the liquid. As such, colloid stains formed by particles with low static friction coefficients were more easily detached by application of a shear force than those dried with higher static friction coefficients.

Acknowledgements

This study was financed by the National Science Foundation, Project No. 0635954; the US Department of Agriculture, Project No. 2005-35102-16316; The Binational Agricultural Research and Development Fund, Project No. IS-3962-07; and the Teresa Heinz Foundation for Environmental Research. The authors thank Dr. Richard Thomas for insightful comments and discussions.

APPENDIX C

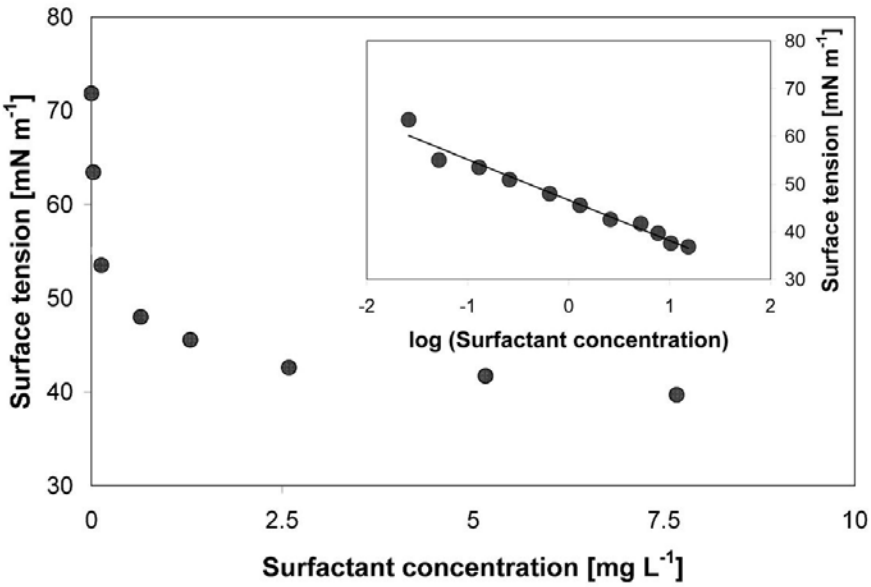

Figure C.1 Change in surface tension with surfactant concentration.

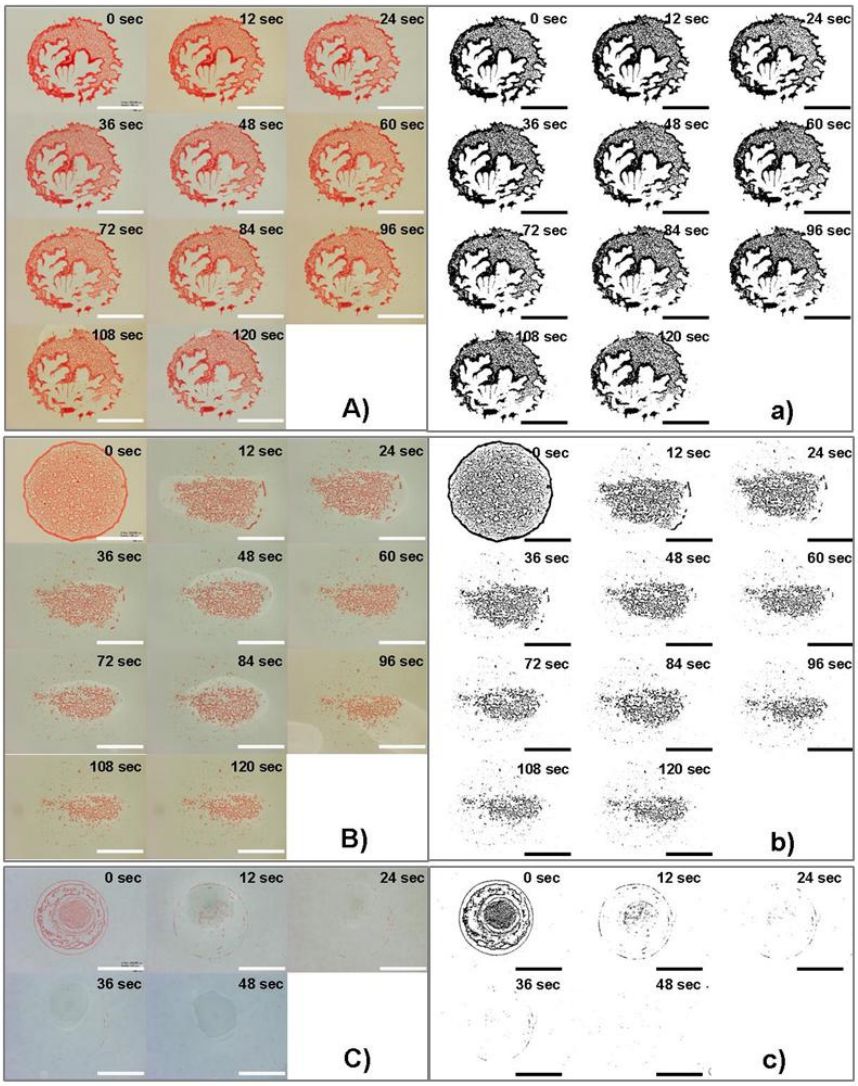

Figure C.2 Sample of sequential images collected during flow displacement tests of colloid stains produced from evaporating droplets containing three different surfactant concentrations. A) Detachment of a colloid stain produced by a droplet containing 0.0 mg L^{-1} initial surfactant concentration. Scale bar = 1000 µm. B) Detachment of a colloid stain produced by a droplet containing 0.13 mg L^{-1} initial surfactant concentration. Scale bar = 1000 µm. C) Detachment of colloids from a stain produced by a droplet containing 7.7 mg L^{-1} initial surfactant concentration. Scale bar = 2000 µm. a, b and c) Are the binarized images.

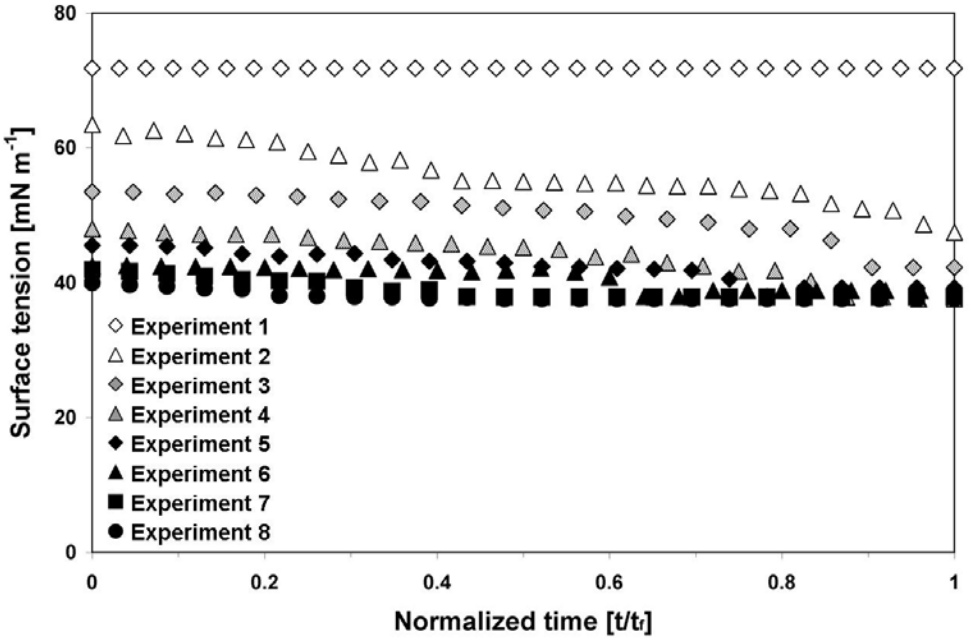

Figure C.3 Time development plots for droplet surface tension at various initial surfactant concentrations.

REFERENCES

Adachi, E., Dimitrov, A.S. and Nagayama, K. (1995) Stripe patterns formed on a glass-surface during droplet evaporation. Langmuir 11, 1057-1060.

Blossey, R. and Bosio, A. (2002) Contact line deposits on cDNA microarrays: A "twin-spot effect". Langmuir 18, 2952-2954.

Busscher, H.J. and van der Mei, H.C. (2006) Microbial adhesion in flow displacement systems. Clinical Microbiology Reviews 19, 127-141.

Byun, M., Hong, S.W., Zhu, L. and Lin, Z.Q. (2008) Self-assembling semicrystalline polymer into highly ordered, microscopic concentric rings by evaporation. Langmuir 24, 3525-3531.

Deegan, R.D. (2000) Pattern formation in drying drops. Physical Review E 61, 475-485.

Deegan, R.D., Bakajin, O., Dupont, T.F., Huber, G., Nagel, S.R. and Witten, T.A. (1997) Capillary flow as the cause of ring stains from dried liquid drops. Nature 389, 827-829.

Deegan, R.D., Bakajin, O., Dupont, T.F., Huber, G., Nagel, S.R. and Witten, T.A. (2000) Contact line deposits in an evaporating drop. Physical Review E 62, 756-765.

Gao, B., Steenhuis, T.S., Zevi, Y., Morales, V.L., Nieber, J.L., Richards, B.K., McCarthy, J.F. and Parlange, J.Y. (2008) Capillary retention of colloids in unsaturated porous media. Water Resources Research 44.

Hogt, A.H., Dankert, J. and Feijen, J. (1986) Adhesion of coagulase-negative staphylococci to methacrylate polymers and copolymers. Journal of Biomedical Materials Research 20, 533-545.

Hong, S.W., Jeong, W., Ko, H., Kessler, M.R., Tsukruk, V.V. and Lin, Z.Q. (2008) Directed self-assembly of gradient concentric carbon nanotube rings. Advanced Functional Materials 18, 2114-2122.

Hu, H. and Larson, R.G. (2005) Analysis of the microfluid flow in an evaporating sessile droplet. Langmuir 21, 3963-3971.

Judai, K., Nishijo, J. and Nishi, N. (2006) Self-assembly of copper acetylide molecules into extremely thin nanowires and nanocables. Advanced Materials 18, 2842.

Kawase, T., Shimoda, T., Newsome, C., Sirringhaus, H. and Friend, R.H. (2003) Inkjet printing of polymer thin film transistors. Thin Solid Films 438, 279-287.

Laurell, T., Nilsson, J. and Marko-Varga, G. (2005) The quest for high-speed and low-volume bioanalysis. Analytical Chemistry 77, 264A-272A.

Ondarcuhu, T. and Joachim, C. (1998) Drawing a single nanofibre over hundreds of microns. Europhysics Letters 42, 215-220.

Picknett, R.G. and Bexon, R. (1977) Evaporation of sessile or pendant drops in still air. Journal of Colloid and Interface Science 61, 336-350.

Shi, Z.L., Wu, S.Q. and Szpunar, J.A. (2006) Self-assembled palladium nanowires by electroless deposition. Nanotechnology 17, 2161-2166.

Shmuylovich, L., Shen, A.Q. and Stone, H.A. (2002) Surface morphology of drying latex films: Multiple ring formation. Langmuir 18, 3441-3445.

Sirringhaus, H., Kawase, T., Friend, R.H., Shimoda, T., Inbasekaran, M., Wu, W. and Woo, E.P. (2000) High-resolution inkjet printing of all-polymer transistor circuits. Science 290, 2123-2126.

Stalder, A.F., Kulik, G., Sage, D., Barbieri, L. and Hoffmann, P. (2006) A Snake-Based Approach to Accurate Determination of Both Contact Points and Contact Angles

Colloids And Surfaces A: Physicochemical And Engineering Aspects 286, 92-103.

Thomas, R.R. (2003) Wetting kinetics study of modified polyimide surfaces containing ionizable functional groups. Langmuir 19, 5763-5770.

Velikov, K.P., Christova, C.G., Dullens, R.P.A. and van Blaaderen, A. (2002) Layer-by-layer growth of binary colloidal crystals. Science 296, 106-109.

Xu, J., Xia, J.F., Hong, S.W., Lin, Z.Q., Qiu, F. and Yang, Y.L. (2006) Self-assembly of gradient concentric rings via solvent evaporation from a capillary bridge. Physical Review Letters 96.

Zevi, Y., Dathe, A., McCarthy, J.F., Richards, B.K. and Steenhuis, T.S. (2005) Distribution of colloid particles onto interfaces in partially saturated sand. Environmental Science and Technology 39, 7055-7064.

CHAPTER 5

ARE PREFERENTIAL FLOW PATHS PERPETUATED BY MICROBIAL ACTIVITY IN THE SOIL MATRIX?[1]

Abstract

Recently, the interactions between soil structure and microbes have been associated with water transport, retention and preferential or column flow development. Of particular significance is the potential impact of microbial extracellular polymeric substances (EPS) on soil porosity (i.e., hydraulic conductivity reduction or bioclogging) and of exudates from biota, including bacteria, fungi, roots and earthworms on the degree of soil water repellency. These structural and surface property changes create points of wetting instability, which under certain infiltrating conditions can result in the formation of persistent preferential flow paths. Moreover, distinct differences in physical and chemical properties between regions of water flow (preferential flow paths) and no-flow (soil matrix) provide a unique set of environmental living conditions for adaptable microorganisms to exist. In this review, special consideration is given to: (1) the functional significance of microbial activity in the host porous medium in terms of feedback mechanisms instigated by irregular water availability and (2) the related physical and chemical conditions that force the organization and formation of unique microbial habitats in unsaturated soils that prompt and potentially perpetuate the formation of preferential flow paths in the vadose zone.

[1] This paper was published as Morales, V.L., et al. (2010), Are preferential flow paths perpetuated by microbial activity in the soil matrix? A review, *Journal of Hydrology*, 393, 29-36.

Introduction and Background

It is widely accepted that preferential flow is the rule rather than the exception in a wide variety of soils [*Dekker and Ritsema*, 1994; *Flury, et al.*, 1994; *Ritsema*, 1999; *Steenhuis, et al.*, 1996]. Additionally, preferential flow is a significant transport mechanism that may account for inaccuracies in water and solute transport predictions [*Ritsema and Dekker*, 2000]. The rising concern about preferential flow (previously referred to as fingering, and recently redefined as column flow in the field) of water in soil is mainly due to the agricultural impacts of reduced soil water retention and bypass of water through the root zone; thus affecting seed emergence, plant growth, and consequently crop yield. In addition, preferential flow is directly implicated with increased risk of groundwater contamination [*Bauters, et al.*, 2000; *Doerr, et al.*, 2007; *Wang, et al.*, 2000] and leaching of agrochemicals into the subsurface. Moreover, localized dry spots (LDS) in golf greens are a result of unwettable soil patches between soil regions that experience preferential flow, and are commonly treated with wetting agents [*Kostka*, 2000]. The ubiquitous occurrence of preferential flow throughout the world, independent of climate type, land use, and soil type and texture [*Andreini and Steenhuis*, 1990; *Baveye, et al.*, 1998a; *Dekker and Ritsema*, 1996a; *Doerr, et al.*, 2007; *Doerr, et al.*, 2006; *Ritsema*, 1999] has proven that it is a common field phenomenon.

Figure 5.1 Preferential flow paths in water repellent dune sand visualized by using dyestuff staining, from Dekker and Ritsema [2000].

Infiltration patterns of preferential flow are distinct as shown in the exposed trench of Figure 5.1. This phenomenon is most commonly attributed to the onset of flow instability at the wetting front of a porous medium, which in natural fields tends be heterogeneous, layered, and often macroporous. The principal cause of column flow, as demonstrated in well characterized and homogeneous media laboratory experiments, is associated with saturation overshoot at the fingertip [*DiCarlo*, 2004]. Here, the region directly behind the wetting front has a high and uniform water saturation, called the finger tip, and is followed by a second region with low and non-uniform water saturation, called the finger tail. However, saturation overshoot does not occur at very low water fluxes or fluxes near the saturated conductivity of the medium. Under field conditions column flow can be enhanced by air entrapment, soil layering (i.e., drastic changes in hydraulic conductivity layers), soil macropores, surface desaturation, and soil water repellency [*Bauters, et al.*, 2000; *Or, et al.*, 2007a; *Wang, et al.*, 2000]. In addition, variable environmental factors that affect soil biological activity (e.g.. temperature, pH, precipitation) further complicate the system by stimulating certain responses that can induced localized and sporadic water

repellence and alter the porosity of the soil. Both, abiotic and biologically derived disturbances of the medium promote column flow. It is thus important to recognize: how preferential flow is initiated, how the flow patterns affect the activity of the soil fauna, and how biological responses to environmental changes affect preferential flow to better understand water transport and retention in soils [*Doerr, et al.*, 2007; *Feeney, et al.*, 2004; *Feeney, et al.*, 2006].

Coating of water-repellent compounds on some soil minerals or soil aggregate surfaces is a result of the slow accumulation of potentially hydrophobic organic compounds produced by plant root exudates, subsurface waxes from plant leaves, and fungal and microbial by-products [*Doerr, et al.*, 2000; *Hallett and Young*, 1999; *Mainwaring, et al.*, 2004; *White, et al.*, 2000]. Furthermore, the soil grain's surface texture has been shown by McHale et al. [2005] to promote the water repellency of soil grains with hydrophobic surface chemistries into super-hydrophobicity by allowing water drops to roll off (i.e., Casey-Baxter 'slippy' conditions) of the dry and rough soil surface. As Dekker and Ritsema [1994] indicate, soils typically display greater water repellency during the summer (rather than during winter or fall) when they are susceptible to falling below a 'critical water content.' Thus, maintaining a minimum moisture content in the soil might prevent an enhanced water-repellency condition from occurring. Recently, irrigation of agricultural lands with wastewater [*Wallach, et al.*, 2005], greywater [*Shafran, et al.*, 2005], or application of sewage sludge to fields [*Hurras and Schaumann*, 2006] as a means to conserve water in water-scarce areas has been found to be responsible for the development of soil water repellency and column flow in arid regions.

Although considerable advances have been made to elucidate the abiotic interrelationships between a soil's physical properties, wetting/drying cycles, water repellency, and column flow, biological feedback mechanisms that support life in such

unpredictable soil environments also contribute to the chemical and physical characteristics known to promote column flow in the first place. In this review, the functional significance of microbial activity on the host porous medium, and the related physical and chemical conditions that force the organization and formation of unique microbial habitats in the vadose zone are considered. A brief description of the physical mechanisms underlying column flow is first provided, followed by a discussion of three biological factors that promote this type of flow by directly or indirectly inducing soil water repellency or changing the medium's hydraulic conductivity. These include: 1) self-organization of microbial organisms at or near column flow regions; 2) the secretion of bacterial compounds that induce soil water repellency, reduce soil porosity, and decrease the soil's hydraulic conductivity; and 3) fungal contributions to soil water-repellency from surface active hydrophobins.

Physics of Column Flow

Early studies of preferential flow ascribed the phenomenon to macropores in the soil medium [*Beven and Germann*, 1982], but more recent findings have shown that unstable infiltration often produces similar flow patterns [*Bauters, et al.*, 2000; *Bundt, et al.*, 2001; *Parlange and Hill*, 1976; *Wang, et al.*, 2000]. Similarly, water repellent soils are well known to have distinct preferential flow patterns [*Bauters, et al.*, 2000; *Dekker and Jungerius*, 1990; *van Ommen, et al.*, 1988] with water moving into the deep soil in columns with dry soil volumes in between, but the physics of this phenomenon is not completely understood.

For soils prone to column flow, a typical preferential solute model divides the soil profile into a distribution soil layer near the soil surface that typically appears saturated, and below, a conveyance zone where preferential flow paths form [*Kim, et al.*, 2005; *Steenhuis, et al.*, 1994]. The distribution zone follows uniform Richards type

infiltration, and conducts water and its solutes into preferential flow paths in the conveyance zone (Figure 5.2). The thickness of the distribution zone in tilled soils can be the depth of the plowed soil [*Kim, et al.*, 2005], while in structured, sandy and water repellent soils it can be limited to 3 to 5 centimeters in depth [*Darnault, et al.*, 2004].

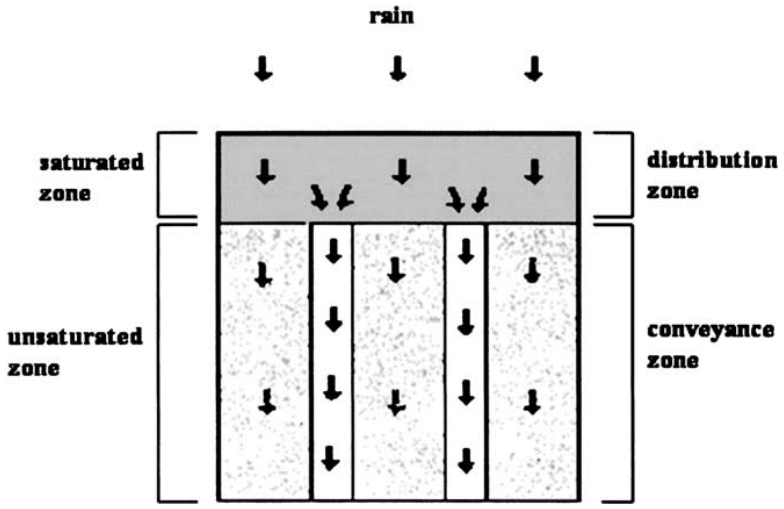

Figure 5.2 Schematic diagram of the flow process in the soil with preferential flow paths, from Kim et al. [2005].

Factors or conditions that trigger wetting front instability either individually or in combination are:

1. An increase of soil hydraulic conductivity with depth, such that coarse-textured soil is overlain by fine-textured soil [*Hill and Parlange*, 1972; *Parlange and Hill*, 1976]
2. Soil water repellency [*Dekker and Jungerius*, 1990; *Raats*, 1973; *Ritsema, et al.*, 1998]
3. Air entrapment [*Hillel*, 1987; *Raats*, 1973]
4. Non-ponding rainfall/irrigation [*Selker, et al.*, 1992; *Wang, et al.*, 2000]

In condition 1, a sharp increase in hydraulic conductivity will increase the velocity of the imbibing water, causing the wetting front to break up into fingers. For condition 2, 'subcritical' water repellency in soils, a concept introduced by Tillman et al. [1989], explains how water infiltration is impeded by repellency despite the appearance of readily wetting soil in the distribution zone because fingers are formed in the conveyance zone below. Bauters et al. [1998] indicate that a ratio as small as 3.13% of hydrophobically treated soil grains to non-repellent grains will make the medium slightly water repellent, and an increase of the ratio to 5% will render the soil extremely water repellent. This evidence shows that small additions of hydrophobic compounds to the medium are not trivial and could induce column flow. In condition 3, large fluxes of infiltrating water lead to air entrapment, where water moves downward in columns, and eventually, compressed air will move upward. Lastly, condition 4 indicates that for density driven displacements, such as non-ponding rainfall/irrigation, the front becomes unstable when the flux, q, is smaller than the soil's conductivity at the maximum water content, $K(\theta_{max})$, close to the wetting front [*Parlange and Hill*, 1976]

$$q < K(\theta_{\max}) \qquad [6.1]$$

This condition mechanistically explains the constriction of water flow during irrigation events, leading to the inevitable formation of fingers that drain out the excess water. The different causes for unstable wetting fronts indicate that the velocity of a wetting front increases with depth, making the front unstable. All the above listed factors can contribute to the small perturbations required to de-stabilize the initially uniform wetting front, and break up the infiltrating water into preferential flow paths.

Initially in the distribution zone, the wetting front is dominated by capillarity, but as irregularities are encountered in the media, gravity becomes the dominant infiltrating force [*de Rooij*, 2000]. Continual drainage cycles of infiltration and

desaturation in soils that experience preferential flow are caused by hysteresis at the finger or column core [*Glass, et al.*, 1989; *Liu, et al.*, 1995; *Wang, et al.*, 2000]. As a result, the patterns of preferential flow paths do not move around much, and actively conduct water for long periods of time [*Bundt, et al.*, 2001; *de Rooij*, 2000]. As de Rooij [2000] explains, once the supply of infiltrating water ceases, the wetted column cores begin drying and water is slowly lost to the surrounding dry soil as a combination of vapor diffusion and liquid water transport until equilibrium is reached. As Liu et al. [1995] point out, the soil in the region of water flow (i.e., preferential flow paths) will remain wetter than the soil in the region of no water flow (i.e., the rest of the soil matrix); thus, subsequent infiltration events will follow old flow paths where the conductivity is higher. Moreover, following the initial wetting and after the columns have stopped expanding laterally, moisture differences between the wet column and the dry soil matrix will be maintained because the matric potential will have also reached equilibrium [*DiCarlo, et al.*, 1999]. This indicates that from a soil water characteristic curve standpoint, column cores are on a drying curve and are considerably wetter at an equal pressure as that of the surrounding dry areas, which are on a wetting curve. For such cases, the non-uniform saturation is an effect of hysteresis that allows pressures to equalize between flow and no flow regions with different saturation levels. These conditions will remain fixed if the wetting/drying cycle is frequent enough to prevent complete soil desiccation or complete saturation that would erase the spatially fragmented soil-moisture hysteresis.

Of the above processes that drive column flow, changes in hydraulic conductivity, water-repellency of certain soil grains, and hysteresis of already formed preferential flow paths are crucial for initiating and maintaining preferential flow in soils with active microfauna. Changes in conductivity are created where active microorganisms reduce the effective porosity of the soil due to biofilm formation near

the surface, such that in coarse textured soils the top soil layer has a lower hydraulic conductivity (from bioclogged pores) than the soil beneath it. Water repellency is created by the secretion of hydrophobic substances by the microfauna during periods of water stress (to reduce localized evaporation from neighboring dry soil), causing preferential flow in any type of soil, independent of particle size. Lastly, hysteresis of wetting-drying cycles will ensure that columns form repeatedly in the same location and persist for extended periods of time. Thus, soil conditions produced by preferential flow impact the growth and activity of microorganisms in the soil, and soil microbial activity accentuates the conditions that trigger preferential flow (Figure 5.3). In essence, the physical processes necessary for preferential flow are strengthened by microbial activity of organisms, and the types of microbial activity are responses to the environmental conditions established by preferential flow, such that the physical and biological processes strengthen each other and perpetuate preferential flow.

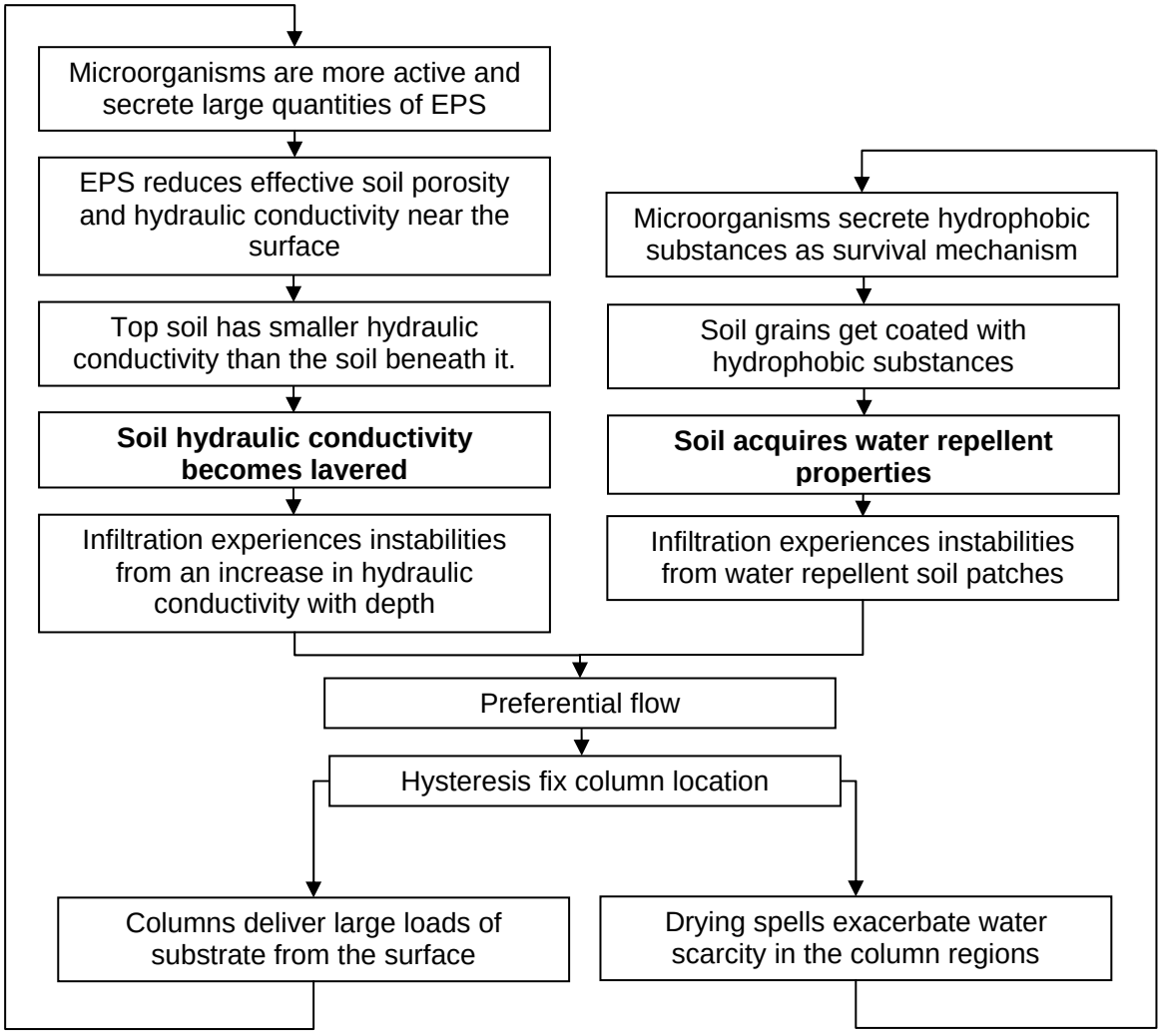

Figure 5.3 Schematic diagram of the feedback mechanisms between microbial activity and preferential flow paths.

Preferential Flow Paths as Biological 'Hot Spots'

The distinct physico-chemical properties of spatially separated soil compartments, particularly at regions of water flow, stimulate deliberate organization of "hot spots" or zones of elevated biological activity in the soil [*Bundt, et al.*, 2001; *Lee*, 1985; *Pivetz and Steenhuis*, 1995]. The different environmental living conditions that support highly active microbial zones are predominantly affected by the greater

amount of oxygen, moisture and nutrient availability in the preferential flow paths than in the rest of the soil matrix, which explains why certain soils experience enhanced degradation of organic compounds transported through preferential flow paths [*Pivetz and Steenhuis*, 1995]. Advective transport of dissolved substrate in preferential pathways is thus a prominent mechanism that supports such highly active microbial zones. Since the distances traversed by migrating microbes are comparable in scale to the separation between individual preferential flow paths, the investment to relocate to a better suited microenvironment is a feasible and worthwhile operation for microorganisms.

Many prokaryotes and fungi are able to sense gradients of nutrients and toxic substances by chemotaxis or quorum sensing, and consequently move/grow towards or away from the source of the compound. Dispersion, and thus colonization of new surfaces with better habitat conditions may be achieved by bacteria that actively use pili or flagella for motility, are transported by interception with flowing water, or are carried away by sorption to a mobile colloid. This ability to relocate can contribute greatly to the altered distribution of organic matter in soils. As the year long study by Bundt et al. [2001] reported, carbon (C) concentrations in preferential flow paths were 10 to 70% greater than in the matrix of a forest soil after measuring temporal and spatial variations between flow and no-flow regions from freshly exposed trenches. Similarly, organic nitrogen (N) concentrations, effective cation exchange capacity (CEC) and base saturation levels were observed to hold similar elevated levels in the preferential flow paths. The high organic matter content in the preferential flow paths was attributed to three main sources: greater proportion of living or decayed roots in flow paths than in the matrix, preferential input of dissolved organic matter from the surface, and enhanced release of microbial biomass C from rewetting of relatively dry soil.

Even with the ability of microorganisms to relocate toward more favorable conditions, the transport mechanisms that allow exuded enzymes to be intercepted by flowing water and carry decomposition products away from cells are largely dependent on the abrupt water fluxes at and near preferential flow paths. In this way, irregular and non-homogeneous infiltration patterns can result in inhibitory scenarios for soil biota if soluble exo-enzymes and other catalytic products are too quickly swept away by convection, thus destroying the return on energy invested in making them. Alternatively, toxic decomposition products may not get carried off fast enough from the vicinity of the propagating microbes [*Ekschmitt, et al.*, 2005] and can otherwise result in self-intoxication. For these reasons, it appears that only resilient microorganisms with the ability to cope with extreme environmental fluctuations by remaining anchored and hydrated will be fit enough to survive in soils prone to finger flow.

It is clear that favorable conditions for microbial activity in the soil depend on the balanced combination of substrate and moisture availability, allowance for gas exchange with the atmosphere, and a moderate rate of transport of excreted/exuded toxic compounds around the cell. Because of these preferences, enhanced microbial activity tends to exaggerate differences in habitat quality between regions where these necessities are met (typically at or near preferential flow regions) and where they are not (in the soil matrix). Furthermore, the enhanced activity and colonization patterns have been contentiously coined as either stochastic or forced organization events by various studies [*Doerr, et al.*, 2007; *Ekschmitt, et al.*, 2005; *Or, et al.*, 2007b], depending on the quality of substrate available intrinsically in the soil or delivered freshly by the fingers. In either case, it is sensible to catalog preferential flow paths as biological ‘hot spots’ from reported evidence of increased biological activity in locations where columns form. Although a set of complex feedback mechanisms must

exist for microorganisms to cope with harsh environmental stresses [*Or, et al.*, 2007b], the specific responses from bacteria experiencing fluctuations associated preferential flow is a research area that has been under-explored.

Impact of Bacterial Compounds on Porous Media

The vadose zone is characterized by its spatial fragmentation and highly dynamic hydration conditions, ranging from complete saturation to wilting point soil moisture. Accordingly, microorganisms must respond to unpredictable and harsh environmental conditions near the soil surface in order to remain viable. A typical adaptation for microbes to cope with soil dehydration and rapid chemical fluctuations of the flowing soil water is through physiological adjustments, such as biosynthesis of extracellular polymeric substances (EPS) [*Or, et al.*, 2007b]. From experimental and theoretical evidence, it is commonly accepted that biofilm surface attachment with EPS is the prevailing lifestyle of bacteria in soil [*Chang and Halverson*, 2003; *Fenchel*, 2002; *Young and Crawford*, 2004]. The EPS structure buffers microcolonies from abrupt hydrating or dehydrating conditions, dampens rapid fluctuations of aqueous temperature, controls the diffusional pathways that deliver resources to the colony, and anchors the cells to soil surfaces [*Or, et al.*, 2007a; *Or, et al.*, 2007b]. However, the synthesized EPS can and often modify physical and chemical characteristics of the soil that cause preferential flow by reducing the effective soil porosity (i.e., pore clogging) when the EPS is hydrated, or by making certain portions of the soil hydrophobic when the EPS dries up.

Bioclogging: Microbes modify their microenvironment by synthesizing and excreting EPS in order to shelter themselves from temporal variations of the variable porous media they reside in [*Or, et al.*, 2007b]. However, because there is a lack of consensus regarding the spatial distribution and properties of biofilms and microbial

aggregates in unsaturated and fragmented conditions, calculations on physical and hydrological processes typically ignore the impact of microbial activity on the porous medium characteristics. Undoubtedly, soil structural properties are affected by EPS synthesis; particularly in terms of altered pore geometry as a result of bioclogging. These two factors can significantly reduce the porosity and hydraulic conductivity (up to 96 and 98% respectively) [*Cunningham, et al.*, 1991] between soil layers and consequently promote conditions that can support preferential flow [*Thullner, et al.*, 2002].

As Or et al. [2007a] point out, at the onset of drying conditions microbial colonies respond by enhanced production of EPS if enough free organic C is readily available. Two key benefits of EPS synthesis during periods of limited water availability are its high water holding capacity and desiccation tolerance. The biopolymer responds to its immediate environmental hydration status by altering its morphology. Under electron microscopy (Figure 5.4) these structural changes are obvious and range from soft and spongy under wet conditions, to stiff and flat when dried (Roberson and Firestone, 1992). In certain types of soils, like those with high clay content, the open EPS structure can enhance soil transport properties [*Czarnes, et al.*, 2000] by physically separating mineral particles from each other [*Baveye, et al.*, 1998b]. While the presence of EPS typically enhances the soil's water holding capacity, in certain cases, hydrated EPS layer can also reduce available pore spaces for flow if the microbes inhabit naturally well-drained soils [*Cunningham, et al.*, 1991; *Kim and Fogler*, 2000; *Nevo and Mitchell*, 1967; *Seki, et al.*, 1998; *Vandevivere and Baveye*, 1992].

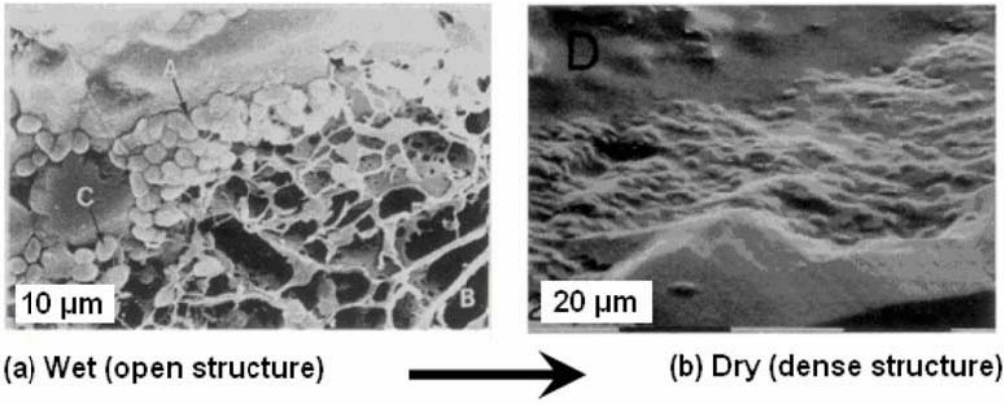

Figure 5.4 Morphological changes of bacterial extracellular polymeric substance on desiccation and on rehydration, from Roberson and Firestone [1992].

The reduction of effective soil porosity is due to a combined effect of biomass accumulation, microbially-induced mineral precipitation, and biogenic gas bubble formation [*Baveye, et al.*, 1998b], although most published studies focus on biomass accumulation to explain pore occlusion with conventional mathematical models (e.g. Hagen-Poiseulle equation and the Kozeny-Carmen equation). In addition to soil bioclogging from biomass growth, it is important to note that microbial populations can produce biofilm layers that are unsustainably thick so nutrients may not diffuse quickly enough to sustain the cells located in the deepest regions. It is suspected that soil bioclogging from microorganism overgrowth may be attributed to surface inputs of the substrate rich irrigation water. The shear force from flowing soil water often enhances biomass sloughing from such regions undergoing endogenous decay. At times, however, partial removal of built up biofilm occurs spontaneously without any change in the flow rate or quality of the applied solution. Although the sloughed material can facilitate permeability recovery at the source, the biofilm fragments may congest other pores in deeper soil layers [*Metcalf and Eddy*, 2002].

It is apparent that microbial activity near the soil surface can clog the topsoil by EPS overproduction in nutrient rich soils. Thus, a layer of reduced hydraulically conductive soil will be formed near the surface overlaying more conductive soil beneath (similar to the effect observed by Hill and Parlange, [1972]), promoting points of instability for imbibing water fronts to break up into columns. It is also sensible to assume that colonies that settle near preferential flow paths (because of substrate supply and moisture availability) must experience mechanical limitations for biofilm growth from the shear forces of the flowing water. Even so, the successful colonization of areas where substrate and moisture abound (i.e. at or near fingers) could potentially change the soil's distribution of conductive pores significantly to fix the location where fingers repeatedly form, and therefore perpetuate preferential flow.

Hydrophobic soil particle surfaces: Typical field trends show that water repellent compounds and soil water repellency (as measured by the Water Drop Penetration Test) are a main cause of preferential flow [*Bond and Harris*, 1964; *Jamison*, 1945]. Soil water repellency has been reported to be common among soils characterized by large particles and in soils of shallow depth [*Bauters, et al.*, 2000; *Bundt, et al.*, 2001; *Ekschmitt, et al.*, 2005]. Partial coating of hydrophobic EPS on soil minerals can modify significantly the matric potential of the medium by increasing the soil-water contact angle and the water head entry value [*Bauters, et al.*, 2000], which consequently lead to preferential flow. This phenomenon may not be obvious in fields that appear to take up water readily, but localized partially-hydrophobic soil particles impede the rate of infiltration and trigger finger formation between unwettable soil patches [*Or, et al.*, 2007b].

Studies on the role of bacterial extracellular polymeric substances in soil water repellence development, such as the one by Schaumann et al. [2007], report that changes to soil wettability after being coated with specific biofilms depend on the

bacterial strain producing it. Other studies have focused on the ability of exopolysaccharides to act as biosurfactants in order to increase the solubility of hydrophobic substances in the soil and make them available for the cells embedded in the EPS matrix [*Ekschmitt, et al.*, 2005]. In addition, reports on wax-degrading bacteria state that such organisms may change the water-repellency of soils through biosurfactant production and direct consumption of hydrophobic waxes [*Roper*, 2005]. Furthermore, the solubilization of hydrophobic substances by (bio)surfactants may facilitate their distribution throughout the soil, which even in small quantities can exacerbate the soil's water-repellency to a great degree and produce preferential flow.

Undoubtedly, the morphological and surface chemical adjustments of EPS alter the characteristics of the soil matrix and the hydrological processes within it in such ways that the potential of a soil type to experience enhanced preferential flow is increased. Two main means by which this occurs are: 1. a decrease the porosity, and thus the hydraulic conductivity, of coarse soils that would otherwise drain well, and 2. induced soil water repellency when EPS dries out and becomes hydrophobic. Both these changes impede water infiltration and consequently create points of instability where columns can form in soils of any particle size.

Influence of Fungal Compounds on Soil Water-Repellency

Fungi have long been suspected to be implicated in the development of soil water repellency [*Bond and Harris*, 1964; *Feeney, et al.*, 2004; *Feeney, et al.*, 2006; *Savage, et al.*, 1969; *White, et al.*, 2000]. They are known to produce highly surface active hydrophobins as a protection mechanism against desiccation stress [*Hakanpaa, et al.*, 2004], and in addition use them as a surfactant to lower the pore water surface tension and aid hyphae to breach the surface of the soil water and grow into air filled voids [*Wessels*, 2000]. In addition to helping the organism survive dry spells, fungal

exudates may also be used as a future food source and as a protective coating that creates harsh microenvironments to keep competitors at bay. Soil fungi have various survival mechanisms to resort to if environmental stresses are high, such as the ability to restore repellency levels in their microenvironment within a couple of weeks of being physically disturbed by soil management practices such as tillage [*Hallett, et al.*, 2005].

As Wessels [2000] and Hallett [2007] point out, fungal exudates are commonly amphiphilic in nature. The polar/apolar charactersistics of exudates are further complicated by the amount of available moisture in the surrounding region. As Hallett [2007] explains, exudates tend to be strongly hydrophilic when wet, but below a critical moisture threshold the hydrophilic surfaces bond strongly with each other and with soil particles leaving an exposed hydrophobic surface as illustrated in Figure 5.5. Therefore, if fungi-containing soil dries beyond this critical water content, the soil behavior can shift abruptly from wettable to non-wettable; yielding soil patches where wetting fronts become unstable and the conditions for finger formation are again satisfied. Although prolonged wetting and field saturation can allow soils to regain wettability, inevitable draining and the occurrence of successive and prolonged drying periods can resume soil water repellency [*Doerr, et al.*, 2000; *Kostka*, 2000; *McHale, et al.*, 2005].

As in the case of bacteria induced water repellency, the effect that fungal hydrophobins have on the porous medium will depend on the proportion of soil particles coated with the hydrophobic surfaces. The fraction of the soil surface area affected, which varies considerably with soil texture, will also determine the magnitude of the effect. Sandy soils have the lowest surface area to volume ratio, so a hydrophobic coating will alter a larger proportion of the particles than for a loamy or

clayey soil with a surface area that is several orders of magnitude greater, thus making the sandy porous medium more prone to experience finger flow infiltration.

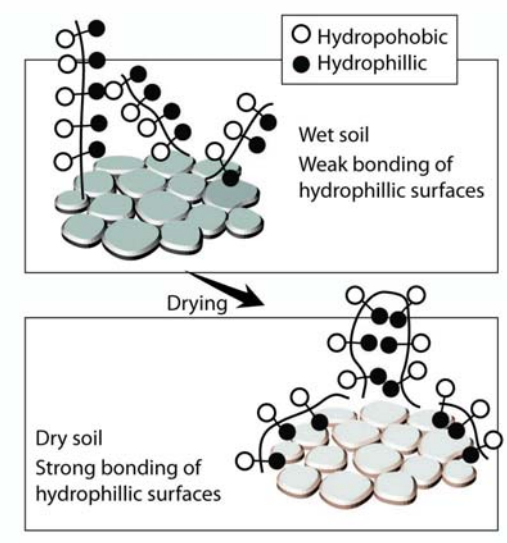

Figure 5.5 The transient nature of water repellency caused by hydrophilic-hydrophobic and hydrophilic-surface bonding during drying, from Hallett [2007].

Agricultural and woodland soil studies have shown a strong correlation between fungal biomass (measured as ergosterol concentrations) and the level of repellency within agricultural soils [*Feeney, et al.*, 2006]. Soils with fairy ring symptoms have been reported to have characteristic of hydrophobic hyphal surfaces and depressed grass growth [*Dekker and Ritsema*, 1996b]. A study by Fidanza et al. [2007] found significantly higher water repellence and reduced soil moisture in necrotic zones that were clearly infested with basydiomycete fungi, but the levels of pH, total nitrogen, magnesium, calcium, cation exchange capacity, and organic matter were not consistently different between the necrotic and healthy turfgrass zones. Few studies are available on specific fungal compounds that may be responsible for the observed increase in soil water repellency. Nonetheless, Fenney et al. [2004] studied

the correlation between glomalin (a specific arbuscular mycorrhizal-fungal exudate) and potting soil repellency. Although inconclusive, this study has not disproved the suspicion that glomalin may be somehow implicated in soil water repellency due to its particularly high adhesive and hydrophobic properties [*Wright and Upadhyaya*, 1998].

Conclusion

Undoubtedly, both bacteria and fungi have the potential to greatly affect the porous media by altering soil water retention and its natural physical properties. Reduced effective porosity can arise from the high concentration of microbes in areas where basic survival requirements are met (such as in the vicinity of preferential flow paths), which can lead to: abundant production of extracellular polymers by highly active microbial cells; sloughing events of this polymeric material caused by overgrowth, starvation or shearing; and release of gaseous byproducts of decomposition and endogenous decay. Heightened soil water repellence may be caused by exuded compounds from fungi and bacteria that are either intrinsically hydrophobic, change their surface properties to become hydrophobic when desiccated, or liberate with biosurfactants existing hydrophobic compounds in the soil. Whichever combination of the above phenomena may be present in the soil, their activation is brought about mainly as a response to recurring water stress. And as indicated in the section describing the physics behind finger flow, the effects of such activities contribute in theory to the physical and chemical conditions that generate preferential flow in soils. In any case, more basic work is still needed before the feedback mechanisms between soil microorganisms and the ever changing environmental conditions in the vadose zone are fully understood. Special attention should be given to soil flora responses to the rapid environmental changes experienced in soils prone to preferential flow.

Acknowledgements

This study was financed in part by the Binational Agricultural Research and Development Fund, Project No. IS-3962-07. The authors thank Dr. Janice Thies, Dr. Louis Dekker, the reviewers, and the associate editor Dr. Wilfred Otten for helpful discussions and insightful comments.

REFERENCES

Andreini, M. S., and T. S. Steenhuis (1990), Preferential paths of flow under conventional and conservation tillage, *Geoderma*, *46*, 85-102.

Bauters, T. W. J., et al. (1998), Preferential flow in water-repellent sands, *Soil Science Society of America Journal*, *62*, 1185-1190.

Bauters, T. W. J., et al. (2000), Physics of water repellent soils, Elsevier Science Bv.

Baveye, P., et al. (1998a), Influence of image resolution and thresholding on the apparent mass fractal characteristics of preferential flow patterns in field soils, *Water Resources Research*, *34*, 2783-2796.

Baveye, P., et al. (1998b), Environmental impact and mechanisms of the biological clogging of saturated soils and aquifer materials, *Critical Reviews in Environmental Science and Technology*, *28*, 123-191.

Beven, K., and P. Germann (1982), Macropores and water-flow in soils, *Water Resources Research*, *18*, 1311-1325.

Bond, R. D., and J. R. Harris (1964), The influence of the microflora on physical properties of soils. L Effects associated with filamentous algae and fungi, *Australian J Soil Res*, *2*, 111-122.

Bundt, M., et al. (2001), Preferential flow paths: biological 'hot spots' in soils, *Soil Biology & Biochemistry*, *33*, 729-738.

Chang, W. S., and L. J. Halverson (2003), Reduced water availability influences the dynamics, development, and ultrastructural properties of Pseudomonas putida biofilms, *Journal of Bacteriology*, *185*, 6199-6204.

Cunningham, A. B., et al. (1991), Influence of biofilm accumulation on porous-media hydrodynamics, *Environmental Science & Technology*, *25*, 1305-1311.

Czarnes, S., et al. (2000), Root- and microbial-derived mucilages affect soil structure and water transport, *European Journal of Soil Science*, *51*, 435-443.

Darnault, C. J. G., et al. (2004), Preferential flow and transport of Cryptosporidium parvum oocysts through the vadose zone: Experiments and modeling, *Vadose Zone Journal*, *3*, 262-270.

de Rooij, G. H. (2000), Modeling fingered flow of water in soils owing to wetting front instability: a review, Elsevier Science Bv.

Dekker, L. W., and P. D. Jungerius (1990), Water repellency in the dunes with special reference to The Netherlands, *Catena, Supplement*, 173-183.

Dekker, L. W., and C. J. Ritsema (1994), Fingered flow - The creator of sand columns in dune and beach sands, *Earth Surface Processes and Landforms*, *19*, 153-164.

Dekker, L. W., and C. J. Ritsema (1996a), Preferential flow paths in a water repellent clay soil with grass cover., *Water Resources Research*, *32*, 1239-1249.

Dekker, L. W., and C. J. Ritsema (1996b), Uneven moisture patterns in water repellent soils, Elsevier Science Bv.

DiCarlo, D. A. (2004), Experimental measurements of saturation overshoot on infiltration, *Water Resources Research*, *40*, 10.

DiCarlo, D. A., et al. (1999), Lateral expansion of preferential flow paths in sands, *Water Resources Research*, *35*, 427-434.

Doerr, S. H., et al. (2007), Water repellence of soils: new insights and emerging research needs, *Hydrological Processes*, *21*, 2223-2228.

Doerr, S. H., et al. (2006), Occurrence, prediction and hydrological effects of water repellency amongst major soil and land-use types in a humid temperate climate, *European Journal of Soil Science*, *57*, 741-754.

Doerr, S. H., et al. (2000), Soil water repellency: its causes, characteristics and hydro-geomorphological significance, *Earth-Science Reviews*, *51*, 33-65.

Ekschmitt, K., et al. (2005), Strategies used by soil biota to overcome soil organic matter stability - why is dead organic matter left over in the soil?, Elsevier Science Bv.

Feeney, D. S., et al. (2004), Does the presence of glomalin relate to reduced water infiltration through hydrophobicity?, *Canadian Journal of Soil Science*, *84*, 365-372.

Feeney, D. S., et al. (2006), Impact of fungal and bacterial biocides on microbial induced water repellency in arable soil, *Geoderma*, *135*, 72-80.

Fenchel, T. (2002), Microbial behavior in a heterogeneous world, *Science*, *296*, 1068-1071.

Fidanza, M. A., et al. (2007), Preliminary investigation of soil chemical and physical properties associated with type-I fairy ring symptoms in turfgrass, *Hydrological Processes*, *21*, 2285-2290.

Flury, M., et al. (1994), Susceptibility of soils to preferential flow of water - A field-study, *Water Resources Research*, *30*, 1945-1954.

Glass, R. J., et al. (1989), Mechanism for finger persistence in homogeneous, unsaturated, porous media: Theroy and verification, *Soil Science*, *148*, 60-70.

Hakanpaa, J., et al. (2004), Atomic resolution structure of the HFBII hydrophobin, a self-assembling amphiphile, *Journal of Biological Chemistry*, *279*, 534-539.

Hallett, P. D. (2007), An introduction to soil water repellency, paper presented at 8th International Symposium of Adjuvants for Agrochemicals, Hand Multimedia, Christchurch, New Zealand, Columbus, Ohio.

Hallett, P. D., et al. (2005), Role of fungi on soil water repellency, paper presented at European Geosciences Union, Vienna, Austria.

Hallett, P. D., and I. M. Young (1999), Changes to water repellence of soil aggregates caused by substrate-induced microbial activity, *European Journal of Soil Science*, *50*, 35-40.

Hill, D. E., and J. Y. Parlange (1972), Wetting front instability in layered soils, *Soil Science Society of America Proceedings*, *36*, 697-&.

Hillel, D. (1987), Unstable flow in layered soils - A review, *Hydrological Processes*, *1*, 143-147.

Hurras, J., and G. E. Schaumann (2006), Properties of soil organic matter and aqueous extracts of actually water repellent and wettable soil samples, *Geoderma*, *132*, 222-239.

Jamison, V. C. (1945), The penetration of irrigation and rain water into sandy soils of Central Florida, *Soil Science Society of America*, *10*, 25-29.

Kim, D. S., and H. S. Fogler (2000), Biomass evolution in porous media and its effects on permeability under starvation conditions, *Biotechnology and Bioengineering*, *69*, 47-56.

Kim, Y. J., et al. (2005), Equation for describing solute transport in field soils with preferential flow paths, *Soil Science Society of America Journal*, *69*, 291-300.

Kostka, S. J. (2000), Amelioration of water repellency in highly managed soils and the enhancement of turfgrass performance through the systematic application of surfactants, Elsevier Science Bv.

Lee, K. E. (1985), *Earthworms: Their Ecology and Relationships with Soils and Land Use*, Academic Press, Sydney, Australia.

Liu, Y. P., et al. (1995), A soil water hysteresis model for fingered flow data, *Water Resources Research*, *31*, 2263-2266.

Mainwaring, K. A., et al. (2004), Role of heavy polar organic compounds for water repellency of sandy soils, *Environmental Chemistry Letters*, *2*, 35-39.

McHale, G., et al. (2005), Water-repellent soil and its relationship to granularity, surface roughness and hydrophobicity: a materials science view, *European Journal of Soil Science*, *56*, 445-452.

Metcalf, and Eddy (2002), *Wastewater Engineering: Treatment and Reuse*, McGraw-Hill Science Engineering.

Nevo, Z., and R. Mitchell (1967), Factors affecting biological clogging of sand associated with ground water recharge, *Water Research*, *1*, 231-&.

Or, D., et al. (2007a), Extracellular polymeric substances affecting pore-scale hydrologic conditions for bacterial activity in unsaturated soils, *Vadose Zone Journal*, *6*, 298-305.

Or, D., et al. (2007b), Physical constraints affecting bacterial habitats and activity in unsaturated porous media - a review, *Advances in Water Resources*, *30*, 1505-1527.

Parlange, J. Y., and D. E. Hill (1976), Theoretical-analysis of wetting front instability in soils, *Soil Science*, *122*, 236-239.

Pivetz, B. E., and T. S. Steenhuis (1995), Biodegradation and bioremediation - Soil matrix and macropore biodegradation of 2,4-D, *Journal of Environmental Quality*, *24*, 564-570.

Raats, P. A. C. (1973), Unstable wetting fronts in uniform and nonuniform soils, *Soil Science Society of America Journal*, *37*, 681-685.

Ritsema, C. J. (1999), Special issue - Preferential flow of water and solutes in soils - Preface, *Journal of Hydrology*, *215*, 1-3.

Ritsema, C. J., and L. W. Dekker (2000), Preferential flow in water repellent sandy soils: principles and modeling implications, Elsevier Science Bv.

Ritsema, C. J., et al. (1998), Modeling and field evidence of finger formation and finger recurrence in a water repellent sandy soil, *Water Resources Research*, *34*, 555-567.

Roper, M. M. (2005), Managing soils to enhance the potential for bioremediation of water repellency, *Australian Journal of Soil Research*, *43*, 803-810.

Savage, S. M., et al. (1969), Contribution of some foil fungi to natural and heat-induced water repellency in sand, *Soil Science Society of America Proceedings*, *33*, 405-&.

Schaumann, G. E., et al. (2007), Influence of biofilms on the water repellency of urban soil samples, *Hydrological Processes*, *21*, 2276-2284.

Seki, K., et al. (1998), Effects of microorganisms on hydraulic conductivity decrease in infiltration, *European Journal of Soil Science*, *49*, 231-236.

Selker, J. S., et al. (1992), Wetting front instability in homogeneous sandy soils under continuous infiltration, Soil Sci Soc Amer.

Shafran, A. W., et al. (2005), Effects of surfactants originating from reuse of greywater on capillary rise in the soil, I W a Publishing.

Steenhuis, T. S., et al. (1994), A simple equation for predicting preferential flow solute concentrations, *Journal of Environmental Quality*, *23*, 1058-1064.

Steenhuis, T. S., et al. (1996), Fingered flow in unsaturated soil: From nature to model - Introduction, *Geoderma*, *70*, 83-85.

Thullner, M., et al. (2002), Interaction between water flow and spatial distribution of microbial growth in a two-dimensional flow field in saturated porous media, *Journal of Contaminant Hydrology*, *58*, 169-189.

Tillman, D. R., et al. (1989), Water-repellency and its measurement by using intrinsic sorptivity, *Australian Journal of Soil Research*, *27*, 637-644.

van Ommen, H. C., et al. (1988), A new technique for evaluating the presence of preferential flow paths in nonstructured soils, *Soil Science Society of America*, *52*, 1192-1193.

Vandevivere, P., and P. Baveye (1992), Saturated hydraulic conductivity reduction caused by aerobic bacteria in sand columns, *Soil Science Society of America*, *56*, 1-13.

Wallach, R., et al. (2005), Soil water repellency induced by long-term irrigation with treated sewage effluent, *Journal of Environmental Quality*, *34*, 1910-1920.

Wang, Z., et al. (2000), Effects of soil water repellency on infiltration rate and flow instability, Elsevier Science Bv.

Wessels, J. G. H. (2000), Hydrophobins, unique fungal proteins, *Mycologist*, *14*, 153-159.

White, N. A., et al. (2000), Changes to water repellence of soil caused by the growth of white-rot fungi: studies using a novel microcosm system, *Fems Microbiology Letters*, *184*, 73-77.

Wright, S. F., and A. Upadhyaya (1998), A survey of soils for aggregate stability and glomalin, a glycoprotein produced by hyphae of arbuscular mycorrhizal fungi, *Plant and Soil*, *198*, 97-107.

Young, I. M., and J. W. Crawford (2004), Interactions and self-organization in the soil-microbe complex, *Science*, *304*, 1634-1637.

CHAPTER 6

CONCLUSIONS AND RECOMMENDATIONS FOR FUTURE WORK

Conclusions

Colloidal transport in the subsurface has gained astounding attention over the past few decades as enhanced transport of contaminants in aquifers, permeability of oil and gas reservoirs, and on-site remediation strategies became topics of concern in various fields of environmental science and engineering. Our understanding of the complex mechanisms governing colloidal transport has come a long way; however, currently developed theories are still insufficient to effectively describe the behavior of these particles in chemically and physically heterogeneous natural systems.

It has been established that colloids can and do facilitate the transport of otherwise sluggish or immobile contaminants by carrying them much faster and further than would be otherwise predicted with traditional solute transport models [*McCarthy and McKay*, 2004]. A substantial fraction of work to date has focused on investigating colloid transport in saturated systems, but attention is quickly being shifted to the more complex –and perhaps more imperative to understand— transport in unsaturated systems. Interest in unsaturated transport has grown because the vadose zone is the critical connection between above surface or shallow contaminant sources and the deeper groundwater.

Natural systems have complex solution chemistries and media surface characteristics that greatly affect colloid attachment and mobilization rates. The effects of individual factors of aqueous chemistry, particularly those involving ionic and surfactant concentration are considered to be well understood. In general, natural media renders unfavorable conditions for colloid deposition in subsurface environments due to electrostatic repulsion between the generally negatively charged

colloids and the porous medium through which they travel. In addition to the above mentioned characteristics that control colloid transport in saturated porous media, transport in the vadose zone is further complicated by the presence of air. This gaseous phase significantly controls the partitioning of colloids between water and solid in various proposed interfaces.

Incorporation of relevant chemical and physical factors into predictive models remains a challenge when describing colloid transport and fate in heterogeneous natural systems. Although the effects of key parameters have been thoroughly studied and assumed to be well understood, such characteristics in the liquid and solid phase are not uniformly distributed spatially nor temporally to be applied at scales pertinent to environmental processes.

The research presented in this dissertation offers a as a mechanistic understanding of the enhanced transport of colloids in complex and organic matter rich solutions, interactions of colloids with the triple contact line (the air-water-solid interface), and the in-homogeneous infiltration patters observed in the field that could further expedite the transport of contaminants through the vadose zone. Chapter 1 offers a review of knowledge gaps that remain void in the pursuit to understand how colloids and pathogens move in the environment. In particular, this chapter emphasizes the current problem of studying variables that are only pertinent to specific and small scales (e.g., interface, pore, column, pedon), but which cannot be efficiently upscaled to the watershed, catchment, or even field level, which are of true environmental concern. Chapter 2 presents a thorough mechanistic understanding of the effect that dissolved organic matter has on colloid transport. The findings of this chapter reveal that organic matter endows colloids with soft particle properties, and this steric hindrance is the repulsive force that promotes enhanced particle transport even under favorable conditions. Moreover, the presence of dissolved organic matter

adds a new layer of complexities to the system that prevents it from following well accepted trends with changes in pH and ionic strength. In this work it was reported for the first time that increasing solution pH resulted in a decrease in transport, while addition of the non-indifferent electrolyte $CaCl_2$ at low concentrations improved the suspension stability. Chapter 3 uses the polymeric characteristics found in Chapter 2 to deterministically predict attachment efficiency values (α) with an empirical correlation equation that accounts for London van der Waals (N_{LO}), electrostatic (N_{E1}), and electrosteric (N_{LEK}) forces. The proposed attachment efficiency correlation does a notable job at fitting the experimentally observed data. Chapter 4 explores the interaction of colloids with a dynamic air-water-solid interface to define the conditions under which capillary forces can successfully immobilize particles. Information gathered on the magnitude of the capillary forces acting on the colloid at the triple interface helps explain the strength of attachment of colloids to the substrate when the system is subject to evaporation. Chapter 5 indicates that two main physico-chemical conditions that trigger infiltration through preferential flow paths (hydraulic conductivity changes with depth and soil-water repellency) are in many cases generated by microbial activity. This chapter proposes that the strategies of microorganisms to survive in fickle micro-environments of soils that experience preferential flow infiltration may, in fact, perpetuate this type of in-homogeneous imbibition. Specifically, the profuse formation of biofilm to protect bacterial cells against severe changes in moisture and nutrient availability can lead to bioclogging, while desiccation of fungal exudates and biofilms is suspected to afford soil grain surfaces with hydrophobic characteristics.

Beyond revealing a detailed mechanistic understanding of simplified sub-micron and column-scale colloidal processes, it is hoped that the scientific discoveries reported in this dissertation will contribute to the greater body of knowledge in

environmental engineering and other fields where similar processes are observed. While it is clear that more work needs to be done to fully understand the colloidal processes that drive fate and transport at environmentally relevant scales, a shift toward investigating phenomena that can be effectively measured or considered in large scale models is in order. The large scale effect and ubiquity of the selected topics of investigation here presented show great promise in meeting this requirement.

Recommendations for Future Work

Scale Dependence of Biocolloid Transport Processes

It is clear that a vast amount of work has been done to understand the processes governing colloid and biocolloid transport in the environment. However, our basic understanding of colloid fate and transport is limited by the itemization of processes as physical, chemical, or biological at the various studied scales (i.e., interface-, collector-, pore-, column-, plot-, field-, and watershed-scales) that may not reveal information that can be upgraded or effectively quantified at large scales of environmental concern. Future work on this topic may include: A thorough assessment of the appropriateness of reported physico-chemical-biological trends across all scales, particularly from the detailed investigations carried out at the smaller scales to the more stochastic larger scales of greater environmental engineering relevance. For example, do cell motility, pore geometry, and degree of surface roughness, known to be relevant at the pore scale, truly affect the transport of bacteria at the watershed-scale?

Effect of DOM on Colloid Transport

There are three possible routes that can be explored to further the understanding of colloidal transport in organic matter-rich porous media based on the

findings reported in the earlier chapter titled: Impact of Dissolved Organic Matter on Colloid Transport in the Vadose Zone: Deterministic Approximation of Transport Deposition Coefficients from Polymeric Coating Characteristics.

Polymeric Characteristics Threshold for Increased Mobility

The results in Chapter 2 show that (polymeric) dissolved organic matter (DOM) layer characteristics required to shift colloid stability from electro*static* to electro*steric* and consequently improve its mobility through a porous medium include non-zero values of adsorbed layer thickness (d), polymeric shell density (Φ), and surface potential (ψ_o). Because each of these characteristics differentially contributed to what has been defined as steric stability for the conditions tested, it is apparent that either a threshold of each characteristic or a grouped characteristic threshold ($(d/a) \cdot \Phi \cdot \psi_o$) must exist beyond which steric stability is not significantly afforded to the suspended colloids and mobility is accordingly no longer improved.

It is clear from the results previously presented that by changing the solution chemistry (in terms of pH and $CaCl_2$ addition), the suspension will shift from having soft particle-like behavior to hard sphere-like behavior. For example, preliminary data suggests that a small concentration of a metal cations (e.g., 2.7 mg L^{-1} of Ca^{2+}) can improve the mobility of colloid-DOM complexes, by enhancing the chelation of DOM strands onto colloid surfaces without significantly neutralizing the charge, compressing the electric double layer, and/or increasing the polymeric shell density (see Figure 6.1).

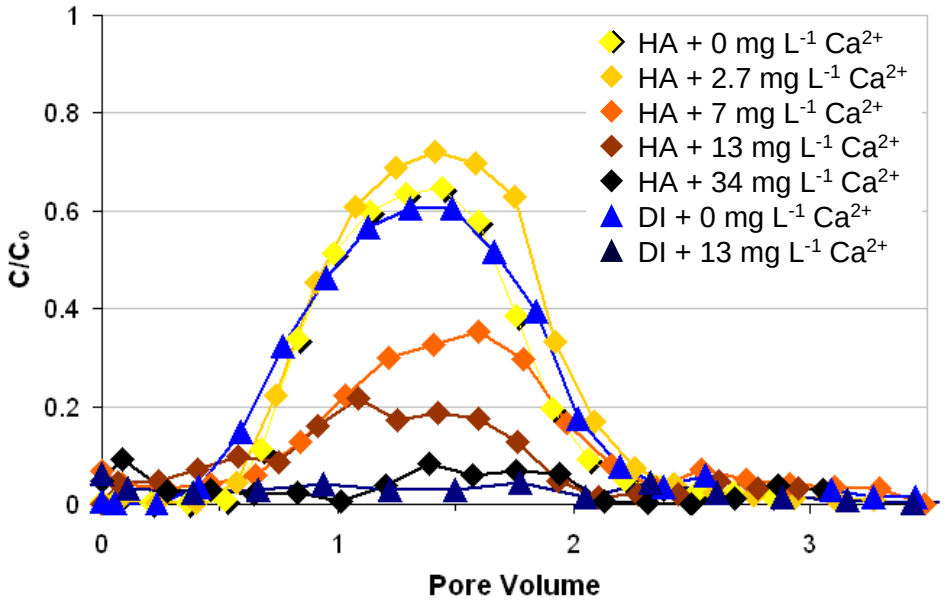

Figure 6.1 Breakthrough curves of experiments with dissolved HA concentrations of 20 mg of dissolved humic acid (HA) organic carbon L^{-1} or deionized water (DI) for no dissolved organic carbon at various concentrations of calcium cations (Ca^{2+}).

A similar trend is observed for changes in pH, where increasing pH will reduce the adsorption of DOM onto colloid surfaces (Γ_c). However, pH also affects the intra-molecular electric repulsion (i.e., protonation of functional groups), which inevitably affects *d*. As indicated in Table 2.1, the values of *d* are low at pH 4, peak at pH 6, and hit a minimum thickness at pH 9. Therefore, it is suspected that an optimal pH value (probably in the circumneutral range) must allow a sufficient mass of DOM to be adsorbed uniformly onto colloid surfaces with a large enough *d*. Since the data presented in Chapter 2 is sparse, the collection of data with higher resolution is suggested to explore these threshold values that can shift suspensions from being electrostatically stabilized to sterically stabilized.

Hydrophobic interactions: Visual data on the transport of colloids through organic matter rich unsaturated media indicate that hydrophobic expulsion might be a process responsible for the favorable retention of humic acid-colloid complexes at air-water interfaces (AWI). Thus, it is recommended that "hydrophobic" interactions be explored to corroborate the increase in hydrophobic behavior resulting in hydrophobic expulsion of HA-colloid complexes when solution composition promotes retention. An approach to do this may follow [*van Oss*, 2003] theory for apolar interactions, which extends classic DLVO theory to include Lifshitz van der Waals (LW), electric double layer (EL), and Lewis acid-base (AB) particle interactions. In the same work, quantitative determination of the LW and AB free energies is achieved with an advancing contact angle method.

Reversible retention of flocculation bridges: As indicated in Chapter 2, the deposition coefficient for HA was in general much smaller than for the non-sterically stabilized colloids in DI and FA solutions (i.e., mass transfer at the AWI was significantly slower than at retention sites involving the solid-water interface (SWI)), suggesting that retention processes at the AWI may actually be *reversible* rather than *slower* when retention occurs at the SWI. It is possible that the soft interfacial surface of the AWI could be easily perturbed with slight changes in saturation that promote re-entrance of colloidal complexes into the mobile liquid phase where they can continue to be transported. Thus, it is recommended that additional experiments be carried out to test the remobilization of DOM-colloid complexes retained in flocculation bridges by solution chemistry or flow transients.

Pathogen Attachment to Fresh Produce Surfaces

A project based on the findings of Chapter 4 would explore the solution compositions responsible for the exceptionally strong attachment of pathogens onto

fresh produce surfaces. It is clear from the findings in Chapter 4 that liquids with high surface tension properties may promote evaporative deposition of pathogenic biocolloids at (primary) energy minima where they can be, as far as conventional produce washing practices, irreversibly attached. Therefore, understanding the composition of irrigation water in terms of substances that affect the liquid's surface tension and Coulombic interactions may shed some light on what modifications can be made to promote weak deposition of inadvertent biocolloids. This is important to improve the efficacy of raw produce washing procedures and better protect food safety.

REFERENCES

McCarthy, J. F., and L. D. McKay (2004), Colloid transport in the subsurface: Past, present, and future challenges, *Vadose Zone Journal*, *3*, 326-337.

van Oss, C. J. (2003), Long-range and short-range mechanisms of hydrophobic attraction and hydrophilic repulsion in specific and aspecific interactions., *Journal of Molecular Recognition*, *16*, 177-190.